Master's Research Thesis

DEFINING THE MEIOTIC FUNCTIONS OF THE CHECKPOINT PROTEIN DPB11.

by

Thomas Garnell,

Student ID: 14299528

Date:30/09/2023

Supervisors

Stephen Gray

Ed Bolt

……

Table of Contents:

Abstract:

DNA damage repair checkpoints identify unrepaired DNA double-strand breaks (DSBs), activating checkpoint kinase Mec1, typically with its accessory protein Dpb11, alongside various downstream effectors responsible for halting cell cycle progression. Recent work has identified Dpb11-dependent (Mordes, Nam and Cortez, 2008) and independent (Navadgi-Patil and Burgers, 2009) functions of Mec1 during mitosis. During the initial stage of meiosis, a specialised cell cycle state that generates haploid gametes from a starting diploid cell, DSBs are introduced throughout the genome, some of which repair as crossover events linking homologous chromosomes. Previous work has shown that not only does Mec1 undertake a checkpoint function inhibiting entry into the first meiotic division until DSBs are repaired, but it also stimulates DSB break formation and instigates interhomolog biased repair. Our work aims to investigate Dpb11's currently undefined roles during meiosis and explore the requirements of Dpb11 in Mec1 activity.

To accurately characterise the meiotic phenotype of removal of Dpb11, we created Dpb11 and Mec1 meiotic depleted (*dpb11-md/mec1-md*) strains by placing the expression of these genes under the Clb2 promoter, known only to be expressed outside of meiosis. In addition, we created N and C terminally 6His-3HA tagged Dpb11 and Mec1 to investigate protein expression and potential post-translational modifications (PTMs). Characterisation of meiotic depleted strains via spore viability and sporulation efficiency indicate roles of Mec1 both dependent and independent on Dpb11. Analysis of *tag-dpb11* and *dpb11-tag* strains indicated that C-terminus and N-terminus tags do not impair potential Dpb11 activity during meiosis. The meiotic phenotype of *tag-dpb11-md* and *dpb11-tag-md* indicates that integration of the P^{CLB2} has impacted Dpb11s expression; however, to what extent remains unclear. Our data suggests that Dpb11 has independent roles from Mec1 as the addition of a *dpb11-md* mutation into *mec1-md* strains showed a difference in spore viability and sporulation efficiency compared to single mec1-md strains. It remains unclear if Dpb11 has any roles dependent on Mec1 due to variation between the *dpb11-md mec1-md* double mutant meiotic phenotypes. Finally, *mec1-md* had lower spore viability and sporulation efficiency when compared to the *dpb11-md* strains, suggesting that Mec1 has roles that are not dependent on Dpb11 during meiosis.

Acknowledgements:

Firstly, I would like to thank my supervisor, Stephen. Many times, throughout the year, I stumbled, and honestly, without your optimism, encouragement and guidance, I would have probably lost my way. I am terrible at expressing myself, and sometimes rocks are more social than I am, but I'd like to sincerely express my thanks for the help you have provided me throughout the year and all the times you put up with my forgetfulness. Next, I'd like to thank Ryan. All your encouragement helped me get to where I am today, and I will honestly miss the conversations we had together; you helped me push through even when I felt helpless. I'd also like to thank Katie. Your optimism was contagious and kept me in high spirits even in the worst of times; you were there to talk to me when I needed it, which meant a lot, even if I'm not great at showing it. A final big thank you to everyone in the lab who was there for me whenever I needed help. I appreciate it.

Chapter 1: Introduction

Meiosis underpins gametogenesis (Maine, 2013), ensuring the chromosome number does not double each reproductive cycle (Gray *et al.*, 2013). During meiosis, two primary processes drive genetic diversity within gametes: crossover formation (Börner, Kleckner and Hunter, 2004) during prophase I and independent assortment (Burgess, Powers and Mell, 2017) during metaphase I. Successful crossover between homologous chromosomes requires the introduction of DNA double-strand breaks (DSBs) (Neale and Keeney, 2006) into the genome via a programmed mechanism (Claeys Bouuaert *et al.*, 2021); however, occasionally DSBs are formed at incorrect locations. If left unrepaired, these DSBs can drive genomic instability and potentially result in cell apoptosis (Kaye *et al.*, 2004; Shrivastav, De Haro and Nickoloff, 2008). As such, a checkpoint mechanism detects unrepaired DSBs and pauses the cell cycle before chromosome segregation (Roeder, 2000), preventing the loss of genetic information. The target of this research, Dpb11, plays a vital role in the mitotic DNA Damage checkpoint (Puddu *et al.*, 2008) and potentially plays a role during the meiotic DNA Damage checkpoint. To aid in characterising Dpb11, the rapidly proliferating species *Saccharomyces cerevisiae (S. cerevisiae)* was chosen (Salari and Salari, 2017). Research into Dpb11's roles during meiosis could hint at unexplored mechanisms of Dpb11's human homolog TopBP1 (Garcia, Furuya and Carr, 2005). However, compared to human germ cells, *S. cerevisiae* cells have some notable differences during meiosis, so it is essential first to explore them in depth.

1.1 Meiosis

The lack of a nitrogen source in the presence of a nonfermentable carbon source can initiate meiosis within budding *S. cerevisiae* A/α diploid cells (Mitchell, 1994). Meiosis can occur outside of nitrogen-deficient environments, but nitrogen starvation halts further cell growth and mitotic division, making it a helpful tool in researching the meiotic characteristics of *S. cerevisiae* strains (Mitchell, 1994). Deprivation of nitrogen and alkalisation from the uptake of nonfermentable carbon source potassium acetate (KAc) triggers the activation of the transcription factor Ime1 (Smith *et al.*, 1990), which, through its interaction with the DNA binding protein Ume6, associates with the promoter of IME2 alongside other genes associated with the early stages of meiosis (Esposito *et al.*, 1969; Rubin-Bejerano *et al.*, 1996). These genes are necessary until meiotic prophase I exit (Smith and Mitchell, 1989; Chu *et al.*, 1998). IME2 encodes for the kinase Ime2 (Guttmann-Raviv, Martin and Kassir, 2002) that, along with Cyclin-Dependent Kinase 1 (cdc28/CDK1), controls *S. cerevisiae's* progression through meiosis (Enserink and Kolodner, 2010; MacKenzie and Lacefield, 2020) with Ime2 being required for the transition between G phase and the pre-meiotic S phase (Dirick *et al.*, 1998) due to the inactivity of G1-CDK (Colomina, 1999). Ime2 is also responsible for forming S-CDK, Cdk1 bound to Clb5 and Clb6, which is required for premeiotic S-phase DNA replication (Smith *et al.*, 1993; Stuart and Wittenberg, 1998).

DNA replication during pre-meiotic S-phase is followed by the first stage of meiosis I, prophase I. Prophase I is split into five substages characterised by the transient formation of the synaptonemal complex (SC), a proteinaceous structure responsible for holding homologous chromosomes together (Hosoya and Miyagawa, 2021). The first substage is leptotene, in which chromosomes begin to condense and align on proteinaceous axial elements and programmed double-strand breaks (more details in 1.2) are introduced throughout the genome by Spo11 endonuclease, initiating recombination (Baker *et al.*, 1976; Keeney, 2001; Scherthan *et al.*, 2007). During the transition between leptotene and the second substage of prophase I, zygotene, telomeres cluster together at the yeast centrosome, forming a "bouquet" structure that tightly binds the chromosomes within the nuclear membrane. (Esponda and Giménez-Martín, 1972; Trelles-Sticken, Loidl and Scherthan, 1999). During zygotene, the synaptonemal complex begins to form in-between the homologous chromosome pairs aided by S-CDK and the coiled-coil protein Zip1 acting as a central element of the complex (Zickler and Kleckner, 2015), and DSBs undergo processing, resulting in the formation of either non-recombinant products or intermediates known as joint-molecules (JMs) (Winter, 2012). After the completion of synapsis, the third substage, pachytene, begins. Matured synaptonemal complexes bridge the homologous chromosome pairs together, aiding DNA strand invasion and the formation of Holliday junction recombination intermediates (Allers and Lichten, 2001; Börner, Kleckner and Hunter, 2004). JMs containing Holliday junctions do not entirely resolve, and spindle pole bodies (SPBs) duplicate but do not separate (Broach, Pringle and Jones, 1991). The synaptonemal complex breaking apart usually characterises the exit from pachytene; however, due to *S. cerevisiae's* small genome, it results in rapid disassembly and the inability to identify characteristics associated with diplotene (Dresser and Giroux, 1988; Winter, 2012). Instead, resolving JMs as crossovers (Allers and Lichten, 2001) and separating SPBs (Broach, Pringle and Jones, 1991) act as markers for the end of pachytene. The homologues remain tightly merged in locations where the crossovers occurred (chiasmata) (Parvinen and Söderström, 1976).

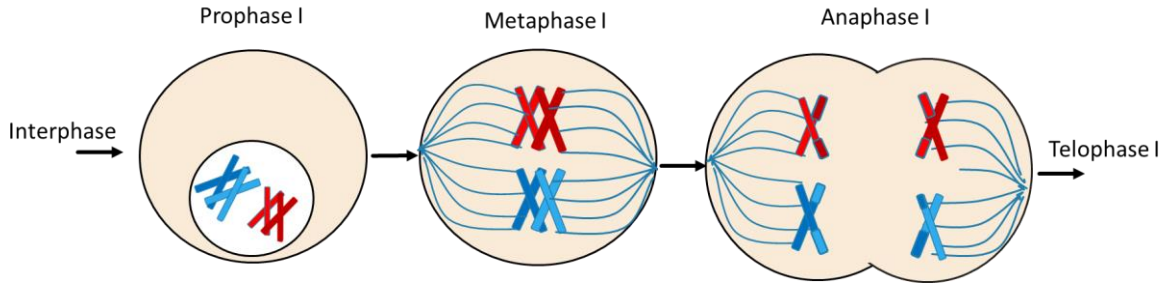

Figure 1.1: Genetic crossover during meiosis I. Genetic crossover occurs during prophase I, where chromosomes condense and align on proteinaceous axial elements. The introduction of double-strand breaks facilitates crossover between chromosome pairs, which form joint-molecules. Crossovers between the chromosome pairs create tension following the binding of spindle fibres during metaphase I. This results in their positioning at the metaphase and ensures correct chromosome segregation. The chiasmata and microtubules then pull the chromosome pairs to separate poles. Image adapted from (MacKenzie and Lacefield, 2020).

The second phase of meiosis I, metaphase I, requires the kinetochores from homologous chromosome pairs fusing to microtubules from opposite poles (Figure 1.1) (Petronczki, Siomos and Nasmyth, 2003). This fusion creates tension at crossovers between the chromosome pairs and results in their positioning at the metaphase plate, with their orientation being independent of each other (Petronczki, Siomos and Nasmyth, 2003). Similar to prophase I, CDK activity plays a vital role in the transition between metaphase I and anaphase I (Figure 1.2). During anaphase I, the chiasmata dissolve, and the homologous chromosomes are pulled to opposite poles by the attached microtubules (McIntosh, 2021; Gottlieb, Gulani and Tegay, 2023). As the homologs reach opposing poles, nuclear envelopes form around them in telophase I, the final phase of meiosis I (Gottlieb *et al.*, 2023). Meiosis I is followed by cytokinesis, where the two diploid daughter cells undergo interkinesis, a brief form of interphase excluding the duplication of genetic material to prepare the cell for meiosis II (Russell, 2010). No further programmed DSBs are introduced during meiosis II as *S. cerevisiae* cells commence spore formation (Figure 1.3) and complete meiosis.

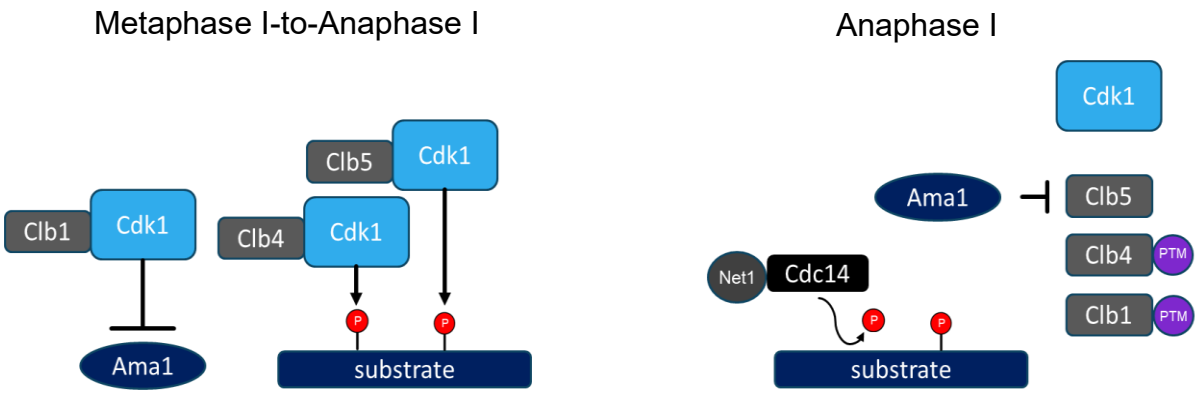

Figure 1.2: CDK1 activity during *Saccharomyces Cerevisiae* Meiosis I. As *S. cerevisiae* cells transition between metaphase I and anaphase I, CDK-Clb1 inhibits Ama1 whilst Cdk1-Clb4 and Cdk1-Clb2 freely phosphorylate CDK substrate. Downregulation of CDK1-Clb1 during anaphase I then allows Ama1 to target Clb5 for degradation. Clb1 and Clb4 are post-translationally modified, which further downregulates CDK activity. Additionally, CDK substrates are partially dephosphorylated by FEAR pathway activated Cdc14. These processes result in an overall reduction in CDK activity during Anaphase I, which facilitates spindle disassembly. Diagram adapted from (MacKenzie and Lacefield, 2020)

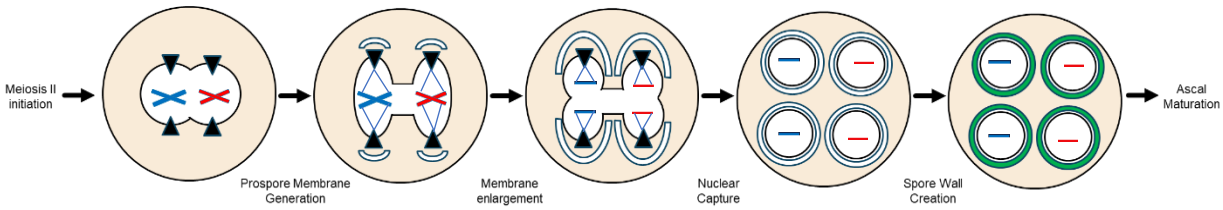

Figure 1.3: Spore formation within *Saccharomyces cerevisiae*. Meiotic plaque created at spindle pole bodies (Black Triangles) consolidates secretory vesicles into prospore membranes (Dark blue (outlined) crescents). The membranes surround the nucleus, generating a spore wall (green). Ascal maturation then concludes spore formation. This diagram was adapted from (Mösch and Taxis, 2012, Neiman, 2005)

1.2 Role of DSBs during Meiosis:

Programmed DNA double-strand breaks (DSBs) during leptotene are essential for meiotic recombination as they provide the environment for strand invasion and the formation of crossovers between homologous chromosome pairs (Claeys Bouuaert *et al.*, 2021). Programmed DSBs are generated through the covalent binding of DNA topoisomerase type-2-related enzyme Spo11 along with ten partner proteins (*S. cerevisiae*) (Keeney, 2001) to DNA and the subsequent endonucleolytic

cleavage by Mre11 endonuclease and Sae2 either side of Spo11 complex (Figure 1.4) (Keeney and Kleckner, 1995; Liu, Wu and Lichten, 1995; Neale, Pan and Keeney, 2005; Claeys Bouuaert *et al.*, 2021). Mre11 exonuclease resects towards the DSB, eventually liberating Spo11 covalently bound to the oligonucleotide (Neale, Pan and Keeney, 2005; Garcia *et al.*, 2011). The DSB ends are then resected by Exo1 exonuclease to create single-stranded tails (Zakharyevich *et al.*, 2010). Single-stranded DNA (ssDNA) can then initiate DNA repair by invading homologous duplex DNA with RecA-like strand exchange proteins Rad51 and Dmc1 (Neale and Keeney, 2006). Repair of DSBs via recombination can lead to two outcomes: non-crossover events (NCOs) which primarily arise from synthesis-dependent strand annealing (SDSA), or crossovers (COs) which are generated through the formation of double Holliday junction (dHJ) intermediates (Allers and Lichten, 2001; McMahill, Sham and Bishop, 2007; Claeys Bouuaert *et al.*, 2021). Homologous linkages, along with sister chromatid cohesion, ensure correct alignment on the meiotic spindle and enable accurate chromosome separation during meiosis I (Székvölgyi and Nicolas, 2010; Claeys Bouuaert *et al.*, 2021).

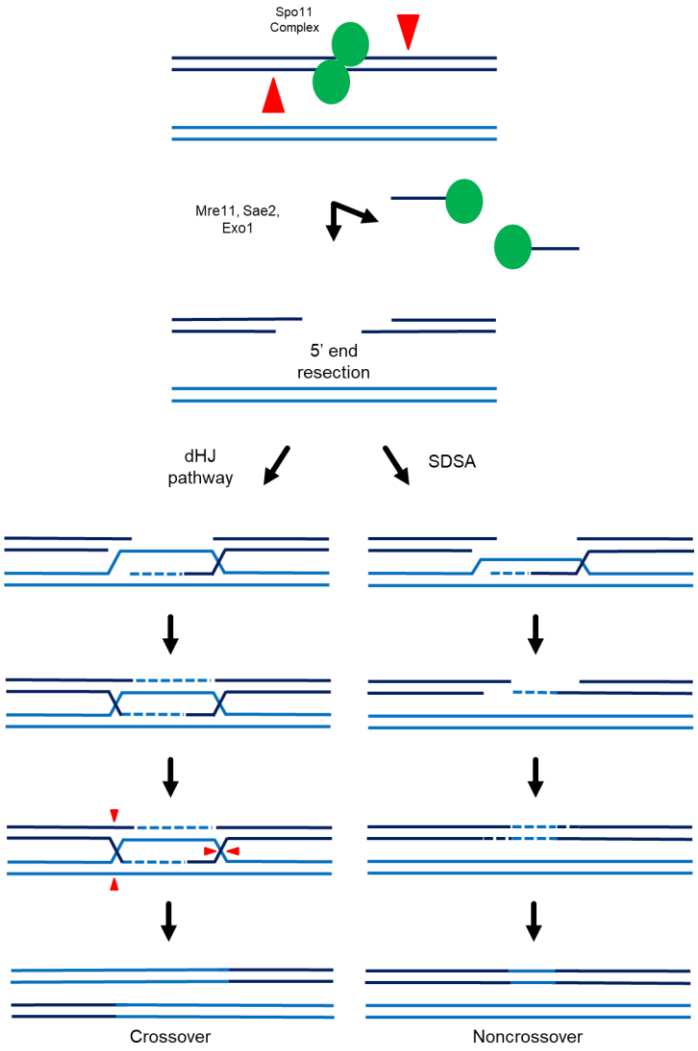

Figure 1.4: Spo11 facilitates DSB generation. Spo11 and its partner proteins covalently bind to DNA, facilitating DNA cleavage by Mre11 and Sae2. Mre11 exonuclease resects towards the DSB, liberating the Spo11 oligonucleotide. Exo1 exonuclease then resects the DNA to create single-strand tails. Repair of DSBs then leads to non-crossover events, which arise from SDSA or crossovers via double holiday junction repair. Diagram adapted from (Neale and Keeney, 2006)

1.3 Meiotic checkpoint

DSBs can be instigated outside of predicted locations due to environmental factors such as ionizing radiation or DNA replication across nicked DNA alongside the production of programmed DSBs during meiosis (Cartagena-Lirola *et al.*, 2008). Both aim to be repaired; however, if left unresolved, unrepaired DSBs can cause chromosomal rearrangements, loss or gain of genetic information, and apoptosis (Featherstone and Jackson, 1999; Shrivastav, De Haro and Nickoloff, 2008). The DNA damage checkpoint is responsible for identifying unrepaired DSBs during mitosis. In contrast, the pachytene checkpoint (recombination checkpoint) appears during meiosis (prophase I/ pachytene) and is

responsible for delaying chromosome segregation, preventing miss-segregation or loss/gain of genetic material resulting in aneuploid gametes (Roeder, 2000; Hochwagen and Amon, 2006).

Both checkpoints are mechanically similar but have a couple of notable differences. Following the detection of an unrepaired DSB, the DNA damage checkpoint requires Rad9 to mediate Rad53 phosphorylation via Mec1 activity (Lydall *et al.*, 1996; Gilbert, Green and Lowndes, 2001), whereas the pachytene checkpoint involves Mek1 kinase, Red1, and Hop1 (Carballo *et al.*, 2008). Hop1 phosphorylation relies on Mec1 and Tel1, subsequently activating Mek1 kinase. (Niu *et al.*, 2005; Carballo *et al.*, 2008). It has been suggested that this is due to the inability of Rad53 to reach the site of meiotic recombination, as during meiosis, exogenous DSBs will result in Rad53 phosphorylation (Cartagena-Lirola *et al.*, 2008).

During mitosis, the DNA damage checkpoint requires two independent complexes to localise to a DSB to arrest the cell cycle effectively. In *S. cerevisiae,* these are the Mec1-Ddc2 complex (Rouse and Jackson, 2002) and the doughnut-like, Rad17, Mec3, and Ddc1 (9-1-1) clamp (Majka and Burgers, 2003). A clamp loader complex consisting of Rad24 and RFC (Rfc1 and four Rfc2-5 subunits) loads the 9-1-1 clamp onto partial duplex DNA in an ATP-dependent interaction (Majka and Burgers, 2003). Further ATP hydrolysis then allows the clap to slide along the DNA until it reaches a region of ssDNA associated with a DSB (Majka and Burgers, 2003). Replication protein A (RPA) coats ssDNA (ssDNA-RPA) (Alani *et al.*, 1992), promoting clamp loading at 5' junctions (Majka, Niedziela-Majka and Burgers, 2006).

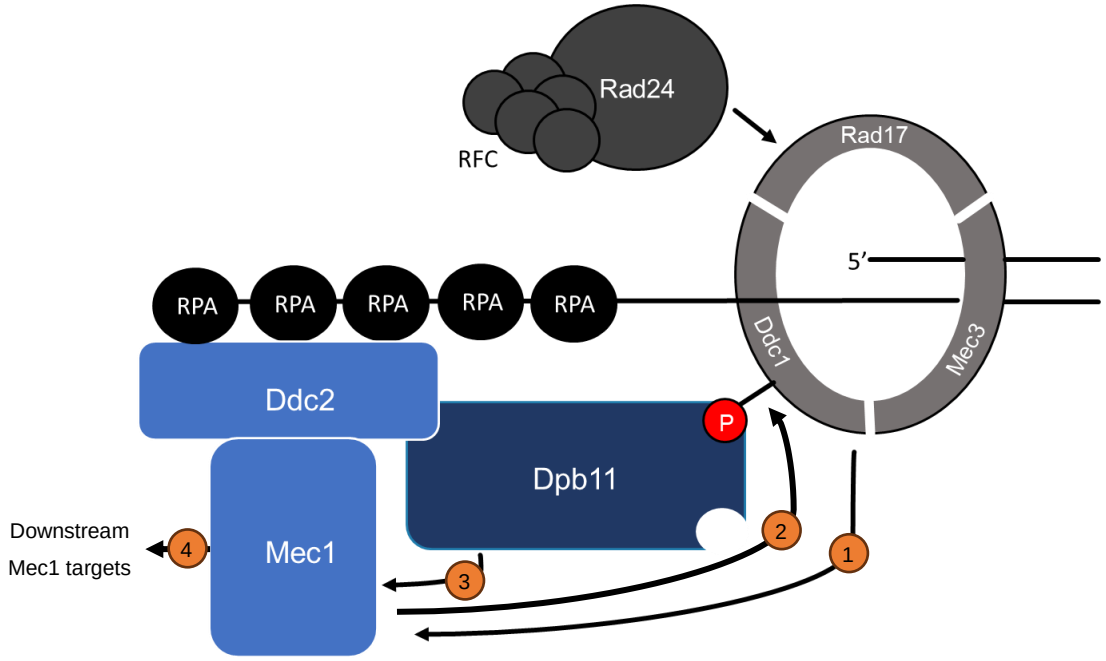

Figure 1.5: Activation of Mec1 kinase activity via Dpb11 Binding to the Ddc2-Mec1 complex within a DNA damage repair checkpoint. Following the independent localisation of the 9-1-1 clamp and Mec1-Ddc2 complex to a DSB, Ddc1s C-terminal activates Mec1 (1). Activated Mec1 then phosphorylates Ddc1 (2), which recruits Dpb11, further activating Mec1 activity (3/4) (Further details in 1.4.1). Diagram adapted from (Dubrana et al., 2007, Bonilla, Melo and Toczyski, 2008). Research conducted by (Mordes, Nam and Cortez, 2008).

Mitosis entry checkpoint kinase 1 (Mec1), a member of the PIKK family, forms a 1:1 stable complex with its regulatory subunit Ddc2 (Majka, Niedziela-Majka and Burgers, 2006), which is recruited to DSBs by the ssDNA-RPA complex (Dubrana *et al.*, 2007). With both the 9-1-1 clamp and Mec1-Ddc2 complex localised at a DSB, the unstructured C-terminal tail present on Ddc1 (9-1-1 subunit) activates Mec1 (Figure 1.5) (Bonilla, Melo and Toczyski, 2008), which in turn phosphorylates Ddc1. Phosphorylated Ddc1 then recruits Dpb11, further activating Mec1 activity (Figure 1.5) (further details in 1.4.1) (Puddu *et al.*, 2008; Deshpande *et al.*, 2017). During mitosis, the activated Mec1 is responsible for phosphorylating histone H2A at Ser129, promoting the recruitment and phosphorylation of Rad9 (Figure 1.6) (Gilbert, Green and Lowndes, 2001; Ho *et al.*, 2022). Additionally, Mec1 phosphorylates Mrc1, a checkpoint mediator and a component of the replication fork (Osborn and Elledge, 2003). Phosphorylated Mrc1 dissociates from Pol ϵ and facilitates the phosphorylation of Rad53 by Mec1 (Alcasabas *et al.*, 2001; Zou and Elledge, 2003; Chen *et al.*, 2014; Ho *et al.*, 2022). Phosphorylated Rad53 promotes cell cycle arrest (Gardner, Putnam and Weinert, 1999) and DNA repair (Sun *et al.*, 1996). It has more recently been shown to arrest leading and lagging strand DNA synthesis (He and Zhang, 2022) and bind to the promoters of genes responsible for encoding proteins responsible for multiple cellular functions (Sheu *et al.*, 2022). As mentioned earlier, the upstream targets of Mec1 differ between the DNA damage checkpoint and the meiotic pachytene checkpoint; instead of Rad9, Mec1 phosphorylates Hop1, which binds to the meiosis-specific paralog of Rad53, Mek1. Similar to Rad53,

Mek1 is required to halt the cell cycle progression (Prugar *et al.*, 2017), but it has also been shown to promote interhomolog bias (Callender *et al.*, 2016) and aid in strand invasion (Chen *et al.*, 2015). Downstream targets of Mec1 are well documented, but potential differences in the mechanism for activating Mec1 via Dpb11 and any potential roles Dpb11 plays during meiosis have yet to be characterised.

1.4 Dpb11

DNA replication regulator DNA Polymerase B II (Dpb11) was first characterised in 1995 by Araki et al., where it was discovered to have dual roles within *Saccharomyces cerevisiae* (Araki *et al.*, 1995). Dpb11 was shown to form a subunit of DNA polymerase II (Epsilon) where it helps it load onto pre-replication complexes at origins during DNA replication (Masumoto, Sugino and Araki, 2000), but was also discovered to play a role in the yet to be characterised cell cycle checkpoint. During their research, analysis of the open reading frame predicted that Dpb11 had a molecular weight of 87-kDa protein, which was later confirmed along with the lethality of dpb11 knockouts (Araki *et al.*, 1995).

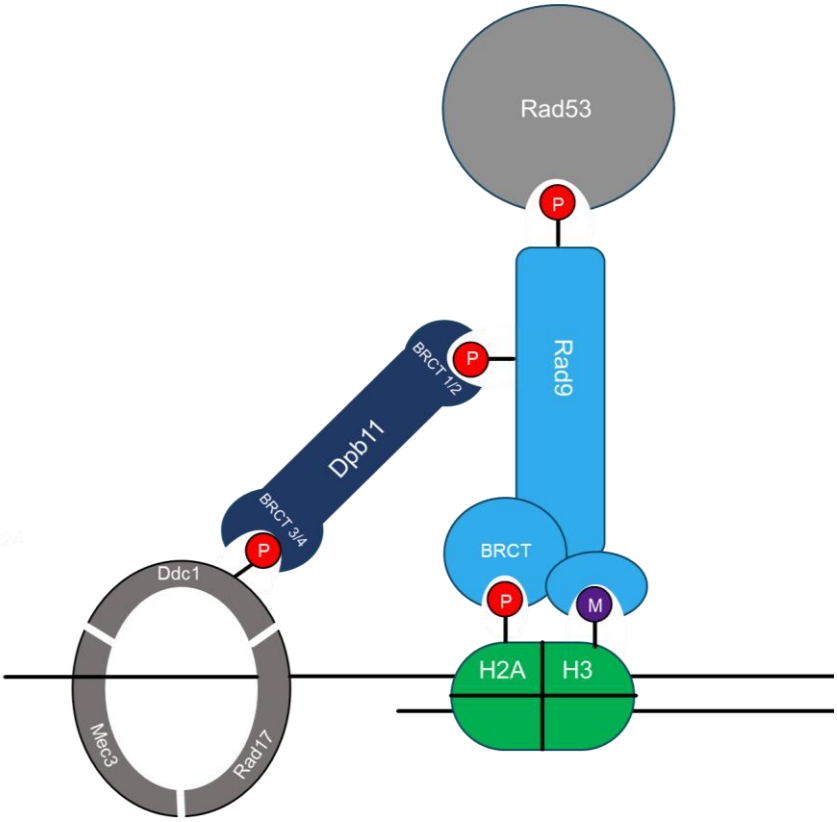

Figure 1.6: Dpb11 forms a central multi-BRCT-domain module with Rad9 and the 9-1-1 checkpoint clamp. Mec1 phosphorylation of H2A promotes the recruitment of Rad9 to a DSB. Dpb11 then facilitates the activation of Rad53 by forming a central multi-BRCT-domain module between Mec1 phosphorylated Ddc1 (9-1-1 subunit) (BRCT 3/4 domain) and Mec1 phosphorylated Rad9 (BRCT 1/2 domain). Diagram adapted from (Cussiol et al., 2015).

Later bioinformatics analysis discovered that Dpb11 contains four BRCA1 C Terminus (BRCT) domains (Bork *et al.*, 1997) which act as phospho-protein binding domains (Yu *et al.*, 2003). More recently, in 2015, Dpb11 was shown to act as a central multi-BRCT-domain module in the coordination of replication initiation, checkpoint signalling and DNA repair where each of its BRCT domains binds to a different target molecule to coordinate the activity of these proteins (more details in 1.4.1, Figure 1.6) (Cussiol *et al.*, 2015).

1.4.1 Dpb11 activates the Mec1–Ddc2 complex

In 2008, research by Daniel A. Mordes, Edward A. Nam, and David Cortez shed light on the previously unconfirmed activation of Mec1 kinase by Dpb11. Dpb11's human homolog TopBP1 was previously shown to activate the Mec1-Ddc2 homolog ATR-ATRIP via its ATR activation domain (AAD) (Kumagai *et al.*, 2006). An equivalent homologous region was not present at the BRCA1 C-terminal of Dpb11, so it remained unclear if any interactions between Dpb11 and Mec1 occurred (Mordes, Nam and Cortez, 2008).

Truncation of the C-terminus of Dpb11 identified a physical interaction with Ddc2 where Dpb11 acts as a central multi-BRCT-domain module between the Ddc2-Mec1 complex and the 9-1-1 clamp (Mordes, Nam and Cortez, 2008). The identified region was situated following Dpb11s BRCT domains and was found to be responsible for the direct activation of Mec1 (Figure 1.5) (Mordes, Nam and Cortez, 2008). This Mec1 activation domain functions similarly to the AAD within TopBP1 (Mordes, Nam and Cortez, 2008). Interestingly, it was revealed that the phosphorylation of Dpb11 by Mec1 enhances subsequent Mec1 kinase activity (Figure 1.5). This hyper-kinase activity occurs once a protein-protein interaction between Dpb11 and Ddc2-Mec1 establishes a positive feedback loop mechanism (Mordes, Nam and Cortez, 2008). This research was conducted in vitro and within mitotic cells. Therefore, no conclusions could be made on Dpb11's roles within the pachytene checkpoint, but it does provide evidence for theoretical interactions that could occur during meiosis.

Research in 2009 explored clamp loader-dependent Mec1 hyperphosphorylation on downstream targets (Vialard *et al.*, 1998; Navadgi-Patil and Burgers, 2009). Results from this study aligned with the predicted mechanism as Mec1's initial activation required a direct interaction with the C-terminal region of the 9-1-1 subunit Ddc1, and further kinase activity requires the indirect recruitment of Dpb11 to a DSB (Navadgi-Patil and Burgers, 2009). Importantly, it indicated that Dpb11 was needed to activate Mec1 during the G2 phase of the cell cycle but was not required for G1 phase checkpoint activation (Navadgi-Patil and Burgers, 2009). Dpb11's absence during G1 could indicate that it potentially doesn't

play a role during the pachytene checkpoint, and any observed phenotypic changes in meiotic-depleted Dpb11 strains result from Dpb11s interactions with other targets.

1.4.1 Dpb11's interaction with other targets

As mentioned, Dpb11 binds to the phosphorylated Ddc1 subunit of the 9-1-1 checkpoint clamp via its BRCT (3/4) domain (Puddu *et al.*, 2008). With this interaction as an anchor, Dpb11 activates Mec1 using its Mec1 activation domain (Mordes, Nam and Cortez, 2008). Dpb11 has also been shown to form a central multi-BRCT-domain module with Rad9 at the DNA Damage checkpoint (Pfander and Diffley, 2011). Following its phosphorylation by CDK, Rad9 binds to Dpb11's BRCT 1/2 domain, facilitating the phosphorylation of Rad9 by Mec1 (Pfander and Diffley, 2011). Phosphorylated Rad9 then recruits Rad53, triggering the cell cycle's halting (Cartagena-Lirola *et al.*, 2008). A second pathway involved in the further recruitment of Rad9 to sites of DNA damage has also been observed (Pfander and Diffley, 2011).

Competition of Dpb11s BRCT 1/2 domain by the Slx4/Rtt107 scaffold complex (Figure 1.7) (Princz, Gritenaite and Pfander, 2015) has been shown to dampen checkpoint signalling of the DNA damage checkpoint as it outcompetes Rad9, resulting in reduced Mec1-dependent Rad9 phosphorylation (Figure 1.8) (Ohouo *et al.*, 2013). Although theorised, no further repair functions have been identified by the Slx4-Dpb11 complex (Princz, Gritenaite and Pfander, 2015). Although Rad9 is not present within the pachytene checkpoint, the dampening of Dpb11-dependent signals may exist during meiosis due to competitive binding within Dpb11's BRCT domains. During the G2/M phase of the cell cycle, there is evidence of Dpb11 bound to the Slx4/Rtt107 scaffold complex, engaging in interactions with the endonuclease Mus81-Mms4 (Figure 1.8) (Gritenaite *et al.*, 2014). It has been hypothesised that this complex may have a role in resolving MMS-induced joint molecules (Cussiol *et al.*, 2015; Princz, Gritenaite and Pfander, 2015).

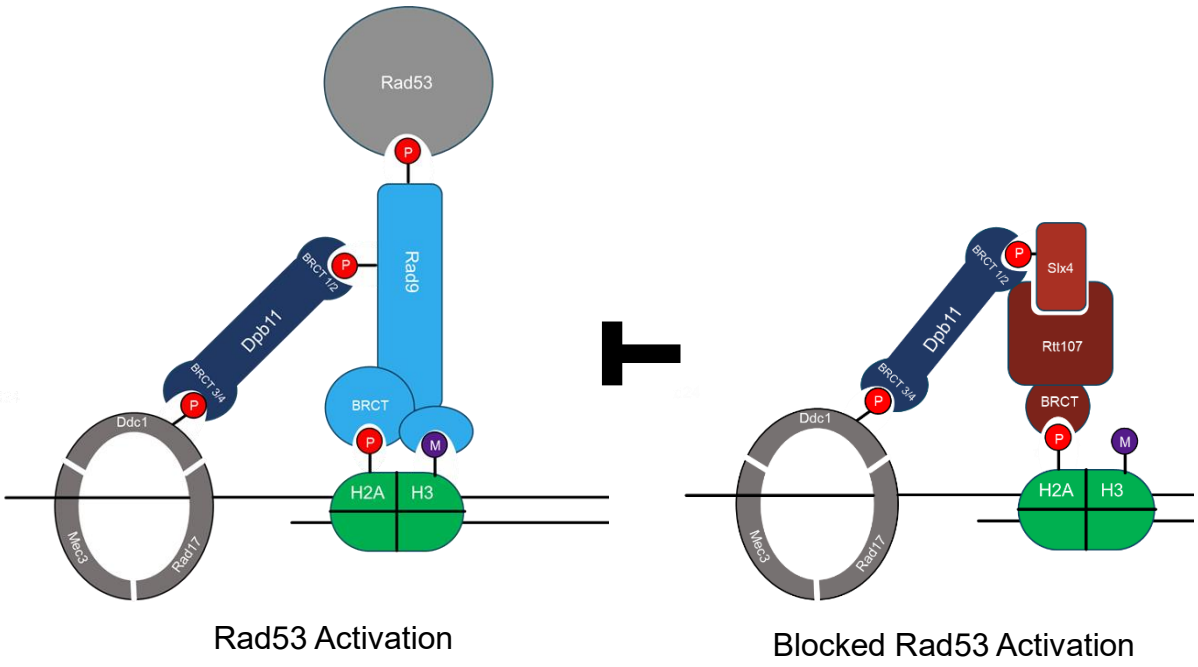

Figure 1.7: Dampening of Rad53 activation via competition with the Slx4/Rtt107 complex. The binding of the Slx4/Rtt107 complex to Mec1 phosphorylated H2A competes with Rad9. This results in the blocked activation of Rad53 by phosphorylated Rad9. Diagram adapted from (Cussiol et al., 2015).

Dpb11 has multiple binding partner proteins that elicit unique signal responses outside of its roles within the DNA damage checkpoint mechanism. Starting during late M phase/G1 phase the Mcm2-7 complex is loaded onto double-stranded DNA (dsDNA) origins (Evrin *et al.*, 2009; Remus *et al.*, 2009; Dhingra *et al.*, 2015). The recruitment of Cdc45 and GINS (Complex comprised of Psf1, Psf2, Psf3, and Sld5) to Mcm2-7 during S phase results in the formation and activation of the Cdc45·Mcm2-7·GINS replication fork helicase (CMG complex) (Ilves *et al.*, 2010; Labib, 2010; Dhingra *et al.*, 2015). Notably, Dpb11 facilitates the recruitment of Cdc45 to Mcm2-7, however, binds directly to Mcm2-7 and Cdc45, competes with GINS and prevents the premature formation of the CMG complex (Dhingra *et al.*, 2015). Dpb11 then binds to ssDNA extruded from Mcm2-7 dissociating from Cdc45 and Mcm2-7 and no longer competes with GINS enabling the formation of the CMG complex (Dhingra *et al.*, 2015). In addition, Dpb11 has been shown to directly interact with GINS participating in both the initiation and elongation stages of chromosomal DNA replication (Takayama *et al.*, 2003; Tanaka *et al.*, 2007).

Interestingly, before migrating to origins, Dpb11 forms a fragile preloading complex with S phase CDK (S-CDK)-phosphorylated Sld2, Pol ε and GINS an important part of the CDK regulation of DNA replication (Muramatsu *et al.*, 2010). Dpb11 forms a central multi-BRCT-domain module with the S-CDK-phosphorylated ssDNA binding proteins Sld2 and Sld3 facilitating their interaction with Cdc45, GINS and other replication proteins and is required for the initiation of DNA replication (Figure 1.8) (Tanaka *et al.*, 2007; Mordes, Nam and Cortez, 2008; Cussiol *et al.*, 2015).

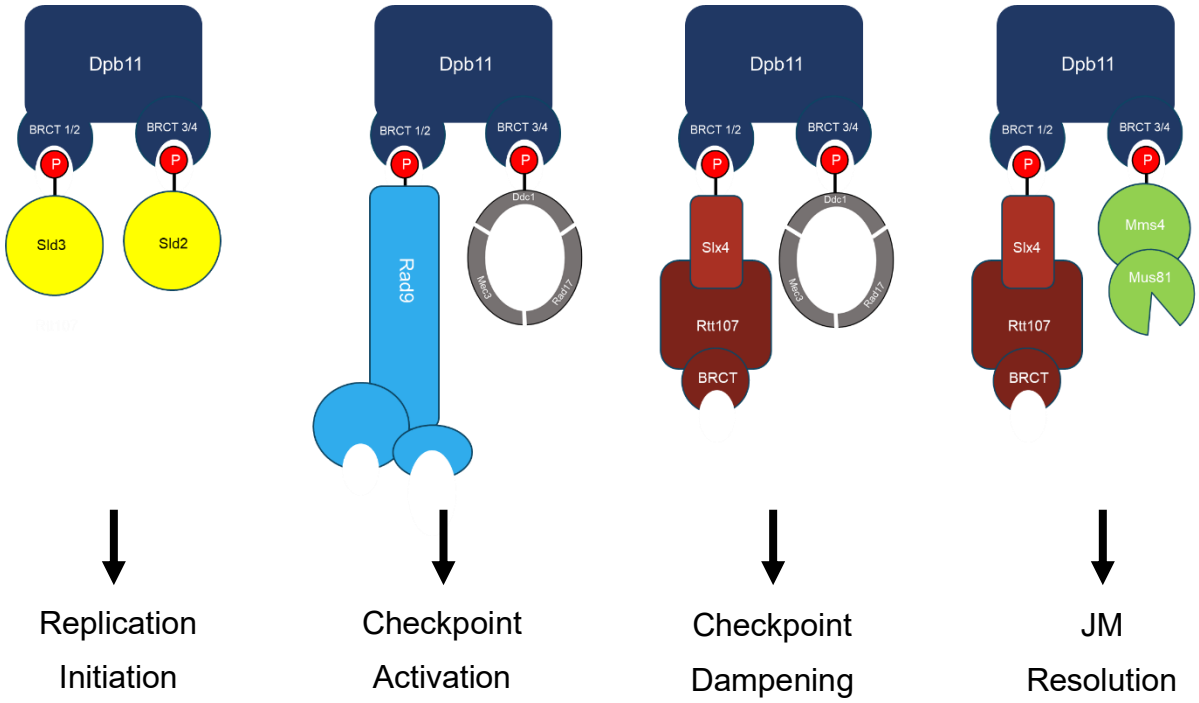

Figure 1.8: Dpb11's activation of downstream pathways. Besides Mec1 activation, Dpb11 forms a central multi-BRCT-domain module with various targets, resulting in replication initiation, checkpoint activation and joint molecule resolution. Notably, competition between Rad9 and Slx-Rtt107 results in the dampening of checkpoint activation. Figure adapted from (Cussiol et al., 2015).

1.5 Aim:

Our work aims to investigate Dpb11's currently undefined roles during meiosis and explore the requirements of Dpb11 in Mec1 activity. This will be accomplished by studying the usage of P^{CLB2} to generate meiotic-depleted (md) strains.

- Generate haploid and diploid mutants, *tag-dpb11, dpb11-md, tag-mec1* and *mec1-md* mutants.
- Construct double mutants *dpb11-md mec1-md, tag-dpb11 mec1-md,* and *dpb11-md tag-mec1* to explore the epistatic relationship between these genes in meiosis.
- Analyse/Compare the spore viability and sporulation efficiency of the mutant strains.
- Explore the use of nanopore sequencing, post-translational modification analysis, and DNA-damaging agents to characterise the mutant strains.

Chapter 2: Materials and Methods

2.1 Materials

2.1.1 Strains

Table 2-1: Catalogue of *Saccharomyces cerevisiae* strains.

Nottingham YSG Number	Mating Type	Genotype	Notes
YSG1	a	ade8	pre-existing: Used for replica-plating
YSG2	p	ade8	Pre-existing: Used for replica-plating
YSG3	a	ho::LYS2, lys2, ura3, arg4-nsp, leu2::hisG, his4X::LEU2, nuc1::LEU2	Pre-existing: WT phenotype
YSG4	p	ho::LYS2, lys2, ura3, arg4-nsp, leu2::hisG, his4X::LEU2, nuc1::LEU2	Pre-existing: WT phenotype
YSG5	a/p	ho::LYS2/', lys2/', ura3/', arg4-nsp/', leu2::hisG/', his4X::LEU2/', nuc1::LEU2/'	Pre-existing YSG3 x YSG4: WT phenotype
YSG15	p	ho::LYS2, lys2, ura3, arg4-nsp, leu2::hisG, his4X::LEU2, nuc1::LEU2, pCLB2-3HA-MEC1::KanMX	Pre-existing: P^{CLB2} MEC1 strain
YSG29	a	ho::LYS2, lys2, ura3, leu2::hisG, trp1::hisG, THR1::mCerulean-TRP1	Pre-existing: Used for Crossover Frequency
YSG33	p	ho::LYS2, lys2, ura3, leu2::hisG, trp1::hisG, CEN8::tdTomato-LEU2	Pre-existing: Used for Crossover Frequency
YSG236	a/p	ho::LYS2/', lys2/', ura3/', leu2::hisG/', trp1::hisG/', THR1::mCerulean-TRP1/THR1, CEN8::tdTomato-LEU2/CEN8	Pre-existing YSG29 x YSG33: Used for Crossover Frequency
YSG518	a	ho::LYS2, lys2, ura3, arg4-nsp, leu2::hisG, his4X::LEU2, nuc1::LEU2, 6xHis-3xHA-DPB11::KanMX	Pre-existing: YSG3 DPB11 tag transformation
YSG519	a	ho::LYS2, lys2, ura3, arg4-nsp, leu2::hisG, his4X::LEU2, nuc1::LEU2, 6xHis-3xHA-DPB11::KanMX	Pre-existing: YSG3 DPB11 tag transformation
YSG520	p	ho::LYS2, lys2, ura3, arg4-nsp, leu2::hisG, his4X::LEU2, nuc1::LEU2, 6xHis-3xHA-DPB11::KanMX	Pre-existing: YSG4 DPB11 tag transformation
YSG521	p	ho::LYS2, lys2, ura3, arg4-nsp, leu2::hisG, his4X::LEU2, nuc1::LEU2, 6xHis-3xHA-DPB11::KanMX	Pre-existing: YSG4 DPB11 tag transformation
YSG678	a	ho::LYS2, lys2, ura3, leu2::hisG, trp1::hisG, THR1::mCerulean-TRP1, pCLB2-3HA-DPB11::KanMX	Pre-existing: YSG29 Transformation pCLB2-DPB11
YSG680	p	ho::LYS2, lys2, ura3, leu2::hisG, trp1::hisG, CEN8::tdTomato-LEU2, pCLB2-3HA-DPB11::KanMX	Pre-existing: YSG33 Transformation pCLB2-DPB11
YSG681	p	ho::LYS2, lys2, ura3, leu2::hisG, trp1::hisG, CEN8::tdTomato-LEU2, pCLB2-3HA-DPB11::KanMX	Pre-existing: YSG33 Transformation pCLB2-DPB11
YSG767	a/p	ho::LYS2/', lys2/', ura3/', leu2::hisG/', trp1::hisG/', THR1::mCerulean-TRP1/THR1, CEN8::tdTomato-LEU2/CEN8, pCLB2-3HA-DPB11::KanMX/'	YSG678x680 Colony A
YSG768	a/p	ho::LYS2/', lys2/', ura3/', leu2::hisG/', trp1::hisG/', THR1::mCerulean-TRP1/THR1, CEN8::tdTomato-LEU2/CEN8, pCLB2-3HA-DPB11::KanMX/'	YSG678x680 Colony B
YSG769	a/p	ho::LYS2/', lys2/', ura3/', leu2::hisG/', trp1::hisG/', THR1::mCerulean-TRP1/THR1, CEN8::tdTomato-LEU2/CEN8, pCLB2-3HA-DPB11::KanMX/'	YSG678x681 Colony A
YSG782	a/p	ho::LYS2/', lys2/', ura3/', leu2::hisG/', trp1::hisG/', THR1::mCerulean-TRP1/THR1, CEN8::tdTomato-LEU2/CEN8, pCLB2-3HA-DPB11::KanMX/'	YSG678x680 Colony C

YSG783	a/p	ho::LYS2/', lys2/', ura3/', leu2::hisG/', trp1::hisG/', THR1::mCerulean-TRP1/THR1, CEN8::tdTomato-LEU2/CEN8, pCLB2-3HA-DPB11::KanMX/'	YSG678x680 Colony D
YSG784	a/p	ho::LYS2/', lys2/', ura3/', leu2::hisG/', trp1::hisG/', THR1::mCerulean-TRP1/THR1, CEN8::tdTomato-LEU2/CEN8, pCLB2-3HA-DPB11::KanMX/'	YSG678x680 Colony E
YSG785	a/p	ho::LYS2/', lys2/', ura3/', leu2::hisG/', trp1::hisG/', THR1::mCerulean-TRP1/THR1, CEN8::tdTomato-LEU2/CEN8, pCLB2-3HA-DPB11::KanMX/'	YSG678x680 Colony F
YSG786	a/p	ho::LYS2/', lys2/', ura3/', leu2::hisG/', trp1::hisG/', THR1::mCerulean-TRP1/THR1, CEN8::tdTomato-LEU2/CEN8, pCLB2-3HA-DPB11::KanMX/'	YSG678x681 Colony B
YSG787	a/p	ho::LYS2/', lys2/', ura3/', leu2::hisG/', trp1::hisG/', THR1::mCerulean-TRP1/THR1, CEN8::tdTomato-LEU2/CEN8, pCLB2-3HA-DPB11::KanMX/'	YSG678x681 Colony C
YSG788	a/p	ho::LYS2/', lys2/', ura3/', leu2::hisG/', trp1::hisG/', THR1::mCerulean-TRP1/THR1, CEN8::tdTomato-LEU2/CEN8, pCLB2-3HA-DPB11::KanMX/'	YSG678x681 Colony D
YSG789	a	ho::LYS2, lys2, ura3, arg4-nsp, leu2::hisG, his4X::LEU2, nuc1::LEU2, pCLB2-3HA-MEC1::KanMX	YSG3 pCLB2-MEC1 Transformation B
YSG790	a	ho::LYS2, lys2, ura3, leu2::hisG, trp1::hisG, THR1::mCerulean-TRP1, pCLB2-3HA-MEC1::KanMX	YSG29 pCLB2-MEC1 Transformation A
YSG791	p	ho::LYS2, lys2, ura3, leu2::hisG, trp1::hisG, CEN8::tdTomato-LEU2, pCLB2-3HA-MEC1::KanMX	YSG33 pCLB2-MEC1 Transformation A
YSG792	p	ho::LYS2, lys2, ura3, leu2::hisG, trp1::hisG, CEN8::tdTomato-LEU2, pCLB2-3HA-MEC1::KanMX	YSG33 pCLB2-MEC1 Transformation A
YSG793	a	ho::LYS2, lys2, ura3, arg4-nsp, leu2::hisG, his4X::LEU2, nuc1::LEU2, pCLB2-3HA-DPB11::KanMX	YSG3 pCLB2-DPB11 Transformation B
YSG794	p	ho::LYS2, lys2, ura3, arg4-nsp, leu2::hisG, his4X::LEU2, nuc1::LEU2, pCLB2-3HA-DPB11::KanMX	YSG4 pCLB2-DPB11 Transformation A
YSG795	p	ho::LYS2, lys2, ura3, arg4-nsp, leu2::hisG, his4X::LEU2, nuc1::LEU2, pCLB2-3HA-DPB11::KanMX	YSG4 pCLB2-DPB11 Transformation B
YSG796	a/p	ho::LYS2/', lys2/', ura3/', arg4-nsp/', leu2::hisG/', his4X::LEU2/', nuc1::LEU2/', pCLB2-3HA-MEC1::KanMX/'	YSG789xYSG15 Colony A
YSG797	a/p	ho::LYS2/', lys2/', ura3/', arg4-nsp/', leu2::hisG/', his4X::LEU2/', nuc1::LEU2/', pCLB2-3HA-MEC1::KanMX/'	YSG789xYSG15 Colony C
YSG798	a/p	ho::LYS2/', lys2/', ura3/', arg4-nsp/', leu2::hisG/', his4X::LEU2/', nuc1::LEU2/', pCLB2-3HA-MEC1::KanMX/'	YSG789xYSG15 Colony D
YSG829	p	ho::LYS2, lys2, ura3, leu2::hisG, trp1::hisG, CEN8::tdTomato-LEU2, KanMX::pCLB2-3HA-MEC1, pCLB2-3HA-DPB11::KanMX	YSG678xYSG791 Colony 3D
YSG830	a/p	ho::LYS2/', lys2/', ura3/', leu2::hisG/', trp1::hisG/', THR1::mCerulean-TRP1/THR1, CEN8::tdTomato-LEU2/CEN8, KanMX::pCLB2-3HA-MEC1/'	YSG790xYSG791
YSG854	a/p	ho::LYS2/', lys2/', ura3/', leu2::hisG/', trp1::hisG/', THR1::mCerulean-TRP1/THR1, CEN8::tdTomato-LEU2/CEN8, pCLB2-3HA-MEC1::KanMX/'	YSG790xYSG792 Colony C
YSG855	a/p	ho::LYS2/', lys2/', ura3/', leu2::hisG/', trp1::hisG/', THR1::mCerulean-TRP1/THR1, CEN8::tdTomato-LEU2/CEN8, pCLB2-3HA-MEC1::KanMX/'	YSG790xYSG792 Colony G
YSG856	a/p	ho::LYS2/', lys2/', ura3/', leu2::hisG/', trp1::hisG/', THR1::mCerulean-TRP1/THR1, CEN8::tdTomato-LEU2/CEN8, pCLB2-3HA-MEC1::KanMX/'	YSG790xYSG792 Colony F
YSG857	a	ho::LYS2, lys2, ura3, arg4-nsp, leu2::hisG, his4X::LEU2, nuc1::LEU2, 6xHis-3xHA-DPB11::KanMX	DPB11 Tag Transformation x YSG3 Colony B2
YSG858	a	ho::LYS2, lys2, ura3, arg4-nsp, leu2::hisG, his4X::LEU2, nuc1::LEU2, 6xHis-3xHA-DPB11::KanMX	DPB11 Tag Transformation x YSG3 Colony B3
YSG859	a	ho::LYS2, lys2, ura3, arg4-nsp, leu2::hisG, his4X::LEU2, nuc1::LEU2, 6xHis-3xHA-DPB11::KanMX	DPB11 Tag Transformation x YSG3 Colony D3
YSG860	a	ho::LYS2, lys2, ura3, arg4-nsp, leu2::hisG, his4X::LEU2, nuc1::LEU2, 6xHis-3xHA-DPB11::KanMX	DPB11 Tag Transformation x YSG3 Colony C4

YSG861	p	ho::LYS2, lys2, ura3, arg4-nsp, leu2::hisG, his4X::LEU2, nuc1::LEU2, 6xHis-3xHA-DPB11::KanMX	DPB11 Tag Transformation x YSG3 Colony C1
YSG862	p	ho::LYS2, lys2, ura3, arg4-nsp, leu2::hisG, his4X::LEU2, nuc1::LEU2, 6xHis-3xHA-DPB11::KanMX	DPB11 Tag Transformation x YSG3 Colony D1
YSG863	p	ho::LYS2, lys2, ura3, arg4-nsp, leu2::hisG, his4X::LEU2, nuc1::LEU2, 6xHis-3xHA-DPB11::KanMX	DPB11 Tag Transformation x YSG3 Colony C2
YSG864	a/p	ho::LYS2/', lys2/', ura3/', arg4-nsp/', leu2::hisG/', his4X::LEU2/', nuc1::LEU2/', 6xHis-3xHA-DPB11::KanMX'	YSG858 x YSG862 Colony F1.3
YSG865	a/p	ho::LYS2/', lys2/', ura3/', arg4-nsp/', leu2::hisG/', his4X::LEU2/', nuc1::LEU2/', 6xHis-3xHA-DPB11::KanMX'	YSG858 x YSG862 0Colony G
YSG870	p	ho::LYS2, lys2, ura3, arg4-nsp, leu2::hisG, his4X::LEU2, nuc1::LEU2, 6xHis-3xHA-DPB11::KanMX	YSG4 Transformation Colony A
YSG871	a	ho::LYS2, lys2, ura3, leu2::hisG, trp1::hisG, CEN8::tdTomato-LEU2, KanMX::pCLB2-3HA-MEC1, pCLB2-3HA-DPB11::KanMX	YSG678xYSG791 Colony A3
YSG872	p	ho::LYS2, lys2, ura3, leu2::hisG, trp1::hisG, THR1::mCerulean-TRP1, KanMX::pCLB2-3HA-MEC1, pCLB2-3HA-DPB11::KanMX	YSG678xYSG791 Colony A1
YSG873	a	ho::LYS2, lys2, ura3, arg4-nsp, leu2::hisG, his4X::LEU2, nuc1::LEU2, 6xHis-3xHA-DPB11::KanMX	YSG870xYSG4 Colony B2
YSG874	p	ho::LYS2, lys2, ura3, arg4-nsp, leu2::hisG, his4X::LEU2, nuc1::LEU2, 6xHis-3xHA-DPB11::KanMX	YSG870xYSG4 Colony C2
YSG875	a	ho::LYS2, lys2, ura3, arg4-nsp, leu2::hisG, his4X::LEU2, nuc1::LEU2, 6xHis-3xHA-DPB11::KanMX	YSG870xYSG4 Colony C4
YSG876	p	ho::LYS2, lys2, ura3, arg4-nsp, leu2::hisG, his4X::LEU2, nuc1::LEU2, 6xHis-3xHA-DPB11::KanMX	YSG870xYSG4 Colony C5
YSG877	a/p	ho::LYS2/', lys2/', ura3/', arg4-nsp/', leu2::hisG/', his4X::LEU2/', nuc1::LEU2/', pCLB2-3HA-DPB11::KanMX/'	YSG793xYSG794 Colony A
YSG878	a/p	ho::LYS2/', lys2/', ura3/', arg4-nsp/', leu2::hisG/', his4X::LEU2/', nuc1::LEU2/', pCLB2-3HA-DPB11::KanMX/'	YSG793xYSG794 Colony B
YSG879	a/p	ho::LYS2/', lys2/', ura3/', arg4-nsp/', leu2::hisG/', his4X::LEU2/', nuc1::LEU2/', pCLB2-3HA-DPB11::KanMX/'	YSG793xYSG794 Colony C
YSG880	a/p	ho::LYS2/', lys2/', ura3/', arg4-nsp/', leu2::hisG/', his4X::LEU2/', nuc1::LEU2/', pCLB2-3HA-DPB11::KanMX/'	YSG793xYSG794 Colony D
YSG881	a/p	ho::LYS2/', lys2/', ura3/', arg4-nsp/', leu2::hisG/', his4X::LEU2/', nuc1::LEU2/', pCLB2-3HA-DPB11::KanMX/'	YSG793xYSG794 Colony E
YSG882	a/p	ho::LYS2/', lys2/', ura3/', arg4-nsp/', leu2::hisG/', his4X::LEU2/', nuc1::LEU2/', pCLB2-3HA-DPB11::KanMX/'	YSG793xYSG794 Colony F
YSG883	a/p	ho::LYS2/', lys2/', ura3/', arg4-nsp/', leu2::hisG/', his4X::LEU2/', nuc1::LEU2/', pCLB2-3HA-DPB11::KanMX/'	YSG793xYSG795 Colony A
YSG884	a/p	ho::LYS2/', lys2/', ura3/', arg4-nsp/', leu2::hisG/', his4X::LEU2/', nuc1::LEU2/', pCLB2-3HA-DPB11::KanMX/'	YSG793xYSG795 Colony B
YSG885	a/p	ho::LYS2/', lys2/', ura3/', arg4-nsp/', leu2::hisG/', his4X::LEU2/', nuc1::LEU2/', pCLB2-3HA-DPB11::KanMX/'	YSG793xYSG795 Colony C
YSG886	a/p	ho::LYS2/', lys2/', ura3/', arg4-nsp/', leu2::hisG/', his4X::LEU2/', nuc1::LEU2/', pCLB2-3HA-DPB11::KanMX/'	YSG793xYSG795 Colony D
YSG887	a/p	ho::LYS2/', lys2/', ura3/', arg4-nsp/', leu2::hisG/', his4X::LEU2/', nuc1::LEU2/', pCLB2-3HA-DPB11::KanMX/'	YSG793xYSG795 Colony E
YSG888	a/p	ho::LYS2/', lys2/', ura3/', arg4-nsp/', leu2::hisG/', his4X::LEU2/', nuc1::LEU2/', pCLB2-3HA-DPB11::KanMX/'	YSG793xYSG795 Colony F
YSG889	a/p	ho::LYS2/', lys2/', ura3/', arg4-nsp/', leu2::hisG/', his4X::LEU2/', nuc1::LEU2/'	YSG3xYSG4 Colony A
YSG890	a/p	ho::LYS2/', lys2/', ura3/', leu2::hisG/', trp1::hisG/', THR1::mCerulean-TRP1/THR1, CEN8::tdTomato-LEU2/CEN8	YSG29xYSG33 Colony D
YSG891	a/p	ho::LYS2/', lys2/', ura3/', arg4-nsp/', leu2::hisG/', his4X::LEU2/', nuc1::LEU2/'	YSG3xYSG4 Colony E
YSG892	a/p	ho::LYS2/', lys2/', ura3/', arg4-nsp/', leu2::hisG/', his4X::LEU2/', nuc1::LEU2/', 6xHis-3xHA-DPB11::KanMX/'	YSG875xYSG876 Colony A
YSG893	a/p	ho::LYS2/', lys2/', ura3/', arg4-nsp/', leu2::hisG/', his4X::LEU2/', nuc1::LEU2/', 6xHis-3xHA-DPB11::KanMX/'	YSG875xYSG876 Colony B
YSG894	a/p	ho::LYS2/', lys2/', ura3/', arg4-nsp/', leu2::hisG/', his4X::LEU2/', nuc1::LEU2/', 6xHis-3xHA-DPB11::KanMX/'	YSG875xYSG876 Colony C
YSG895	a/p	ho::LYS2/', lys2/', ura3/', arg4-nsp/', leu2::hisG/', his4X::LEU2/', nuc1::LEU2/', 6xHis-3xHA-DPB11::KanMX/'	YSG873xYSG874 Colony A
YSG896	a/p	ho::LYS2/', lys2/', ura3/', leu2::hisG/', trp1::hisG/', THR1::mCerulean-TRP1/THR1, CEN8::tdTomato-LEU2/CEN8, pCLB2-3HA-MEC1::KanMX/'	YSG790xYSG791
YSG928	a	ho::LYS2, lys2, ura3, arg4-nsp, leu2::hisG, his4X::LEU2, nuc1::LEU2, 6xHis-3xHA-DPB11::KanMX, KanMX::pCLB2-3HA-MEC1	YSG858xYSG15 Colony

YSG929	p	ho::LYS2, lys2, ura3, arg4-nsp, leu2::hisG, his4X::LEU2, nuc1::LEU2, 6xHis-3xHA-DPB11::KanMX, KanMX::pCLB2-3HA-MEC1	YSG858xYSG15 Colony
YSG930	a/p	ho::LYS2/', lys2/', ura3/', arg4-nsp/', leu2::hisG/', his4X::LEU2/', nuc1::LEU2/'	YSG5 Duplicate Colony A
YSG931	a/p	ho::LYS2/', lys2/', ura3/', arg4-nsp/', leu2::hisG/', his4X::LEU2/', nuc1::LEU2/'	YSG5 Duplicate Colony B
YSG932	a/p	ho::LYS2/', lys2/', ura3/', arg4-nsp/', leu2::hisG/', his4X::LEU2/', nuc1::LEU2/'	YSG5 Duplicate Colony D
YSG933	a/p	ho::LYS2/', lys2/', ura3/', arg4-nsp/', leu2::hisG/', his4X::LEU2/', nuc1::LEU2/'	YSG5 Duplicate Colony E
YSG934	a/p	ho::LYS2/', lys2/', ura3/', leu2::hisG/', trp1::hisG/', THR1::mCerulean-TRP1/THR1, CEN8::tdTomato-LEU2/CEN8	YSG236 Duplicate Colony A
YSG935	a/p	ho::LYS2/', lys2/', ura3/', leu2::hisG/', trp1::hisG/', THR1::mCerulean-TRP1/THR1, CEN8::tdTomato-LEU2/CEN8	YSG236 Duplicate Colony B
YSG936	a/p	ho::LYS2/', lys2/', ura3/', leu2::hisG/', trp1::hisG/', THR1::mCerulean-TRP1/THR1, CEN8::tdTomato-LEU2/CEN8	YSG236 Duplicate Colony C
YSG937	a/p	ho::LYS2/', lys2/', ura3/', leu2::hisG/', trp1::hisG/', THR1::mCerulean-TRP1/THR1, CEN8::tdTomato-LEU2/CEN8	YSG236 Duplicate Colony D
YSG938	a/p	ho::LYS2/', lys2/', ura3/', leu2::hisG/', trp1::hisG/', THR1::mCerulean-TRP1/THR1, CEN8::tdTomato-LEU2/CEN8	YSG236 Duplicate Colony F
YSG939	a/p	ho::LYS2/', lys2/', ura3/', leu2::hisG/', trp1::hisG/', THR1::mCerulean-TRP1/THR1, CEN8::tdTomato-LEU2/CEN8, pCLB2-3HA-DPB11::KanMX/', KanMX::pCLB2-3HA-MEC1/'	YSG871xYSG872 Colony A
YSG940	a/p	ho::LYS2/', lys2/', ura3/', leu2::hisG/', trp1::hisG/', THR1::mCerulean-TRP1/THR1, CEN8::tdTomato-LEU2/CEN8, pCLB2-3HA-DPB11::KanMX/', KanMX::pCLB2-3HA-MEC1/'	YSG871xYSG872 Colony B
YSG941	a/p	ho::LYS2/', lys2/', ura3/', leu2::hisG/', trp1::hisG/', THR1::mCerulean-TRP1/THR1, CEN8::tdTomato-LEU2/CEN8, pCLB2-3HA-DPB11::KanMX/', KanMX::pCLB2-3HA-MEC1/'	YSG871xYSG872 Colony C
YSG942	a/p	ho::LYS2/', lys2/', ura3/', leu2::hisG/', trp1::hisG/', THR1::mCerulean-TRP1/THR1, CEN8::tdTomato-LEU2/CEN8, pCLB2-3HA-DPB11::KanMX/', KanMX::pCLB2-3HA-MEC1/'	YSG871xYSG872 Colony D
YSG943	a/p	ho::LYS2/', lys2/', ura3/', leu2::hisG/', trp1::hisG/', THR1::mCerulean-TRP1/THR1, CEN8::tdTomato-LEU2/CEN8, pCLB2-3HA-DPB11::KanMX/', KanMX::pCLB2-3HA-MEC1/'	YSG871xYSG872 Colony E
YSG963	a	ho::LYS2, lys2, ura3, arg4-nsp, leu2::hisG, his4X::LEU2, nuc1::LEU2, DPB11-6xHis-3xHA::KanMX	YSG3 DPB11 Tag Transformation A
YSG964	a	ho::LYS2, lys2, ura3, arg4-nsp, leu2::hisG, his4X::LEU2, nuc1::LEU2, DPB11-6xHis-3xHA::KanMX	YSG3 DPB11 Tag Transformation B
YSG965	p	ho::LYS2, lys2, ura3, arg4-nsp, leu2::hisG, his4X::LEU2, nuc1::LEU2, DPB11-6xHis-3xHA::KanMX	YSG4 DPB11 Tag Transformation A
YSG966	p	ho::LYS2, lys2, ura3, arg4-nsp, leu2::hisG, his4X::LEU2, nuc1::LEU2, DPB11-6xHis-3xHA::KanMX	YSG4 DPB11 Tag Transformation B
YSG967	a	ho::LYS2, lys2, ura3, leu2::hisG, trp1::hisG, THR1::mCerulean-TRP1, DPB11-6xHis-3xHA::KanMX	YSG29 DPB11 Tag Transformation A
YSG968	a	ho::LYS2, lys2, ura3, leu2::hisG, trp1::hisG, THR1::mCerulean-TRP1, DPB11-6xHis-3xHA::KanMX	YSG29 DPB11 Tag Transformation B
YSG969	p	ho::LYS2, lys2, ura3, leu2::hisG, trp1::hisG, CEN8::tdTomato-LEU2, DPB11-6xHis-3xHA::KanMX	YSG33 DPB11 Tag Transformation B
YSG970	a	ho::LYS2, lys2, ura3, arg4-nsp, leu2::hisG, his4X::LEU2, nuc1::LEU2, DPB11-6xHis-3xHA::KanMX	YSG3 pCLB2-DPB11 Tag Transformation B
YSG971	a	ho::LYS2, lys2, ura3, leu2::hisG, trp1::hisG, THR1::mCerulean-TRP1, pCLB2-3HA-DPB11::KanMX	YSG29 pCLB2-DPB11 Tag Transformation A
YSG972	a	ho::LYS2, lys2, ura3, leu2::hisG, trp1::hisG, THR1::mCerulean-TRP1, 6xHis-3xHA-DPB11::KanMX	YSG29 Tag DPB11 Transformation A
YSG973	a	ho::LYS2, lys2, ura3, leu2::hisG, trp1::hisG, THR1::mCerulean-TRP1, 6xHis-3xHA-DPB11::KanMX	YSG972 x 33 'C1'
YSG974	p	ho::LYS2, lys2, ura3, leu2::hisG, trp1::hisG, CEN8::tdTomato-LEU2, 6xHis-3xHA-DPB11::KanMX	YSG972 x 33 'D3'
YSG975	a/p	ho::LYS2/', lys2/', ura3/', leu2::hisG/', trp1::hisG/', THR1::mCerulean-TRP1/THR1, CEN8::tdTomato-LEU2/CEN8, 6xHis-3xHA-DPB11::KanMX	YSG973 x YSG974 Colony 1
YSG976	a/p	ho::LYS2/', lys2/', ura3/', leu2::hisG/', trp1::hisG/', THR1::mCerulean-TRP1/THR1, CEN8::tdTomato-LEU2/CEN9, 6xHis-3xHA-DPB11::KanMX	YSG973 x YSG974 Colony 2
YSG977	a/p	ho::LYS2/', lys2/', ura3/', arg4-nsp/', leu2::hisG/', his4X::LEU2/', nuc1::LEU2/', DPB11-6xHis-3xHA::KanMX	YSG963 x YSG965
984	p	ho::LYS2, lys2, ura3, arg4-nsp, leu2::hisG, his4X::LEU2, nuc1::LEU2, pCLB2 DPB11-6xHis-3xHA::KanMX	YSG4 pCLB2-DPB11 Tag Transformation E

985	a	ho::LYS2, lys2, ura3, arg4-nsp, leu2::hisG, his4X::LEU2, nuc1::LEU2, DPB11-6xHis-3xHA::KanMX, pCLB2-3HA-MEC1::KanMX	YSG789 x 965 'C3'
986	p	ho::LYS2, lys2, ura3, arg4-nsp, leu2::hisG, his4X::LEU2, nuc1::LEU2, DPB11-6xHis-3xHA::KanMX, pCLB2-3HA-MEC1::KanMX	YSG789 x 965 'C2'
987	a	ho::LYS2, lys2, ura3, arg4-nsp, leu2::hisG, his4X::LEU2, nuc1::LEU2, pCLB2-3HA-DPB11::KanMX, pCLB2-3HA-MEC1::KanMX	789 x 794 'G1'
988	p	ho::LYS2, lys2, ura3, arg4-nsp, leu2::hisG, his4X::LEU2, nuc1::LEU2, pCLB2-3HA-DPB11::KanMX, pCLB2-3HA-MEC1::KanMX	789 x 794 'G3'
989	a	ho::LYS2, lys2, ura3, arg4-nsp, leu2::hisG, his4X::LEU2, nuc1::LEU2, pCLB2 DPB11-6xHis-3HA::KanMX, pCLB2-3HA-MEC1::KanMX	789 x 984 'H1'
990	p	ho::LYS2, lys2, ura3, arg4-nsp, leu2::hisG, his4X::LEU2, nuc1::LEU2, pCLB2 DPB11-6xHis-3HA::KanMX, pCLB2-3HA-MEC1::KanMX	789 x 984 'H4'
991	p	ho::LYS2, lys2, ura3, arg4-nsp, leu2::hisG, his4X::LEU2, nuc1::LEU2, pCLB2 DPB11-6xHis-3HA::KanMX, pCLB2-3HA-MEC1::KanMX	789 x 984 'F1'
992	a	ho::LYS2, lys2, ura3, leu2::hisG, trp1::hisG, THR1::mCerulean-TRP1, pCLB2 DPB11-6xHis-3xHA::KanMX	971 x 33 'C3 '
993	p	ho::LYS2, lys2, ura3, leu2::hisG, trp1::hisG, CEN8::tdTomato-LEU2, pCLB2 DPB11-6xHis-3xHA::KanMX	971 x 33 'A2'
994	a	ho::LYS2, lys2, ura3, leu2::hisG, trp1::hisG, THR1::mCerulean-TRP1, 6xHis-3xHA-DPB11::KanMX, pCLB2-3HA-MEC1::KanMX	790 x 974 'K4'
995	p	ho::LYS2, lys2, ura3, leu2::hisG, trp1::hisG, CEN8::tdTomato-LEU2, 6xHis-3xHA-DPB11::KanMX, pCLB2-3HA-MEC1::KanMX	790 x 974 'K3'
996	a	ho::LYS2, lys2, ura3, leu2::hisG, trp1::hisG, THR1::mCerulean-TRP1, DPB11-6xHis-3xHA::KanMX, pCLB2-3HA-MEC1::KanMX	790 x 969 'G2'
997	p	ho::LYS2, lys2, ura3, leu2::hisG, trp1::hisG, CEN8::tdTomato-LEU2, DPB11-6xHis-3xHA::KanMX, pCLB2-3HA-MEC1::KanMX	790 x 969 'G1'
998	a	ho::LYS2, lys2, ura3, leu2::hisG, trp1::hisG, THR1::mCerulean-TRP1, pCLB2 DPB11-6xHis-3HA::KanMX, pCLB2-3HA-MEC1::KanMX	790 x 993 'B3'
999	p	ho::LYS2, lys2, ura3, leu2::hisG, trp1::hisG, CEN8::tdTomato-LEU2, pCLB2 DPB11-6xHis-3HA::KanMX, pCLB2-3HA-MEC1::KanMX	790 x 993 'B4'
1000	a/p	ho::LYS2/', lys2/', ura3/', arg4-nsp/', leu2::hisG/', his4X::LEU2/', nuc1::LEU2/', DPB11-6xHis-3xHA::KanMX/'	963 x 965 A
1001	a/p	ho::LYS2/', lys2/', ura3/', arg4-nsp/', leu2::hisG/', his4X::LEU2/', nuc1::LEU2/', DPB11-6xHis-3xHA::KanMX/'	963 x 965 B
1002	a/p	ho::LYS2/', lys2/', ura3/', arg4-nsp/', leu2::hisG/', his4X::LEU2/', nuc1::LEU2/', DPB11-6xHis-3xHA::KanMX/'	963 x 965 C
1003	a/p	ho::LYS2/', lys2/', ura3/', arg4-nsp/', leu2::hisG/', his4X::LEU2/', nuc1::LEU2/', DPB11-6xHis-3xHA::KanMX/'	964 x 965 A
1004	a/p	ho::LYS2/', lys2/', ura3/', arg4-nsp/', leu2::hisG/', his4X::LEU2/', nuc1::LEU2/', DPB11-6xHis-3xHA::KanMX/'	964 x 965 B
1005	a/p	ho::LYS2/', lys2/', ura3/', arg4-nsp/', leu2::hisG/', his4X::LEU2/', nuc1::LEU2/', DPB11-6xHis-3xHA::KanMX/'	964 x 965 C
1006	a/p	ho::LYS2/', lys2/', ura3/', arg4-nsp/', leu2::hisG/', his4X::LEU2/', nuc1::LEU2/', pCLB2 DPB11-6xHis-3HA::KanMX/'	970 x 984 A
1007	a/p	ho::LYS2/', lys2/', ura3/', arg4-nsp/', leu2::hisG/', his4X::LEU2/', nuc1::LEU2/', pCLB2 DPB11-6xHis-3HA::KanMX/'	970 x 984 B
1008	a/p	ho::LYS2/', lys2/', ura3/', arg4-nsp/', leu2::hisG/', his4X::LEU2/', nuc1::LEU2/', pCLB2 DPB11-6xHis-3HA::KanMX/'	970 x 984 C
1009	a/p	ho::LYS2/', lys2/', ura3/', arg4-nsp/', leu2::hisG/', his4X::LEU2/', nuc1::LEU2/', 6xHis-3xHA-DPB11::KanMX/', pCLB2-3HA-MEC1::KanMX/'	928 x 929 A
1010	a/p	ho::LYS2/', lys2/', ura3/', arg4-nsp/', leu2::hisG/', his4X::LEU2/', nuc1::LEU2/', 6xHis-3xHA-DPB11::KanMX/', pCLB2-3HA-MEC1::KanMX/'	928 x 929 B
1011	a/p	ho::LYS2/', lys2/', ura3/', arg4-nsp/', leu2::hisG/', his4X::LEU2/', nuc1::LEU2/', 6xHis-3xHA-DPB11::KanMX/', pCLB2-3HA-MEC1::KanMX	928 x 929 C
1012	a/p	ho::LYS2/', lys2/', ura3/', arg4-nsp/', leu2::hisG/', his4X::LEU2/', nuc1::LEU2/',DPB11-6xHis-3xHA::KanMX/', pCLB2-3HA-MEC1::KanMX/'	985 x 986 A
1013	a/p	ho::LYS2/', lys2/', ura3/', arg4-nsp/', leu2::hisG/', his4X::LEU2/', nuc1::LEU2/',DPB11-6xHis-3xHA::KanMX/', pCLB2-3HA-MEC1::KanMX/'	985 x 986 B
1014	a/p	ho::LYS2/', lys2/', ura3/', arg4-nsp/', leu2::hisG/', his4X::LEU2/', nuc1::LEU2/',DPB11-6xHis-3xHA::KanMX/', pCLB2-3HA-MEC1::KanMX/'	985 x 986 C
1015	a/p	ho::LYS2/', lys2/', ura3/', arg4-nsp/', leu2::hisG/', his4X::LEU2/', nuc1::LEU2/',DPB11-6xHis-3xHA::KanMX/', pCLB2-3HA-MEC1::KanMX/'	985 x 986 D
1016	a/p	ho::LYS2/', lys2/', ura3/', arg4-nsp/', leu2::hisG/', his4X::LEU2/', nuc1::LEU2/',DPB11-6xHis-3xHA::KanMX/', pCLB2-3HA-MEC1::KanMX/'	985 x 986 E

1017	a/p	ho::LYS2/', lys2/', ura3/', arg4-nsp/', leu2::hisG/', his4X::LEU2/', nuc1::LEU2/', pCLB2-3HA-DPB11::KanMX/', pCLB2-3HA-MEC1::KanMX/'	987 x 988 A
1018	a/p	ho::LYS2/', lys2/', ura3/', arg4-nsp/', leu2::hisG/', his4X::LEU2/', nuc1::LEU2/', pCLB2-3HA-DPB11::KanMX/', pCLB2-3HA-MEC1::KanMX/'	987 x 988 B
1019	a/p	ho::LYS2/', lys2/', ura3/', arg4-nsp/', leu2::hisG/', his4X::LEU2/', nuc1::LEU2/', pCLB2-3HA-DPB11::KanMX/', pCLB2-3HA-MEC1::KanMX/'	987 x 988 C
1020	a/p	ho::LYS2/', lys2/', ura3/', arg4-nsp/', leu2::hisG/', his4X::LEU2/', nuc1::LEU2/', pCLB2 DPB11-6xHis-3HA::KanMX/', pCLB2-3HA-MEC1::KanMX/'	989 x 990 A
1021	a/p	ho::LYS2/', lys2/', ura3/', arg4-nsp/', leu2::hisG/', his4X::LEU2/', nuc1::LEU2/', pCLB2 DPB11-6xHis-3HA::KanMX/', pCLB2-3HA-MEC1::KanMX/'	989 x 990 B
1022	a/p	ho::LYS2/', lys2/', ura3/', arg4-nsp/', leu2::hisG/', his4X::LEU2/', nuc1::LEU2/', pCLB2 DPB11-6xHis-3HA::KanMX/', pCLB2-3HA-MEC1::KanMX/'	989 x 990 C
1023	a/p	ho::LYS2/', lys2/', ura3/', leu2::hisG/', trp1::hisG/', THR1::mCerulean-TRP1/THR1, CEN8::tdTomato-LEU2/CEN8, 6xHis-3xHA-DPB11::KanMX/'	973 x 974 A
1024	a/p	ho::LYS2/', lys2/', ura3/', leu2::hisG/', trp1::hisG/', THR1::mCerulean-TRP1/THR1, CEN8::tdTomato-LEU2/CEN8, 6xHis-3xHA-DPB11::KanMX/'	973 x 974 B
1025	a/p	ho::LYS2/', lys2/', ura3/', leu2::hisG/', trp1::hisG/', THR1::mCerulean-TRP1/THR1, CEN8::tdTomato-LEU2/CEN8, 6xHis-3xHA-DPB11::KanMX/'	973 x 974 C
1026	a/p	ho::LYS2/', lys2/', ura3/', leu2::hisG/', trp1::hisG/', THR1::mCerulean-TRP1/THR1, CEN8::tdTomato-LEU2/CEN8, 6xHis-3xHA-DPB11::KanMX/'	973 x 974 D
1027	a/p	ho::LYS2/', lys2/', ura3/', leu2::hisG/', trp1::hisG/', THR1::mCerulean-TRP1/THR1, CEN8::tdTomato-LEU2/CEN8, 6xHis-3xHA-DPB11::KanMX/'	973 x 974 E
1028	a/p	ho::LYS2/', lys2/', ura3/', leu2::hisG/', trp1::hisG/', THR1::mCerulean-TRP1/THR1, CEN8::tdTomato-LEU2/CEN8, 6xHis-3xHA-DPB11::KanMX/'	973 x 974 F
1029	a/p	ho::LYS2/', lys2/', ura3/', leu2::hisG/', trp1::hisG/', THR1::mCerulean-TRP1/THR1, CEN8::tdTomato-LEU2/CEN8, DPB11-6xHis-3xHA::KanMX/'	968 x 969 A
1030	a/p	ho::LYS2/', lys2/', ura3/', leu2::hisG/', trp1::hisG/', THR1::mCerulean-TRP1/THR1, CEN8::tdTomato-LEU2/CEN8, DPB11-6xHis-3xHA::KanMX/'	968 x 969 B
1031	a/p	ho::LYS2/', lys2/', ura3/', leu2::hisG/', trp1::hisG/', THR1::mCerulean-TRP1/THR1, CEN8::tdTomato-LEU2/CEN8, DPB11-6xHis-3xHA::KanMX/'	968 x 969 C
1032	a/p	ho::LYS2/', lys2/', ura3/', leu2::hisG/', trp1::hisG/', THR1::mCerulean-TRP1/THR1, CEN8::tdTomato-LEU2/CEN8, pCLB2 DPB11-6xHis-3xHA::KanMX/'	992 x 993 A
1033	a/p	ho::LYS2/', lys2/', ura3/', leu2::hisG/', trp1::hisG/', THR1::mCerulean-TRP1/THR1, CEN8::tdTomato-LEU2/CEN8, pCLB2 DPB11-6xHis-3xHA::KanMX/'	992 x 993 B
1034	a/p	ho::LYS2/', lys2/', ura3/', leu2::hisG/', trp1::hisG/', THR1::mCerulean-TRP1/THR1, CEN8::tdTomato-LEU2/CEN8, pCLB2 DPB11-6xHis-3xHA::KanMX/'	992 x 993 C

2.1.2 Plasmids

2.1.2.1 pSG11

pSG11 consists of various features useful in *S. cerevisiae* and *E. coli* research. Kanamycin (KanMX) and Ampicillin (AmpR) resistance genes enable strain selection, whilst 6xHis-3HA is a tag used to characterise protein expression in Western Blots (2.2.7.4). The *NdeI* and *SacI* restriction enzyme cut sites allow the separation of the plasmid backbone region consisting of the high-copy-number ColE1/pMB1/pUC/pBR322 origin of replication (Ori), T7 promotor and AmpR gene for plasmid creation.

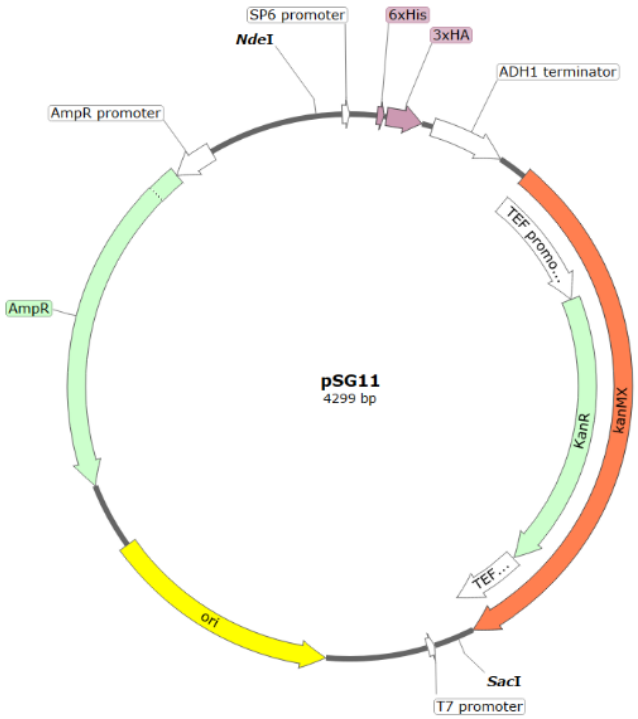

Figure 2.1: pSG11 plasmid.

2.1.2.2 tag-dpb11

The pre-existing N-terminal tagged Dpb11 plasmid consists of Dpb11 upstream and downstream homology regions, the KanMX selection marker within the transformation cassette and the Dpb11 start codon situated before the 6xHis-3HA tag on the N terminal region of the Dpb11 gene. The plasmid backbone contains the Ori, AmpR selection gene.

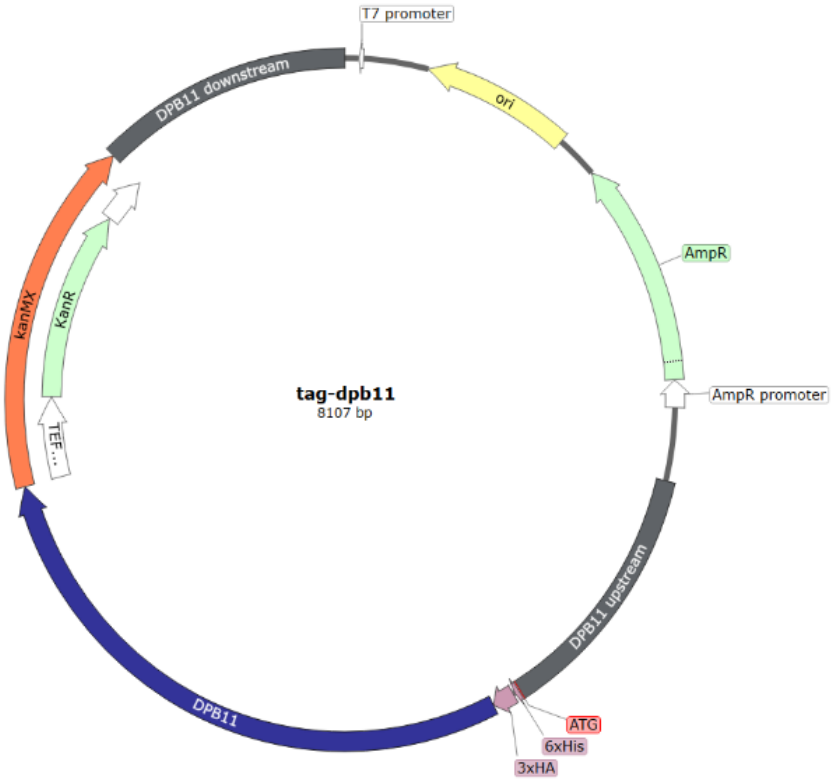

Figure 2.2: *tag-dpb11* plasmid. N-terminally tagged Dpb11 construct.

2.1.2.3 tag-dpb11-md

Identical to the *tag-dpb11* plasmid (2.1.2.2), but with the insertion of the Clb2 promotor region before the start codon to deplete Dpb11 expression during meiosis.

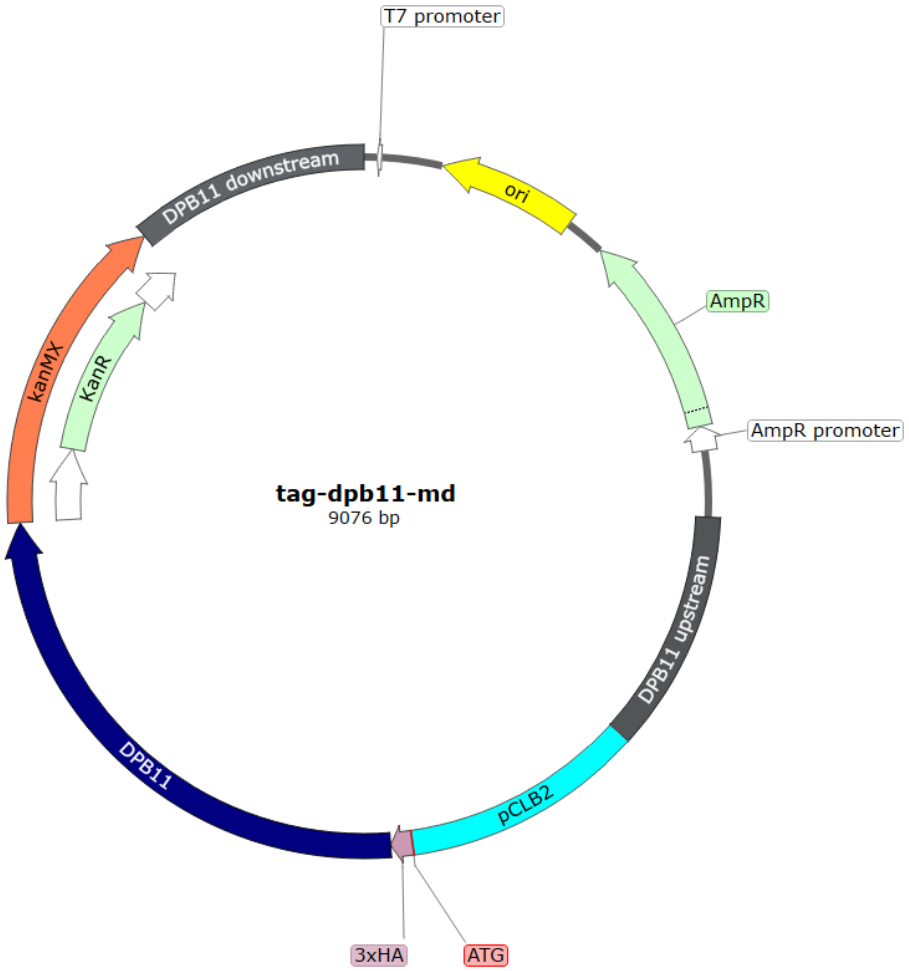

Figure 2.3: *tag-dpb11-md* plasmid. Pre-existing meiotic depleted N-terminally tagged Dpb11 construct.

2.1.2.4 dpb11-tag

The *dpb11-tag* plasmid was constructed using the *tag-dpb11* plasmid (2.1.2.2) as a base. The 6xHis-3HA tag was transferred from the N-terminal region to the C-terminus.

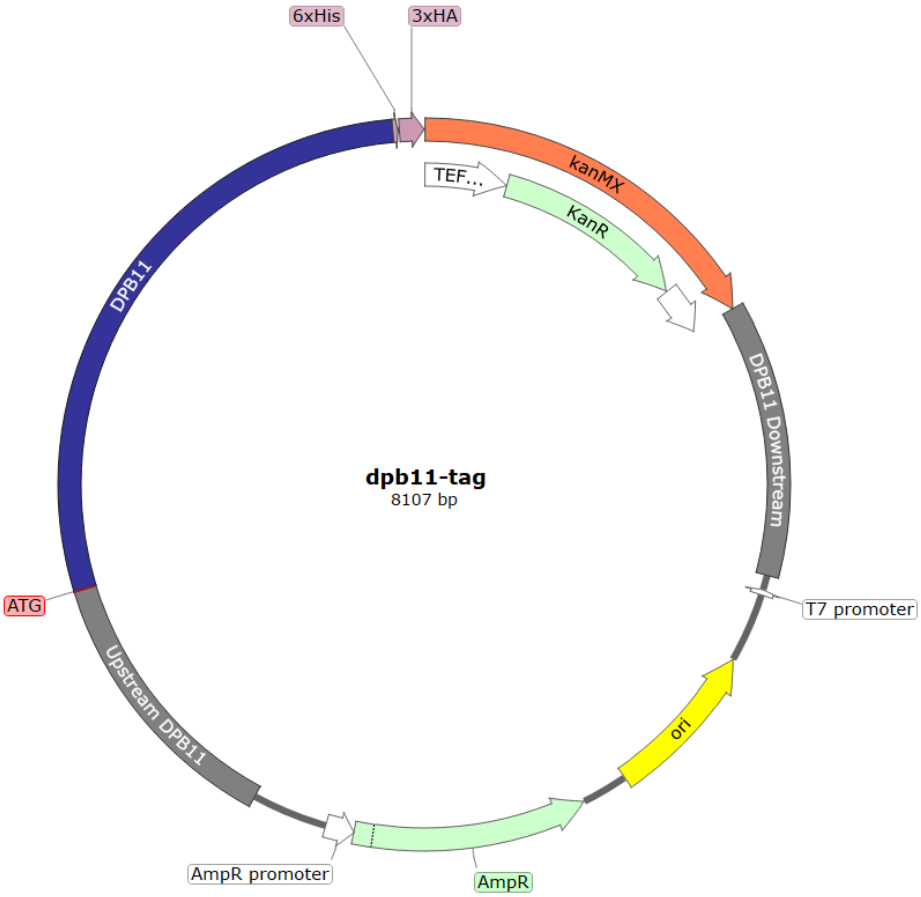

Figure 2.4: *dpb11-tag* plasmid. C-terminally tagged Dpb11 construct.

2.1.2.5 dpb11-tag-md A

The meiotic-depleted *dpb11-tag* (*dpb11-tag-md*) plasmid A was constructed using *tag-dpb11-md (2.1.2.3*) as a base. Construction issues outlined in (Figure 3.10) resulted in halting development and looking for a new method.

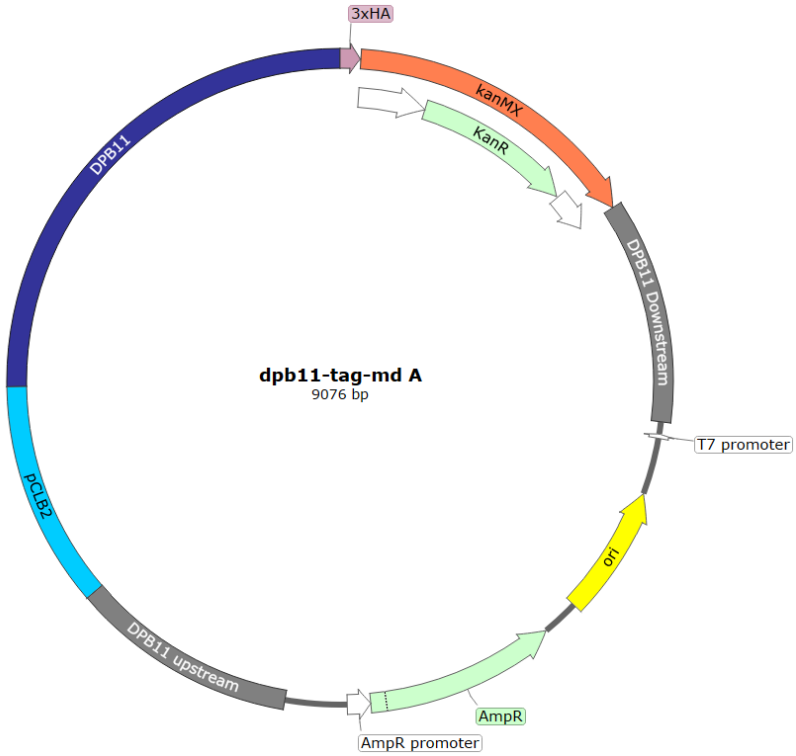

Figure 2.5: *dpb11-tag-md* plasmid A. The first meiotic-depleted N-terminally tagged Dpb11 construct.

2.1.2.6 *dpb11-tag-md* B

Following the issues with constructing *dpb11-tag-md* A (2.1.2.5), a new method was developed using the newly constructed *dpb11-tag* (2.1.2.4) plasmid as a base.

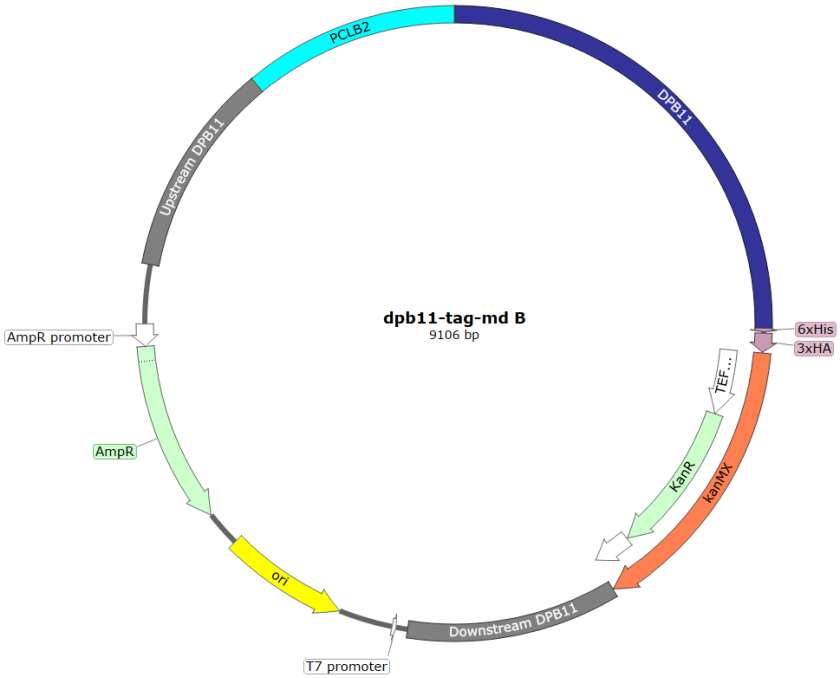

Figure 2.6: *dpb11-tag-md B* plasmid. The second meiotic-depleted N-terminally tagged construct.

2.1.2.7 *tag-mec1* A

The initial N-terminally tagged Mec1 plasmid was designed and created similarly to *tag-dpb11* (2.1.2.2) with the complete downstream and upstream regions acting as homology, the complete Mec1 gene, KanMX selection marker and a base plasmid backbone. Low levels of the Mec1 fragment resulted in the creation of *tag-mec1* B.

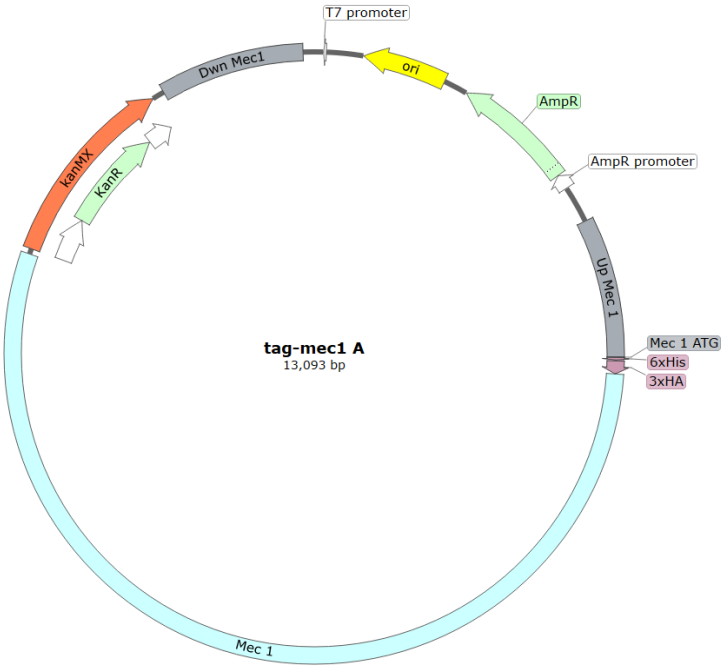

Figure 2.7: *tag-mec1* A plasmid. The first N-terminal tagged Mec1 construct.

2.1.2.8 *tag mec1* B

Since the large Mec1 fragment did not amplify successfully, a second *tag-mec1* plasmid was designed to split the Mec1 fragment into two smaller fragments. One of the fragments continued to not PCR amplify, so a new method was chosen.

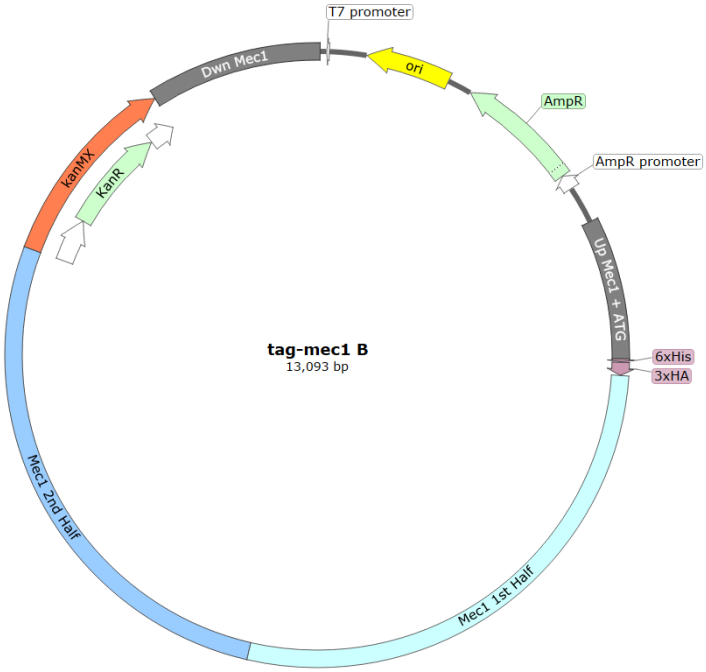

Figure 2.8: *tag mec1* plasmid B. The second N-terminal tagged Mec1 construct.

2.1.2.9 *tag mec1* C

The third N-terminal tagged Mec1 plasmid used Mec1 upstream and the first half of Mec1 as homology; however, the insertion of KanMX between the upstream region and Mec1 ATG would have impacted Mec1 expression. Subsequently, the construction was stopped (See 2.1.2.9).

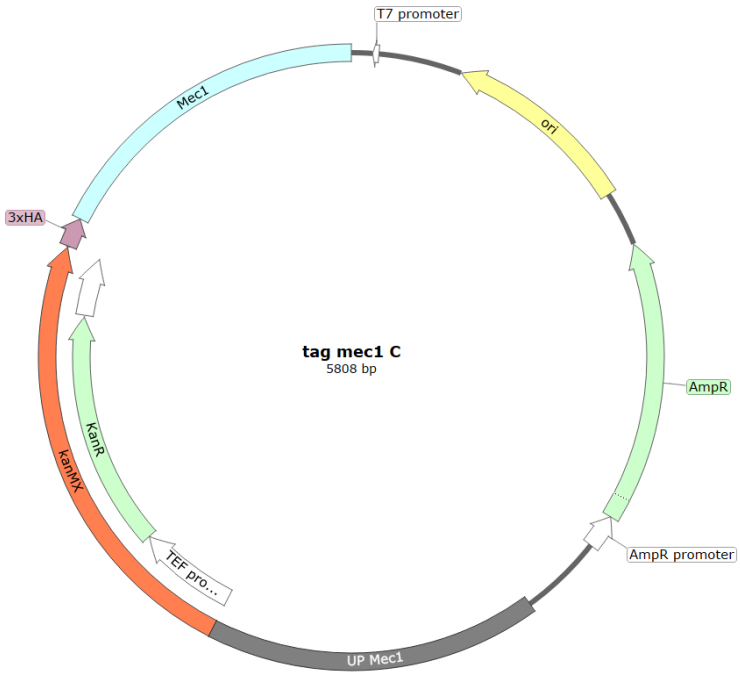

Figure 2.9: *tag mec1* plasmid C. The third N-terminal tagged Mec1 construct.

2.1.2.10 mec1-tag

Following the issues regarding *tag tec1,* it was decided to tag Mec1 C-terminally to avoid any issues. The final 1 kb of Mec1 alongside downstream Mec1 was used as homology (See 2.1.2.10)

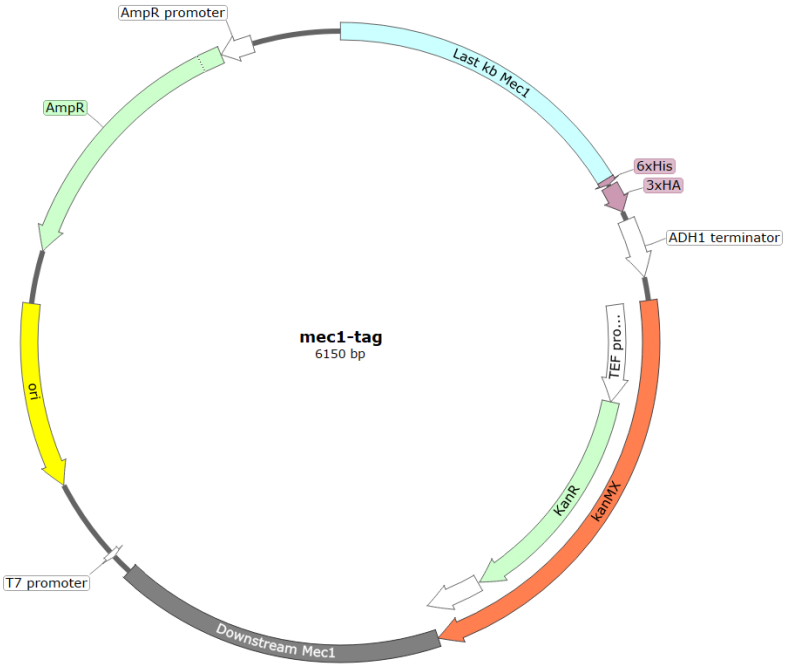

Figure 2.10: *mec1-tag* plasmid. The first C-terminal tagged Mec1 construct.

2.1.3 Primers

Table 2-2: Catalogue of primers.

Primer Number	Primer Name	Sequence
84	MEC1_F-1366	TGTATAAAAGAAGAGGAACGTCCGC
85	MEC1_R+79	GCACCTTTGAATCCACCCCC
590	KanCheckR	GGAATCGAATGCAACCGGCGC
851	TagDPB11_fwd	CGCTGCTCAGAAGCCCTTTCAAGGAATAAC
854	kanMX_rev	GGACTACATTCAGTATAGCGACCAGCATTC
921	DPB11 wholeseq_fwd	TCGAGGGAATAAGACCTGCC
922	DPB11 wholeseq_rev	GGAGCCATTCTTGTGACGGG
951	DPB11 backbone (pCLB2)_fwd	AGATTACGCTGCTCAGAAGCCCTTTCAAG
952	DPB11 backbone (pCLB2)_rev	AGAACAGGGTAGTAATATTAATGCTGCTGATAAAATAC
953	pCLB2-3HA 2_fwd	TAATATTACTACCCTGTTCTTGACGGTC
954	pCLB2-3HA 2_rev	GCTTCTGAGCAGCGTAATCTGGAACGTC
955	DPB11 Diagnostic PCR fwd	CCGCTTCGCATACGGCGGTG
956	DPB11 Diagnostic PCR rev	GGTGGACCCAACAACAAGGAC
1056	KanMX_fwd	GAAGACCGTTAGGACATGGAGGCCCAGAATAC
1057	KanMX_rev	GAGGAAATCTAGGCAGTATAGCGACCAGCATTC
1093	Up + Mec1 ATG_fwd	ATTGTACTGAGAGTGCACCAGGACAGCGGATGGCAGTAG
1094	Up + Mec1 ATG_rev	GATGATGATGCATGCAGTCTTGTGGGCC

1095	6His-3HA_fwd	AGACTGCATGCATCATCATCATCATCATATCTTTTAC
1096	6His-3HA_rev	CGTGTGATTCAGCGTAATCTGGAACGTC
1097	Mec1 + ~50bp Dwn_fwd	AGATTACGCTGAATCACACGTCAAATATCTTG
1098	Mec1 + ~50bp Dwn_rev	CCTCCATGTCATCAAGAGGAAGTTCGTC
1099	KanMX_fwd	TCCTCTTGATGACATGGAGGCCCAGAATAC
1100	KanMX_fwd	TCTGTTGCCGCAGTATAGCGACCAGCATTC
1101	Dwn Mec1_fwd	CGCTATACTGCGGCAACAGACGAACTTC
1102	Dwn Mec1_rev	ATCATCGATGAATTCGAGCTAGGAACTAATAGAACGATTGC
1133	Up MEC1 -503 fwd	AAAAGGCCGCTGAACTACGAGGC
1134	Dwn MEC1 +7577 rev	GTGCGAAACAAGCAATGCCC
1135	DPB11 +174 rev	TCGAATCTATGCTTCACCGC
1136	DPB11 +263 rev	TGTTGCCGTATTAGAGTCCGGC
1170	END+KanMX+Ori+AmpR+ATG_fwd	AGATTACGCTTGAGACATGGAGGCCCAG
1171	END+KanMX+Ori+AmpR+ATG_rev	GCTTCTGAGC CATAGTAATATTAATGCTGCTGATAAAATACCTG
1172	DPB11_fwd	TATTACTATGGCTCAGAAGCCCTTTCAAG
1173	DPB11_rev	GATGATGATGAGAATCTAATTCCTTTGTCTGATTTC
1174	6His-3HA_fwd	ATTAGATTCTCATCATCATCATCATCATATCTTTTAC
1175	6His-3HA_rev	CCATGTCTCAAGCGTAATCTGGAACGTC
1176	3HA_fwd	ATTAGATTCTTACCCATACGATGTTCCTG
1177	3HA_rev	CCATGTCTCAAGCGTAATCTGGAACGTC
1178	KanMX+Ori+AmpR+pCLB2_fwd	AGATTACGCTTGAGACATGGAGGCCCAG
1179	KanMX+Ori+AmpR+pCLB2_rev	GAAAGGGCTTCATCTATAAGATCAATGAAGAGAGAGAGG
1180	DPB11Tag_fwd	CTTATAGATGAAGCCCTTTCAAGGAATAAC
1190	Tag MEC1 CompleteSeq_Fwd	CTCGTGGTATGAGATAAATAAAGAATGGAG
1191	Tag MEC1 CompleteSeq_Rev	TATTAGTCAACTGCGTGAACGG
1192	KanMX +100bp_Rev	CGTAATTTTTGCTTCGCGCCGTGCGG
1203	DPB11-Tag.....Up DPB11_fwd	GATCTTATAGATGGCTCAGAAGCCCTTTC
1204	DPB11-Tag.....Up DPB11_rev	AAGAGCAAATGCGTTGAAAGAAACCTGG
1205	238bp Up DPB11 + pCLB2_fwd	CTTTCAACGCATTTGCTCTTTCCGCTTC
1206	238bp Up DPB11 + pCLB2_rev	TCTGAGCCATCTATAAGATCAATGAAGAGAGAG
1225	DPB11+2125_F	ATGTGCCTACAGAGCAGCCG
1226	Final 1kb of Mec1_fwd	ATTGTACTGAGAGTGCACCAGGGCTATCAACCATTTAG
1227	Final 1kb of Mec1_rev	GATGATGATGCCAAAATGGAAGCCAACC
1228	6His3HA + End + KanMX_fwd	TCCATTTTGGCATCATCATCATCATCATATCTTTTAC
1229	6His3HA + End + KanMX_rev	TGGAAAGTCGCAGTATAGCGACCAGCATTC
1230	Downstream Mec1_fwd	CGCTATACTGCGACTTTCCACCATTTTC
1231	Downstream Mec1_rev	ATCATCGATGAATTCGAGCTTACTTCCGCATTTCTTAC
-	MEC1-Tag CompleteSeq_Fwd	GGCTATCAACCATTTAGGCCGG
-	MEC1-Tag CompleteSeq_Rev	TACTTCCGCATTTCTTACGCA
-	MEC1-Tag NearCompleteSeq_Rev	GGTGCTGTGTATTTTTTCAAGGGC

2.1.4 Chemicals and enzymes

Chemicals and enzymes were purchased from a variety of sources and appropriately stored, © Thermo Fisher Scientific, © Bio-Rad Laboratories, Sigma-Aldrich® and New England Biolabs® as examples.

2.1.5 Media

2.1.5.1 YPD+ALU liquid media

Reagents

- YPD Powder
- Adenine Sulphate 10 mM
- Leucine 20 mM
- Uracil 16 mM

ALU stock was created by dissolving 0.92 g of adenine sulphate, 1.31 g of Leucine, and 0.896 g of Uracil into 500 mL ddH_2O, then autoclaved. 25 g of YPD powder was dissolved in 25 mL of the Adenine, Leucine and Uracil stock and filled to 500 mL with ddH_2O. The YPD + ALU mixture was then autoclaved and stored at room temperature.

2.1.5.2 YPD+ALU plates

Reagents

- YPD Powder
- Adenine, Leucine and Uracil stock
- Bacto agar

YPD+ALU plates were created by following the method mentioned in 2.1.5.1, then adding 7.5 g of Bacto agar per 500 mL. The reagents were mixed using a magnetic stir bar and then autoclaved. Once autoclaved, the liquid media was placed onto the magnetic stirrer whilst hot and left until cool enough to pour.

2.1.5.3 Dissection plates

Reagents

- YPD Powder
- Adenine, Leucine and Uracil stock
- Bacto agar

Following the method mentioned in 2.1.5.2, a 50 mL falcon tube was used to measure 25 mL of YPD+ALU per plate and left to cool on a level surface.

2.1.5.4 G418 plates

A 1 mL aliquot of G418 mixture was added to 500 mL YPD+ALU plate media (2.1.5.2) to give a final concentration of 400 g/ mL, ensuring that the media was at a comfortable hand-holding temperature.

2.1.5.5 YPA

To create YPA, 10 g of yeast extract, 20 g of bacto peptone and 10 g of potassium acetate were added to 1 L of ddH_2O. This was autoclaved and stored at room temperature.

2.1.5.6 2% Potassium Acetate

20 g of potassium acetate was added to 1 L of ddH_2O, then autoclaved and stored at room temperature.

2.1.5.7 100x AAHLTU

To create 100xAAHLTU, a ddH_2O mixture of 1 mg/ mL of Adenine, Arginine, Histidine, Tryptophan, Uracil and 3 mg/ mL of Leucine was gently heated. After filter sterilising, the mixture was stored at 4˚C.

2.1.5.8 Min/TRP/LEU Per 500 mL bottle

7.5 g of agar was autoclaved in 450 mL of water. During the autoclave, 3.35 g of Yeast Nitrogen Base with Ammonium Sulphate (YNB+AS) was added to the appropriate amount of amino acid dropout mix, 20 mL of 50% glucose was added to the YNB+AS + amino acid mix, followed by water, filling the total to 50 mL. After the autoclave was completed, the agar was left to cool, and just before it reached hand-holding temperature, the YNB+AS + amino acid mix was added. Once the mixture reached hand-holding temperature, the plates were poured.

2.1.5.9 LB broth

10 g of tryptone, 5 g of yeast extract, 10 g of NaCl, and 1 L of distilled water were mixed. The pH was then adjusted to 7.0 using 1M NaOH and autoclaved for 25 minutes at 120°C.

2.1.5.10 LB AMP

1 L of LB broth was added to a 2 L Erlenmeyer flask. After adding 15 g of agar, the mixture was autoclaved using a liquid cycle. The mixture was cooled to 50 °C in an H_2O bath. After adequate cooling, 0.5 mL Amp stock was added to the mix before pouring the plates near a hot flame.

2.1.6 Other solutions

2.1.6.1 1M Tris.HCl pH 8.8 with 2% Trichloroethanol (T54801-100G)

60.57 g of Tris Base was added to 440 mL of water and 10 mL of 100% TCE. The pH was adjusted to 8.8 using HCl and brought up to 500 mL volume.

2.1.6.2 4x Stacking Mix pH6.8

6.05 g of Tris Base was added to 40 mL of ddH_2O. The pH was adjusted to 6.8 using HCl, and then the mixture was made up to 100 mL in volume and filter sterilised. 0.4 g SDS was dissolved into the mix without stirring and then stored at 4˚C.

2.1.6.3 10% SDS (Fisher BP166-500)

50 g of SDS stock was dissolved in 500 mL of ddH_2O.

2.1.6.4 50x TAE

242 g Tris-Base was dissolved in 700 mL of water, followed by carefully adding 57.1 mL of 100% Glacial Acetic Acid. Next, 100 mL 0.5 M of EDTA pH 8.0 was added with the volume then adjusted to 1 L. This was stored at room temperature.

2.1.6.5 0.5M EDTA pH 8.0

93.05 g EDTA was dissolved in 400 mL of water, and the pH was adjusted using NaOH. The volume was brought up to 500 mL, autoclaved, and then stored at room temperature.

2.1.6.6 STE

STE was created using 2% SDS, 0.5 M Tris-HCl pH 8.1, 10 mM EDTA, and 1% volume saturated bromophenol blue.

2.1.6.7 2x Loading Buffer

2x Loading Buffer was created using 4% SDS, 100 mM Tris HCl pH 6.8, 20% Glycerol, 1 mM EDTA, and 10% volume saturated bromophenol blue.

2.1.6.8 50% PEG3350 (Sigma 202444-500G)

50 g of PEG3350 stock was dissolved in 100 mL of water, then autoclaved and stored at room temperature.

2.2 Methods

2.2.1 General *Saccharomyces cerevisiae* microbiology

2.2.1.1 Retrieval of *S. cerevisiae* samples from stock

Reagents:

- YPD + ALU plate
- Frozen *S. cerevisiae* strain (See 2.2.1.5 Storage (Freezing))

Equipment

- Sterile sticks
- 30˚C incubator

A scrape was taken from a frozen *S. cerevisiae* strain and spread across half of a YPD+ALU plate using sterile sticks. The plate was then placed into a 30˚C incubator for three days until single colonies could be collected.

2.2.1.2 *S. cerevisiae* inoculation

Reagents:

- YPD + ALU
- Plated *S. cerevisiae* strain

Equipment:

- 30˚C incubator
- Rotator
- Test tubes
- Large sterile sticks

A single colony of *S. cerevisiae* was suspended in 4 mL of protein rich YPD + ALU within a test tube using a sterile stick. The test tube was inserted into a rotator within a 30˚C incubator overnight to reduce self-identification and the formation of multicellular clumps (2015).

2.2.1.3 *S. cerevisiae* mating

Reagents

- Plated *S. cerevisiae* strain
- SDW
- YPD + ALU plate

Equipment

- Hydrophobic plastic
- 30˚C incubator

10 µL of SDW was pipetted onto hydrophobic plastic, following which a single colony of *S. cerevisiae* was mixed into it. A similar-sized colony of *S. cerevisiae* from the opposite mating type was mixed into the droplet using a new pipette tip. The mixed droplet was pipetted onto the edge of a YPD + ALU plate and grown overnight within the 30˚C incubator. This process facilitates the successful mating of *S. cerevisiae* cells within the patch. Following overnight growth, sterile sticks collected the mated cells and spread them across the plate. The plate was then returned to the 30˚C incubator for three days/ until single colonies could be collected.

2.2.1.4 *S. cerevisiae* sporulation

Reagents

- YPD + ALU inoculated *S. cerevisiae* strain
- 2% Potassium acetate
- SDW

Equipment

- Test tubes
- Eppendorf tubes
- Centrifuge
- Rotator
- 30˚C incubator

1.5 mL of inoculated *S. cerevisiae strain* was added to an Eppendorf tube and centrifuged for 1 min at ~15,500 x g. After removing the supernatant, the pellet was resuspended in 1 mL of SDW and spun again for 1 min at ~15,500 x g. The supernatant was removed, and the pellet was resuspended in 3 mL of 2% potassium acetate and left to sporulate in a rotating 30˚C incubator.

2.2.1.5 Freezing down *S cerevisiae* strains

Reagents

- YPD+ALU inoculated *S. cerevisiae* strain
- 50% glycerol

Equipment

- Microscope
- Glass slide
- Coverslip
- Freezer tube
- -80˚C freezer

750 µL of 50% glycerol was added to 750 µL of the inoculated *S. cerevisiae* sample, creating a final concentration of 25% glycerol. The mixture was placed into a labelled freezer tube and stored within a -80˚C freezer. When freezing diploid cells, vortexing the inoculated strain aids with identification due to their significantly slower sedimentation. Accurate identification requires pipetting 10 µL onto a glass slide and visualisation using a microscope.

2.2.2 General *Escherichia coli* microbiology

2.2.2.1 Retrieval *of E. coli* samples from stock

Reagents:

- LB AMP plate
- Frozen *E. Coli* strain (See 2.2.2.3 *E. coli* Storage (Freezing))

Equipment

- Sterile sticks
- 30˚C incubator

Using a similar method to 2.2.1.1, a scrape was taken from a frozen *E. coli* strain and spread across an LB AMP plate using sterile sticks. The plate was placed in the 37˚C incubator overnight to accommodate *E. coli's* faster growth rate.

2.2.2.2 *E. coli* inoculation

Reagents:

- LB AMP
- Plated *E. coli* strain

Equipment:

- 37˚C rotating incubator
- Plastic round bottom tube

3 mL of LB AMP was added to a plastic round bottom tube. A single colony of *E. coli* was suspended in the LB AMP alongside the pipette tip it was transferred on. The tube was placed into a 37˚C, 220 rpm rotating incubator overnight.

2.2.2.3 *E. coli* storage (Freezing)

Reagents

- LB AMP inoculated *E. coli* strain
- 50% glycerol

Equipment

- Freezer tube
- -80˚C freezer

750 µL of 50% glycerol was added to 750 µL of the inoculated *E. coli* strain in a labelled freezer tube in an identical method to 2.2.1.5 *S. cerevisiae Storage*. The tube was then placed into the -80 ˚C freezer.

2.2.3 Nucleic acid extraction from cells

2.2.3.1 Genomic DNA prep

Reagents:

- Spheroplasting buffer
- 100% 2-mercaptoethanol
- 50 mg/ mL zymolyase
- 20% SDS
- 0.5 M EDTA
- 20 mg/ mL proteinase K
- Phenol: chloroform: isoamyl alcohol (25:24:1)
- 3 M NaAc pH 5.2
- 100% ethanol
- 70% ethanol
- 1xTE
- 10 mg/ mL RNAse A
- YPD+ALU inoculated *S. cerevisiae* strain

Equipment:

- Pipette Tips
- 37˚C incubator
- Cut P1000 Pipette Tips
- Centrifuge
- 1.5 mL Eppendorf tubes

1.5 mL of inoculated *S. cerevisiae* strain was transferred to a labelled Eppendorf tube and centrifuged for 1 min at ~15,500 x g. After removing the supernatant, 500 µL spheroplasting buffer containing 1% 2-mercaptoethanol and 0.25 mg/ mL zymolyase was used to resuspend the pellet and incubated at 37˚C. 100 µL 3% SDA/0.1 M EDTA was mixed with 5 µL 20 mg/ mL proteinase K and added to the spheroplasting buffer mix, followed by a 30-minute 37˚C incubation. After cooling for 5 minutes, 500 µL of phenol: chloroform: isoamyl alcohol was mixed into the sample within a fume hood. The sample was mixed vigorously and spun at ~15,500 x g for 5 mins. 450 µL of the top clear phase was removed using a cut P1000 and transferred into a labelled 1.5 mL Eppendorf tube.

50 µL 3M NaAc pH 5.2 and 500 µL 100% EtOH were mixed into the sample. The sample was then centrifuged for 1 minute at ~15,500 x g. After removing the supernatant, 1 mL 70% EtOH was added

and centrifuged for 1 minute at ~15,500 x g. The supernatant was then removed, followed by pulse centrifugation. A pipette was used to remove the excess residue ethanol and then left to air dry for 10 minutes. After the sample was dried, 450 µL of 1xTE was pipetted into the sample and left at 37˚C for 30 minutes. 50 µL 1 mg/ mL RNAse was added and further incubated for 30 minutes at 37˚C. Following this, 50 µL of 3M NaAc and 550 µL 100% EtOH were mixed into the sample and centrifuged for 1 minute at 13,000 rpm. The supernatant was removed, 1 mL 70% EtOH was added, and the sample was centrifuged for 1 minute at ~15,500 x g. After removing the supernatant, the sample was pulse centrifuged, the supernatant was removed again, then dissolved into 100 µL 1xTE and left overnight at 37˚C.

2.2.3.2 Bacterial plasmid mini prep

Reagents:

- *E. coli* LB culture
- Buffer A1
- Buffer A2
- Buffer A3
- Buffer A4
- AW
- AE

Equipment

- Eppendorf tube
- NucleoSpin® Plasmid/ Plasmid (NoLid) Column
- Collection tube
- Centrifuge
- Vortex machine

Bacterial mini-preps were conducted using MACHERY-NAGEL's 'Plasmid DNA Purification' kit. 1-5 mL of the inoculated *E. coli* sample was centrifuged at 11,000 rpm for 30 seconds, and the supernatant was discarded. The pellet was then resuspended in 250 µL Buffer A1 by vortexing. 250 µL Buffer A2 was added and gently mixed by 6-8 inversions. This was left to incubate at room temperature for 5 minutes before mixing with Buffer A3 by 6-8 inversions. The sample was centrifuged at 11,000 rpm for 5 minutes, ensuring the supernatant was clear. A NucleoSpin® Plasmid/ Plasmid (NoLid) Column was placed into a collection tube before the supernatant was decanted and spun for 1 minute at 11,000 rpm. Flowthrough within the collection tube was discarded, and an additional wash step involving 500 µL AW was performed by centrifuging at ~11,100 x g for 1 minute. 600 µL Buffer A4 was added to the sample, followed by a 1 minute ~11,100 x g centrifuge to discard the flowthrough. The sample was centrifuged for 2 minutes at ~11,100 x g to dry the silica membrane. The NucleoSpin® Plasmid/ Plasmid (NoLid)

Column was placed into a 1.5 mL Eppendorf tube before the sample was incubated for 1 minute within 50 µL AE. Following the incubation, the sample was centrifuged at ~11,100 x g for 1 minute with the flow through being collected.

2.2.4 Nucleic acid manipulation

2.2.4.1 PCR

Reagents

- Genomic DNA (2.2.3.1) Sample (diluted 1/10)
- Polymerase Q5x2
- Forward Primer
- Reverse Primer
- SDW

Equipment:

- Pipette Tips
- 1.5 mL Eppendorf tubes
- PCR Machine
- PCR Tubes

Method

New England Biolabs© (NEB) Q5 mix enables PCR amplification, and their Tm Calculator estimates an appropriate annealing temperature for NEB-designed primers. An initial primer mix was created using 10 µL forward primer, 10 µL reverse primer, and 80 µL SDW. A master mix was then created using 5 µL primer mix added to 125 µL Q5 and 115 µL SDW. 1 µL of sample genomic DNA was added to 49 µL of Master mix and placed into a PCR tube.

PCR settings

Initial Denaturation

- Denaturation: 98 ˚C, 5 minutes

PCR- 30 Cycles

- Denaturation: 98˚C, 30 seconds
- Annealing: (Appropriate annealing temperature based on primers in Q5), 30 seconds
- Amplification: 72˚C, ‘1 minute per kb’

Final Amplification

- Amplification: 72˚C, 5 minutes

2.2.4.2 PCR cleanup

Reagents

- PCR Product
- NTI
- NT3
- SDW

Equipment

- NucleoSpin gel and PCR cleanup column
- Collection Tubes
- Centrifuge

PCR cleanup was conducted using MACHERY-NAGEL's 'PCR cleanup Gel extraction' kit. One volume of PCR sample was added to 2 volumes of NTI before being transferred to the 'NucleoSpin® gel and PCR cleanup Column' within a collection tube. The sample was cleaned using 700 µL NT3 buffer and spun for 3 seconds at ~11,100 x g twice, with the supernatant being removed each time. After washing the sample, it was spun dry for 1 minute at ~11,100 x g. 30 µL of SDW was added to each column and then incubated for 1 minute at room temperature. The DNA concentration was then calculated using 2.2.6.3 Nanodrop.

2.2.4.3 Restriction enzyme digestion

Reagents

- Sample plasmid
- Restriction enzymes
- SDW
- Buffer

Equipment

- 37˚C incubator

After deciding the restriction enzyme/s and the associated buffer solution required, 2 µL of buffer solution was added to 1 µL of each restriction enzyme, 5 µL plasmid and SDW to create a final volume of 20 µL. The reaction mixture was left to incubate for 1 hour at 37˚C.

2.2.5 Nucleic acid integration into *Saccharomyces cerevisiae* and *Escherichia Coli*

2.2.5.1 Gibson/HiFi assembly

Reagents

- PCR amplified fragments
- SDW

Equipment

- PCR machine

Using the equation pmols (picomoles) = ((weight in ng) x 1,000) / ((base pairs of the fragment) x 650), the number of pmols of each fragment. If the number of fragments required in the assembly was between 1 and 2, an insert: vector pmol ratio of 2:1 and a total assembly reaction of 0.03-0.2 pmols. Assemblies of 3 or more fragments required a 1:1 insert: vector pmol ratio and a total assembly reaction of 0.2-0.5 pmols. The fragments were diluted in SDW to ensure the correct ratios were achieved. Equal volumes of each diluted fragment (10 µL maximum) were added to 10 µL 2x HIFI master mix with SDW to create a reaction mixture of 20 µL. A PCR machine was used to incubate the reaction mixture at 50˚C for 15 minutes (1-2 fragment assembly) or 1 hour (3+ fragment assembly).

2.2.5.2 Bacterial transformation

Reagents

- DH5alpha cells
- SOC
- Gibson product

Equipment

- 42˚C water bath
- Container of ice
- 37˚C rotating incubator
- Selection plate

2 µL of Gibson product was added to 50 µL of DH5 alpha cells (10 transformations) and incubated on ice for 5 minutes. The reaction mixture was heat shocked at 42˚C for 42 seconds, then incubated on ice for 5 minutes. 100 µL SOC was added to each tube and then incubated on a rotator at 37˚C for 60 minutes. Following incubation, the reaction mixture was spread onto the relevant selection plate and incubated overnight at 37˚C.

2.2.5.3 Yeast transformation

Reagents

- Plated background strains.
- G418 plate
- YPD+ALU
- 1M LiAc
- 100mM LiAc
- 50% PEG3350
- 10mg/ mL Salmon Sperm (ssDNA)

Equipment

- 30˚C Shaking Incubator
- Flask
- 30˚C Incubator
- 42˚C incubator
- Falcon tubes
- Large centrifuge
- Small Centrifuge
- Spreader
- Sterile Sticks

One day before yeast transformation, 30 mL of YPD was placed into a flask. Single colonies from each background strain were incubated in YPD + ALU. These were then placed into the 30˚C Shaking Incubator overnight. After being removed from the shaking incubator, 2 mL of each mutant strain was transferred to a new flask. Fresh YPD + ALU was used to fill the flask to 20 mL, allowing the cells to enter log phase growth. The cells were then placed back into the shaking incubator. This re-inoculation occurs at the start of the day and is grown for 4 hours.

After transferring the inoculated background strains into 50 mL falcon tubes, they were spun at ~3000 x g for 5 minutes. The supernatant was poured off, resuspended in 20 mL of H_2O, and spun for 5 minutes at ~3000 x g. After removing the supernatant, 1 mL of 100 mM LiAc was used to resuspend the pellet and transfer it into a 1.5 mL Eppendorf tube. This was then spun at ~4500 x g for 3 seconds. The supernatant was carefully removed and resuspended in 200 µL 100M LiAc. The sample was then spun for 30 seconds at ~4500 x g.

A transformation mix (1 transformation)

- 50% PEG 3350 240 µL
- 1M LiAc 36 µL
- 10mg/ mL ssDNA 10 µL

- DNA (x µL)
- Water 74 µL
- **Total** **360 µL**

350 µL of transformation mix + 10 µL DNA was added to the tube and vortexed for 1 minute to ensure thorough mixing. The mixture was then incubated at 30˚C for 20 minutes, followed by 20 minutes in the 42˚C bath. After centrifuging at ~4500 x g for 30 seconds with the supernatant removed and carefully resuspended in 1 mL of YPD+ALU and incubated at 30˚C 250 rpm to restart cell activity. After another ~4500 x g centrifugation for 3 seconds, the samples were resuspended in 200 SDW and spread throughout a G418 Selection plate. This was then incubated at 30˚C for 3-4 days. After 3-4 days, successfully grown colonies were re-streaked onto a new G418 selection plate using sterile sticks and returned to the 30˚C incubator to grow for 3-4 days.

2.2.5.4 Replica-plating

Reagents

- Plate
- Selection plates

Replica-plating is a selection process via transferring plated *E. coli* or *S. cerevisiae* colonies to a new plate. The initial plate is pressed against a transfer cloth before the selection plate is pressed against the same cloth. When selecting mating types, a new cloth must be used between each MIN plate.

2.2.6 Nucleic acid screening

2.2.6.1 Gel electrophoresis

Reagents:

- Sample (PCR Products)
- Agarose
- 1xTAE
- Ethidium Bromide
- Gel Loading Dye
- 1kB ladder

Equipment

- Microwaveable Flask

- Gel Electrophoresis
- Microwave
- Hydrophobic plastic

A 0.8% agarose gel was created using 1 g of agarose with 125 mL of TAE within a microwaveable flask. (Different percentage gels were created using different quantities of agarose when necessary.) then microwaved for 2 minutes before being cooled for 30 minutes. After cooling, 12.5 µL of ethidium bromide was gently mixed into the liquid to reduce bubbles. After taping the sides of the electrophoresis gel tray, the liquid was poured onto it. Two 20-lane wells were placed on the tray before cooling for 30 minutes. After the gel had set and the inserts were removed, the gel was submerged in TAE.

10 µL of 1kb ladder was added to the initial well. 10 µL of 6x Gel loading dye was added to 50 µL of each sample, with 20 µL placed within the wells. For samples needing further experimentation, 10 µL of DNA was added to 2 µL 6x Gel loading dye on top of hydrophobic plastic, with 10 µL placed into wells. The gel was then run for 30 minutes at 120V. The gel was carefully transferred to the UV machine, which resulted in visible bands. If necessary, the gel can be run for an extended period to segregate bands accurately.

2.2.6.2 DNA sequencing

Reagents

- Sample
- Primer

10 µL of the sample was sent to the University of Nottingham's Deep Seq facility alongside an appropriate primer that anneals within 500 bp of the site of interest.

2.2.6.3 Nanodrop

Reagents

- Samples
- SDW
- TE

Equipment

- Nanodrop Machine
- Lint-free wipes

Method

Initially, a blank was created using 2 µL of TE or SDW (based on what the DNA is incubated within). 2 µL of each sample was measured against the blank to determine the concentration ng/ µL and 260/280 of DNA. The lint-free wipes were used to clean the probe after each measurement, with SDW as the final sample to clean the machine after use.

2.2.7 Protein biochemistry methods

2.2.7.1 Protein extraction

Reagents

- 10% Trichloroacetic acid
- 0.5mm zirconium/silica beads
- STE
- 2x Loading Buffer
- 100% ß-mercaptoethanol (BME)

Cells inoculated the day prior were pelleted into 2 mL cap tubes before 300 µL of fresh 10% TCA was added to each tube. One scoop of cold silica beads was added to each tube and then vortexed for 10 seconds to ensure the cells were successfully broken open. The supernatant was transferred to a new 1.5 mL tube using a P200 tip. The supernatant was removed and discarded after spinning down for 1 minute at ~15,500 x g. The pellet was then resuspended in 300 µL of STE and boiled for 5 minutes at 95˚C. The supernatant was transferred into a new tube following a 1-minute, ~15,00 x g spin down. The Samples could then be stored at -20˚C for later use. A loading mixture was created using 950 µL of 2x Loading Buffer, and 50 µL 100% BME was added to an equivalent volume of sample (10 µL: 10 µL) prior to loading onto the SDS gel. Similarly, the ladder was diluted 1:1 with 2x Loading Buffer +BME.

2.2.7.2 SDS PAGE

Reagents

- 30% Bis-Acrylamide
- 1M Tris.HCl pH 8.8 with 2% Trichloroethanol
- 10% SDS
- 10% Ammonium Persulphate
- TEMED
- 4x Stacking Mix pH6.8
- 70% Ethanol

- 100% Isopropanol

Protein size	Gel percentage (Approx)
4-40kDa	20%
12-45kDa	15%
10-70kDa	12.5%
15-100kDa	10%
25-200kDa	8%

Before creating a gel, the correct percentage of gel required was decided based on the size of the protein being examined, and all the glassware must be cleaned using 100% Isopropanol (IPOH)/ 70% Ethanol and wiped clean. The front and back glass pieces were sealed using casting clips before being placed onto a casting mould. Before adding any gel mixture,1 mL of water was poured into the cast to check for leaks.

Resolving Gel

7.5% Gel	1 Gel	2 Gels	4 Gels
30% Bis/Acrylamide	2.5 mL	5 mL	10 mL
1M Tris pH8.8 + TCE	2.5 mL	5 mL	10 mL
Water	4.8 mL	9.6 mL	19.2 mL
10% SDS	100 µL	200 µL	400 µL
10% APS	100 µL	200 µL	400 µL
TEMED	10 µL	20 µL	40 µL

Stacking Gel

	1 Gel	2 Gels	4 Gels
30% Bis/Acrylamide	625 µL	1.25 mL	2.5 mL
Stacking Mix	1.25 mL	2.5 mL	5 mL
Water	3.05 mL	6.1 mL	12.2 mL
10% APS	25 µL	50 µL	100 µL
TEMED	10 µL	20 µL	40 µL
TEMED	10 µL	20 µL	40 µL

Due to APS and TEMED causing polymerisation, the resolving gel mix was created in the order provided within the table at a swift speed. Adding a layer of IPOH to the top of the gel allowed it to set flat, and

the resolving gel mix provided a good indication of whether the gel had been set. Once the gel had set, the IPOH was poured off, and the gel was rinsed with ddH_2O and dried using a paper towel. Using the same procedure as the resolving gel, an appropriate stacking mix was created and poured into the cast. A comb was then applied to the stacking mix and left to set. When storing the gel overnight, the gels were completely hydrated in ddH_2O and carefully wrapped in cling film before being placed in the fridge.

When running the gel, 1x SDS running buffer was added to the SDS gel container, ensuring the gels were covered and the centre between the two gels was filled. The comb was carefully removed from each gel, and the wells were checked for misalignment. The gel was run for an appropriate amount of time. In the case of Dpb11, the 50 kDa ladder band reached the bottom of the gel.

2.2.7.3 Gel transfer

Reagents

1) PVDF Membrane
2) Gel
3) Filter paper
4) 100% Ethanol
5) 1x Transfer Buffer

Equipment

- UV Imager
- Filter paper

Whilst running the SDS page, the filter paper was equilibrated by submerging in 1x transfer buffer in a plastic tray. The PVDF membrane was activated in 100% ethanol for ten minutes, ensuring it was completely covered. Once the gel was finished, the loading area and 0.5 cm from the bottom were cut off to avoid curling. The gel was transferred onto a wet gel imaging tray using a scraper to ensure it did not dry out. The TCE within the gel was activated using an initial 1-minute UV exposure, then exposed for shorter periods until the bands were visible but not saturated. After ensuring the protein extraction was successful, the gel was placed into a transfer cassette consisting of filter paper and the activated PVDF gel below and a filter paper above inside a Bio-Rad® transfer tray. A roller was used to remove any bubbles that may have appeared between the filter paper and the gel before the lid was pressed on top and locked. The 2.5A-25V-10M programme was then chosen to transfer the protein between the gel and the membrane.

2.2.7.4 Western blot

Reagents

- 5% BSA/NFDM
- 1xTBST
- Primary antibody
- Secondary antibody
- ECL

Equipment

- Rotator
- UV imager

The membrane containing the transferred proteins was placed protein side inwards into a 50 mL falcon 1tube containing 10 mL of 5% BSA + 1xTBST. This was left to turn for at least 30 minutes at room temperature and then was poured off and replaced with a 10 mL mixture containing 1xTBST and the diluted primary antibody at the correct dilution and left on the rotator overnight. The following day, the membrane was washed thrice in 10 mL 1xTBST for 10 minutes. After the third wash, the membranes were incubated with 10 mL of 1/5000 dilution goat anti-rabbit secondary rabbit in 1xTBST for 1 hour. After the incubation, the mixture was poured off and washed 3x for 10 minutes in 1xTBST. Equal volumes of ECL were incubated with the membrane for one minute, allowing the visualisation of tagged protein using the UV imager.

2.2.8 Phenotyping of *Saccharomyces cerevisiae*

2.2.8.1 Dissection/spore viability calculation

Reagents

- 50 mg/ mL Zymolyase
- SDW
- Dissection plates

Sporulated diploid colonies (2.2.1.4) were imaged under a light microscope to ensure tetrads had formed before taking 1 mL of culture and spinning it down for 1 minute at ~15,500 x g. After removing the supernatant, the pellet was resuspended in 500 µL SDW and incubated at 37˚C for 30 minutes with 2.5 µL of Zymolyase. The sporulation mix was diluted with SDW (1/10), and then 10 µL was pipetted onto a dissection plate and allowed to run down a vertical line to the left-hand side. After allowing them to dry, the tetrads were dissected using a dissection microscope. To calculate the spore viability, The number of spores that successfully grew on a dissection plate was counted and compared to the total number of dissected spores.

2.2.8.2 Sporulation efficiency

Reagents

- Sporulated cells

Equipment

- Microscope
- Glass slide
- Coverslip
- Imaging equipment

10 µL of diploid cells were pipetted onto a microscope slide with a cover slip placed on top. Visual comparison of Haploid and Diploid cells allowed the identification of successful diploid sporulation and potential contamination of both foreign material and haploid cells. Imagining equipment was used to take photos of sporulated diploid cells and allowed the calculation of sporulation efficiency by counting the number of sporulated cells vs. those that have not.

2.2.8.3 Meiotic time course

Reagents

- YPD+ALU
- YPA
- Sporulation Media
- 100xAAHLUTA
- UPH_2O

Equipment

- Large conical Flasks
- Spectrophotometer

Woken-up yeast diploid colonies were inoculated in 20 mL YPD+ALU and placed into a shaking incubator at 250 rpm at 30˚C overnight. 13.5 hours before the first time point, the inoculated diploid colonies were transferred into 200-250 mL YPA to create a final OD_{600} of 0.2. After 13.5 hours, the incubated colonies were spun down at ~3,000 x g for 5 minutes and washed in prewarmed UPH_2O. Following a second ~3,000 x g for 5 minutes spin down, the pellets were resuspended in prewarmed SPM (T_0). Samples were then taken at different time points based on the area of meiosis being examined.

Samples	Details
DNA	10-20 mL Cultures pelleted and stored at -20˚C
Protein	10-20 mL Cultures pelleted and stored at -20˚C
Sporulation Efficiency	Samples were taken at 72hrs, 100 µL added to 500 µL 100% MeOH and stored at -20˚C
Spore Viability	Samples taken at 72hrs, stored at 4 ˚C

Chapter 3: Results and Conclusions

3.1 Construction and analysis of *tag-dpb11* and *tag-dpb11-md* strains

Prior to this study, N-terminal 6xHIS-3xHA tagged Dpb11 (*tag-dpb11*) (YSG518, YSG519, YSG520 YSG521) and N-terminal 6xHIS tagged P^{CLB2} Dpb11 (*tag-dpb11-md*) (YSG678, YSG680, YSG681) strains were generated using standard procedures outlined in Chapter 2 after research conducted by (Pfander and Diffley, 2011) showed that N-terminal His-tagging Dpb11 does not affect its binding characteristics. However, it remains unclear if introducing an N-terminal tag affects the meiotic phenotype of *S cerevisiae* mutants.

3.1.1 Construction and analysis of N-terminal His tagged DPB11 *S. cerevisiae* strains

Tagging Dpb11 at the N-terminal region allows the quantification of protein expression during vegetative and more active cell states, such as during meiosis. Meiotic protein quantification is achieved by taking samples of sporulating cells at different stages of meiosis via a meiotic time course (2.2.8.3) and then performing western blots. During a meiotic time course, cultures synchronously sporulate, enabling a direct comparison of protein expression across various strains. The tag consists of two parts: six consecutive histidine residues (6xHis), which allows the purification via immobilised metal ion affinity chromatography (Hochuli *et al.*, 1988), and three Human influenza hemagglutinin glycoproteins (3xHA) that bind to primary anti-HA antibodies during western blot analysis ((2.2.7.4)(Field *et al.*, 1988))

The background strains used in this research, *S. cerevisiae* SK1 YSG3, YSG4, YSG29, and YSG33, contain ho::LYS2, an insertion of LYS2 into the endonuclease HO gene, which disrupts the activity of the endonuclease HO, subsequently preventing *S. cerevisiae's* ability to switch mating types (Coughlan *et al.*, 2020). Notably, YSG29 has mCerulean-TRP1, a cyan fluorescent protein (Rizzo and Piston, 2005) inserted at THR1, and YSG33 has a tdTomato-LEU2, an orange fluorescent protein (Shaner *et al.*, 2004) inserted at CEN8. Crossover between the THR1 and CEN8 regions during meiosis I results in the movement of the fluorescent proteins between spores, subsequently altering the fluorescence observed (Thacker *et al.*, 2011). This method was developed by D. Thacker et al. as an alternative to the more time-consuming meiotic characterisation by tetrad dissection (Thacker *et al.*, 2011). Initially, we planned to use this method to characterise any alterations in crossover frequency and chromosome segregation caused by mutation. Diploids created from mating YSG3 and YSG4 background strains are denoted as '3 x 4' background strains whilst diploids created from mating YSG29 and YSG33 are denoted as '29 x 33' background strains.

3.1.1.1 Validation of pre-existing *tag-dpb11*

An analysis of the previously generated N-terminal 6xHIS-3xHA tagged DPB11 (*tag-dpb11*) strains YSG518, YSG519, YSG520 and YSG521 was conducted to ensure accurate data collection. These strains were created using YSG3 and YSG4 as a background and should show a WT meiotic phenotype during spore viability and sporulation efficiency analysis. To determine if the 6xHIS-3xHA tag was successfully integrated into the S. cerevisiae genome, a genomic DNA pep was performed on each stain alongside a WT control, followed by nanodrop verification. PCR amplification was performed, amplifying the region 'upstream DPB11' to 132 bp into DPB11 using primers 921 and 956 (Figure 3.1A). Gel electrophoresis identified appropriately sized banding (Figure 3.1B); however, to ensure the 120bp tag was present and in-frame, the samples underwent PCR cleanup prior to DNA Sequencing.

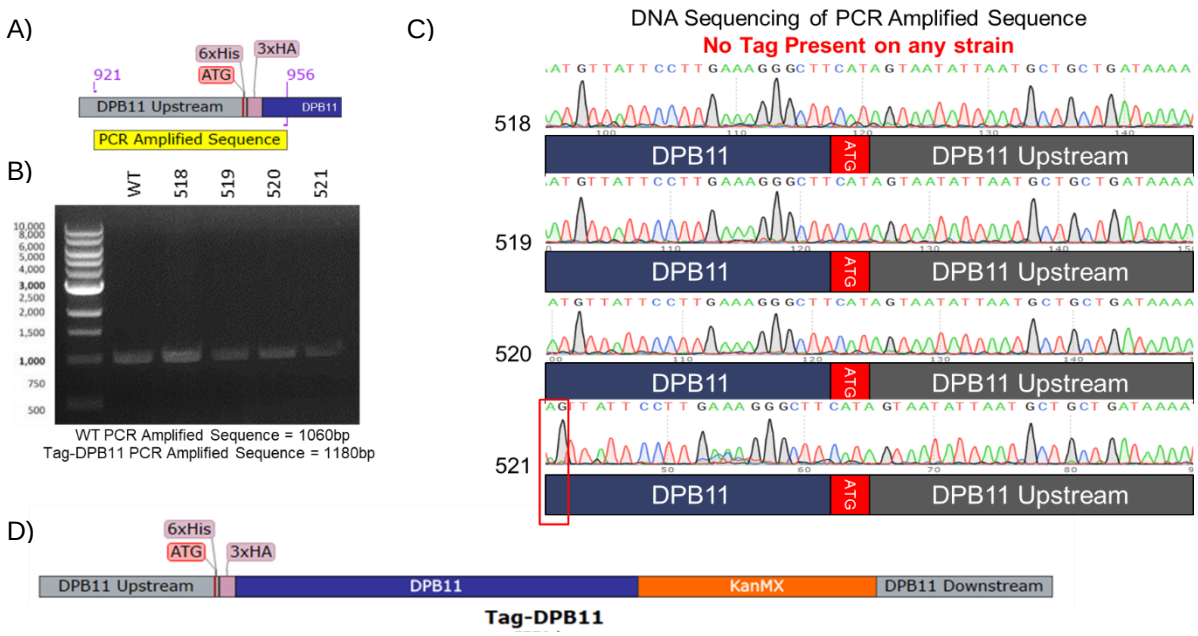

Figure 3.1: Analysis of pre-existing N-terminal *tag-dpb11* strains. A) 1180 bp PCR amplified sequence, including the 6xHIS-3xHA N-terminal tag. B) Gel electrophoresis of the PCR amplified 1180 bp sequence. *tag-dpb11* strains YSG518, YSG519, YSG520 and YSG521 were examined. C) Sequencing results of YSG518, YSG519, YSG520 and YSG521 strains using reverse primer 956. D) The complete 5772 bp *tag-dpb11* cassette.

The samples were sent to the 'Deep Seq' facility alongside the reverse primer 956, annealing 132 bp away from the 6xHIS-3xHA tag (Figure 3.1A). Sequencing results determined that all four strains did not include the 6xHIS-3xHA tag with YSG521 containing a potential point mutation (Figure 3.1C).

3.1.1.2 Construction and validation of *tag-dpb11* strains

After discovering the absence of any tags within the pre-existing *tag-dpb11* strains, the plasmids used to create them were analysed. Commencing with a nanodrop, a full-sequence PCR of the *tag-dpb11* cassette located within plasmids A and B was conducted using primers 921 and 922 (Figure 3.2A). Gel electrophoresis (Figure 3.2B) identified that the amplified region on both plasmids was ~1 kb larger than expected; however, this was missed due to inexperience within the second month of research.

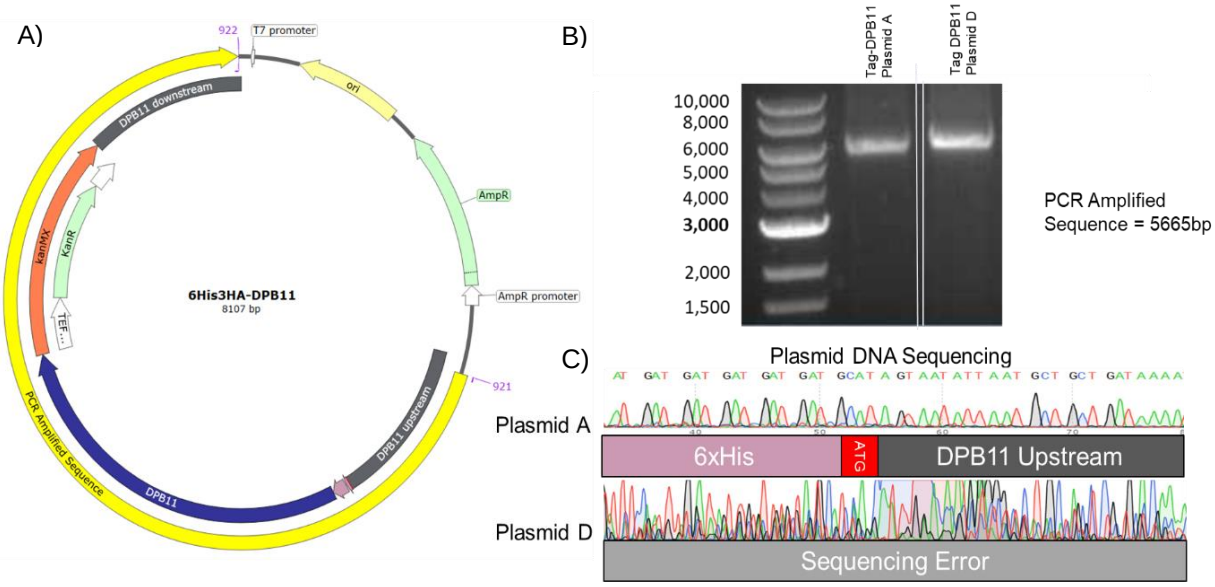

Figure 3.2 Analysis of the pre-existing *tag-dpb11* plasmid. A) 5665 bp PCR amplification of the complete *tag-dpb11* cassette. B) Gel electrophoresis of the complete cassette sequence in plasmids 'A' and 'D'. C) Sequencing results of plasmid 'A' indicate the presence of the 6His-3HA tag in frame within the cassette whilst plasmid 'D' resulted in a sequencing error. Primer used: 956.

Future analysis in Figure 3.5C concluded that, despite the extra length observed within the complete cassette sequence PCR, the plasmid and the transformed strains had no additional base pairs within the cassette region. Continued analysis of the pre-existing plasmids via DNA sequencing (Figure 3.2C) determined that plasmid A contained the 6xHIS-3xHA tag in-frame at the correct location, while plasmid D resulted in a sequencing error (Figure 3.2C). The observed error may indicate foreign material within the sample or mechanical error, so the decision was made to continue research using plasmid A.

Following sequencing, the complete sequence PCR was repeated three times, cleaned up and transformed into the *S. cerevisiae* background strains YSG3, YSG4, YSG29 and YSG33. During

transformation, the cassette sequence traverses both the cell wall and the plasma membrane, subsequently entering the cytosol through a mechanism resembling endocytosis (Kawai *et al.*, 2004). Within the cytosol, the DNA is transferred to the nucleus and integrated into the genome based on homologous regions within the sequence (Kawai, Hashimoto and Murata, 2010). KanMX inserted downstream from the DPB11 gene (Figure 3.1D) provides kanamycin (G418) resistance to strains that have successfully integrated the cassette into their genome (Jimenez and Davies, 1980). Genomic DNA preparation was performed on inoculated colonies that grew on the G418 plates. PCR amplification of the region surrounding the 6xHIS-3xHA tag using primers 921 and 956 identified a larger (likely correct) band in the YSG4 background strain A (4A) (Figure 3.3A). All the PCR fragments were cleaned up and sent to sequencing with primer 956 as a precaution (Figure 3.3C). As predicted, strain 4A had successfully integrated the 6xHIS-3xHA tag at the correct location. Rather than a second yeast transformation, *tag-dpb11* strain 4A was used to integrate the 6xHIS-3xHA into its opposite mating type. After mating *tag-dpb11* strain 4A with YSG3, sporulated diploids were dissected and replica-plated using YSG1 ('A' mating type) min, YSG2 ('α' mating type) min and G418 plates. Min plates do not have the amino acids to facilitate cell growth, so only spores that mate with their opposite mating types can grow, i.e. α mating type spores grown on YSG1 plates. The G418 plate facilitates the identification of the cassette sequence crossing over to the opposite mating type. Three replica-plated YSG3 colonies and three replica-plated YSG4 colonies were selected and labelled YSG858, YSG859, YSG860, YSG861, YSG862, and YSG863 respectively.

The *tag-dpb11* cassette was successfully integrated into the YSG29 background (YSG972 Figure 3.3B/ Figure 3.3C) but was unsuccessful in the YSG33 background. The previously mentioned method transferred the cassette from *tag-dpb11* YSG29 into WT YSG33. The PCR conducted in Figure 3.3A was repeated on all the newly synthesised *tag-dpb11* strains to ensure the cassette was successfully integrated into the correct location within the genome. The labels YSG972, YSG973, and YSG974 were provided to *tag-dpb11* 29, replica-plated *tag-dpb11* 29 and replica-plated *tag-dpb11* 33, respectively. The upstream region of *tag-dpb11* 33 exhibited major overlapping of base pair signals during sequencing (Figure 3.2C); however, this was determined to be a sequencing error rather than a strain mutation. This was potentially a result of DNA contamination during PCR amplification.

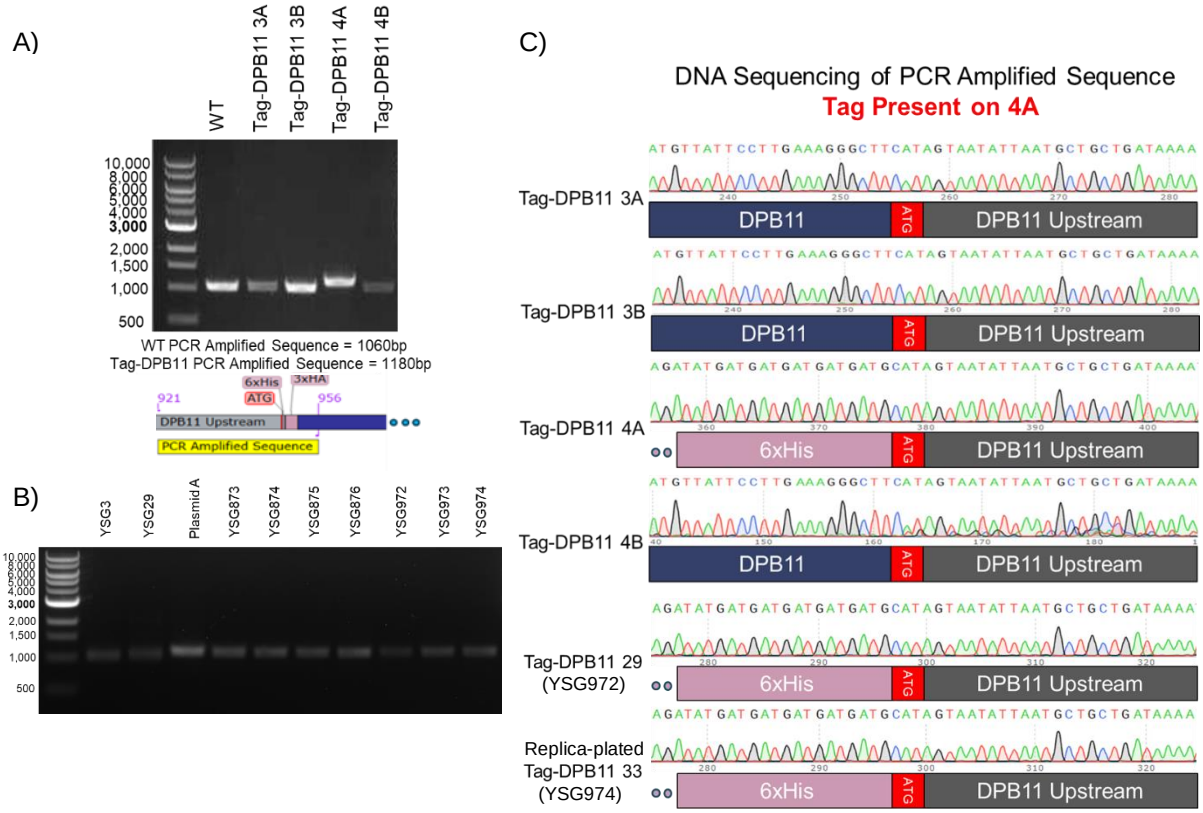

Figure 3.3 Analysis of transformed N-terminal *tag-dpb11* strains. A) Gel electrophoresis of the PCR amplified 1180 bp sequence containing the 6xHIS-3xHA N-terminal tag. Transformed *tag-dpb11* strains 3A, 3B, 4A and 4B were examined. B) Repeat gel electrophoresis of the 1180 bp sequence within *tag-dpb11* strains YSG873, YSG875, YSG874, YSG876, YSG972, YSG973, and YSG974, WT strains YSG3 and YSG29 and Plasmid A. C) DNA sequencing results of transformed *tag-dpb11* strains 3A, 3B, 4A, 4B and 29 along with replica-plated 33. The tag was present and in-frame within the transformed strains 4A, 29 and replica-plated strain 33.

3.1.1.3 Analysis and conclusions of *tag-dpb11* strains

Tetrads serve as a valuable tool in characterising the meiotic phenotype, as the survivability of their spores, when separated and allowed to grow, can reveal any abnormalities that may have occurred during the first and second meiotic divisions. If a mutation has affected a strain's ability to initiate sporulation or affected meiotic divisions, the number of cells showing signs of sporulation will change. In a scenario where the integration of the 6xHIS-3xHA tag at the N-terminal region does not affect the expression and activity of Dpb11, the strains should express a WT meiotic phenotype. Alongside, the premade YSG(3 x 4) WT control diploid YSG5, WT haploid YSG3 was mated with its opposite mating type, YSG4, to form new diploids labelled YSG889, YSG891, YSG930, YSG931, YSG932, YSGG933,

and YSG934. In addition, YSG29 was mated with YSG33 to create diploids (pre-existing) YSG236, YSG890, YSG934, YSG935, YSG936, YSG937, and YSG938 to act as YSG(29 x 33) controls.

Following the creation of controls, (YSG(3 x 4)) *tag-dpb11* diploid strains were created by mating YSG858, YSG859, and YSG860 with YSG861, YSG862, and YSG863. Alongside the WT control diploids, the newly synthesised *tag-dpb11* (YSG864/YSG865) diploids were dissected using a tetrad dissection microscope. Following incubation, the spore viability was determined by comparing the number of spores that successfully grew to the total number of dissected spores. Photographs were also captured of the sporulated cells to determine sporulation efficiency. Initial sporulation data from the newly synthesised *tag-dpb11* (3 x 4*)* diploids was lower than anticipated (Figure 3.4A). The total spore viability of *tag-dpb11* (61%, n = 32, SD = 9%) showed a 36% (p = 3.34e-05) decrease compared to WT (97%, n = 95, SD = 2%), while the *tag-dpb11* sporulation efficiency (38%, n = 559, SD = 11%) showed a 51% (p =4.26e-08) decrease in sporulation efficiency compared to WT (89%, n = 1791, SD = 6%). To calculate the p-value, a two-tailed type 2 T-test was performed between each strain's spore viability and sporulation efficiency rather than the total sporulation efficiency. The lower spore viability and sporulation efficiency observed within the *tag-dpb11* strains was initially believed to result from integrating the tag at the N-terminus of Dpb11. Subsequently, it was decided to create C-terminally tagged DPB11 (*dpb11-tag)* and meiotic depleted C-terminally tagged DPB11 (*dpb11-tag-md)* strains to determine if tagging the N-terminal region was a reason for reducing spore viability and sporulation efficiency (3.2).

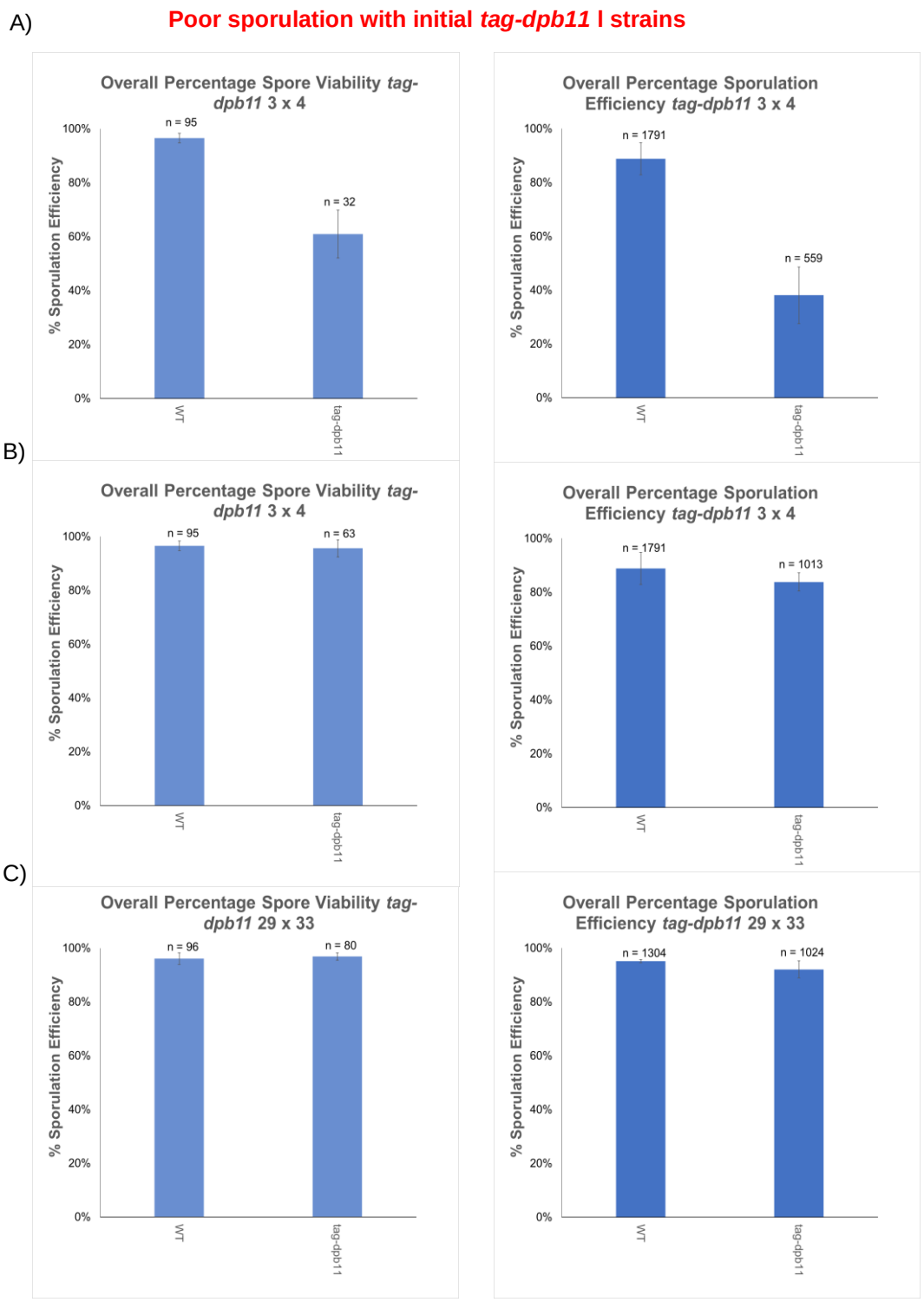

Figure 3.4: Spore viability and sporulation efficiency of *tag-dpb11* mutants. A) Spore viability and sporulation efficiency of (3 x 4) WT control strains and the initial *tag-dpb11* strains YSG864 and YSG865 (p =3.34E-05) (p =4.26E-08) B) Spore viability and sporulation efficiency of the (3 x 4) WT control strains and the *tag-dpb11* strains YSG892, YSG893, YSG894, and YSG895. (p =0.55) (p =0.14) C) Spore viability and sporulation efficiency of the (29 x 33) WT control strains and the *tag-dpb11* strains YSG1023, YSG1024, YSG1025, YSG1026, YSG1027. (p =0.04) (p =0.12) (Spore Viability: N = number of tetrads dissected. Sporulation Efficiency: N = number of sporulated/un-sporulated cells counted, Error Bars = Standard Deviation.)

During the construction of C-terminal *dpb11-tag*, further analysis of the *tag-dpb11* haploid strains created during the initial *tag-dpb11* 4A x WT3 replica-plating was conducted using fresh media. The newly inoculated *tag-dpb11* haploid colonies were labelled YSG873 (YSG3), YSG875 (YSG3), YSG873 (YSG4), and YSG875 (YSG4) alongside the initial *tag-dpb11* 4A transformation that was labelled YSG872. Diploid colonies made from mating these haploids were labelled YSG892, YSG893, YSG894, and YSG895. These new strains showed statistically similar ($p = 0.55$) spore viability (96%, $n = 63$, $SD = 3\%$) compared to WT (97%, $n = 95$, $SD = 2\%$) (Figure 3.4B). The sporulation efficiency (84%, $n = 1013$, $SD = 3\%$) was lower than WT (89%, $n = 1791$, $SD = 6\%$); however, it was not statistically significant ($p = 0.14$). It was theorised that the 5% difference resulted from the sporulation environment as the spore viability remained unchanged between each strain. To further clarify these results, extra sporulated WT and *tag-dpb11* (3 x 4) strains should be photographed and counted in the future.

To see if a similar meiotic phenotype was observed within the *tag-dpb11* (29 x 33) background, YSG972 and YSG973 were mated with YSG974 to create *tag-dpb11* diploid strains YSG1023, YSG1024, YSG1025, YSG1026, YSG1027 and YSG1028. The (29 x 33) *tag-dpb11* spore viability (97%, $n = 80$, $SD = 1\%$) was 1% higher ($p = 0.04$) than WT (96%, $n = 96$, $SD = 2\%$), while the sporulation efficiency (92%, $n = 1024$, $SD = 3\%$) was 3% lower ($p=0.12$) than WT (95%, $n = 1034$, $SD = 1\%$) (Figure 3.4C). Due to the less than 5% variation between *tag-dpb11* and WT within both sporulation efficiency and spore viability, it was concluded that *tag-dpb11* (29 x 33) phenocopies WT.

Thus, it was concluded that integration of the tag at the Dpb11 N-terminus does not affect its expression or activity as this would cause the phenotype to align closer with the inviability observed in Dpb11 knockout cells (Araki *et al.*, 1995). Several factors could have caused the initial erroneous results; however, the most likely is the inadequate washing of the diploids before sporulation. Inadequate washing would result in higher levels of nitrogen, inhibiting the activation of the transcription factor Ime1 (Smith *et al.*, 1990) and genes associated with the early stages of meiosis (Esposito *et al.*, 1969; Rubin-Bejerano *et al.*, 1996). With Ime1 no longer present, Ime2 expression diminishes. Ime2 plays a crucial role in regulating progression through meiosis, so reduced levels of Ime2 expression result in a reduction of sporulation observed in *S.cerevisiae* (Enserink and Kolodner, 2010; MacKenzie and Lacefield, 2020). Repeated spore viability and sporulation efficiency analysis should be completed with strains YSG864 and YSG865 using fresh media to validate this theory.

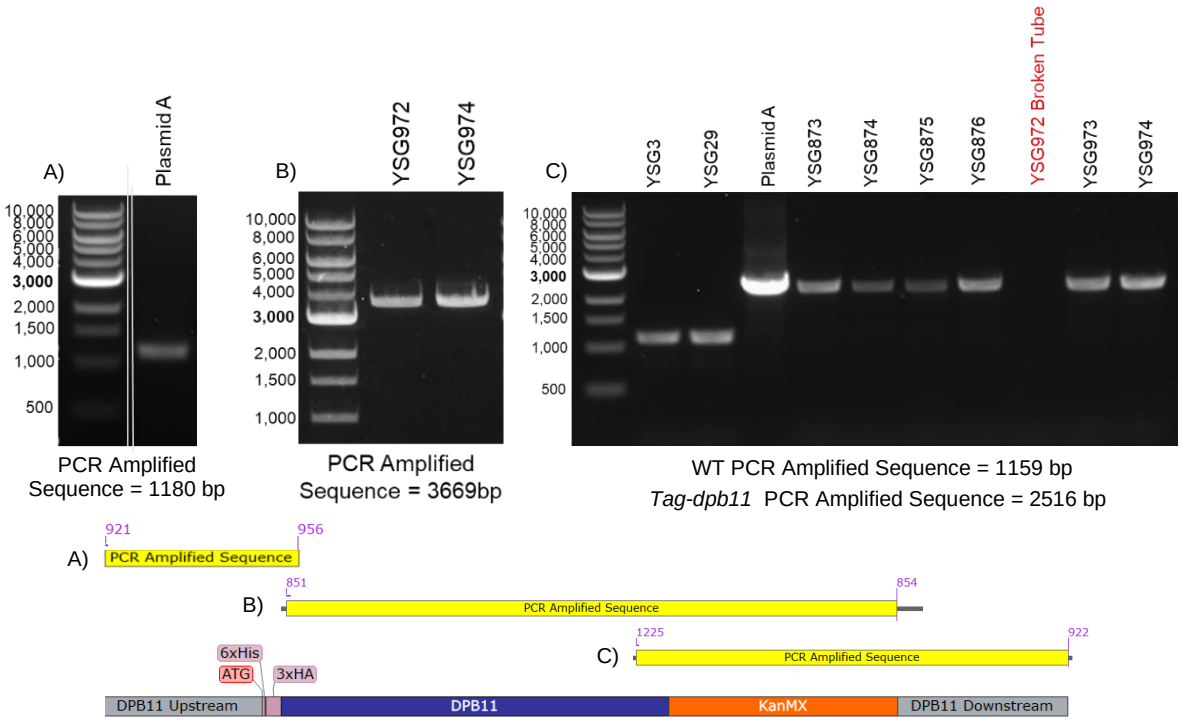

Figure 3.5 Further analysis of *tag-dpb11* mutants via PCR amplification. A) Gel electrophoresis of a PCR amplified 1180 bp sequence within *tag-dpb11* Plasmid A B) PCR amplification of Dpb11 alongside KanMX within *tag-dpb11* transformation 29 (YSG972) and replica-plated *tag-dpb11* strain 33 (YSG974). PCR parameters: primers 851 and 854.

After discovering the additional 1 kb present in the pre-existing cassette sequence, time constraints hindered the design and creation of new *tag-dpb11* strains, so it was necessary to determine where the additional region was inserted into the cassette. Although the *tag-dpb11* strains showed WT meiotic phenotypes, it was essential to clarify if the additional sequence could affect any of the results obtained. PCR amplification of the complete cassette sequence using primers 921 and 922 should indicate any additional sequences transformed into the mutant strain; however, following five attempts on various WT and transformed strains, the PCR was determined to be infeasible as most cases (Only successfully amplified in Figure 3.7) resulted in no PCR product. Subsequently, it was decided that multiple smaller PCRs would be completed along the cassette region.

As the upstream and tag region was previously amplified in Figure 3.3B/Figure 3.5A, it was decided to first PCR amplify the downstream region as an insertion into Dpb11 would likely result in inviable cells. Primers 1225 and 922 amplified the dpb11 downstream region at 69˚C with an extension time of 5 minutes. The extension time was extended to account for a potentially larger-than-expected PCR product. Although one of the tubes opened during PCR amplification resulting in the evaporation of YSG972s PCR product, the remaining transformed strains expressed the correct PCR product and

included no extra sequence in the downstream region. However, a faint secondary band was observed within plasmid A (Figure 3.5C). This secondary band could indicate that following the downstream region, a secondary downstream region (or more) has been integrated into the pre-existing *tag-dpb11* plasmid. If only the region between the upstream and the first downstream region is integrated into the transformed strains, it will exhibit the observed PCR results, and since the integration was downstream of DPB11, it should not affect the expression of tagged Dpb11 even if the extra region was integrated. To validate this theory, a PCR using newly designed primers from DPB11 into the backbone would need to be completed alongside gel electrophoresis of the undigested plasmid to ensure the secondary band was not a result of excess plasmid within the PCR reaction.

The study region within *tag-dpb11* was an insertion into the DPB11 gene itself. A diagnostic PCR of *tag-dpb11* strains YSG972 and YSG974 indicated that despite the successful integration of the *tag-dpb11* cassette, no extra base pairs were integrated into the yeast genome, despite the increased length observed in the initial tag-dpb11 cassette PCR amplification(Figure 3.5C). The complete cassette PCR was repeated using plasmid A (Figure 3.6) as a final identification method. This PCR resulted in a sequence length more accurately representing the 5665 bp sequence.

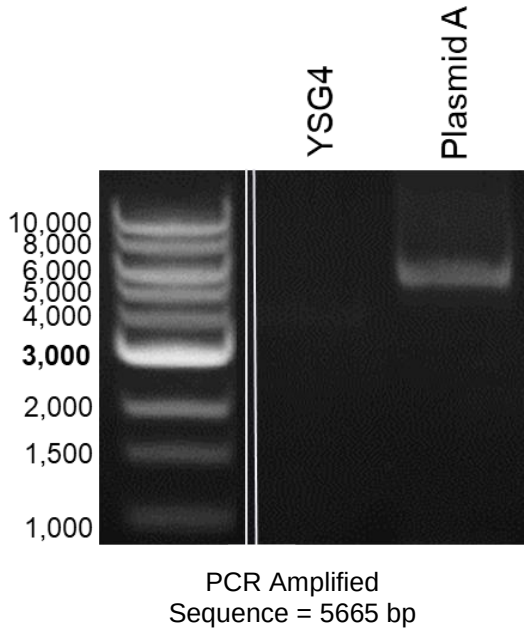

Figure 3.6: PCR amplification of *tag-dpb11* plasmid. A) Gel electrophoresis of the complete sequence PCR of *tag-dpb11* Plasmid A and YSG4. PCR parameters: Primers 921 and 922.

3.1.2 Construction and analysis of meiotic depleted N-terminal His tagged DPB11 *S. cerevisiae* strains

To characterise Dpb11's roles during meiosis, it is vital to determine what happens to cells where it is no longer expressed. The Dpb11 knockout being inviable (Araki *et al.*, 1995) may be due to its requirement in genetic processes outside of meiosis (Tanaka *et al.*, 2013); therefore, a method is needed to deplete Dpb11 levels during meiosis (md). Clb2 is a protein whose expression aligns with this principle (Dahmann and Futcher, 1995). As shown in (Gray *et al.*, 2013), integration of the Clb2 promotor region (P^{CLB2}) upstream of a target gene results in halted expression during meiosis.

3.1.2.1 Construction and validation *tag-dpb11-md* strains

The pre-existing *P^{CLB2}-Tag-DPB11 (tag-dpb11-md)* strains YSG678, YSG680, and YSG681 were made in the YSG29, YSG33 and YSG33 backgrounds, respectively. Following inoculation and DNA preparation, the same diagnostic PCR, as noted in Figure 3.1A, was performed on each strain alongside a WT control. This PCR was especially useful as, if the sequence was integrated incorrectly, a secondary WT band would be located at 1060 bp alongside the expected 2149 bp sequence. Using the same parameters/ machine as *tag-dpb11* resulted in the first PCR amplification producing no product as a 2-minute extension time was below NEB's recommended 1 minute per 1000 bases amplification time (*Guidelines for PCR Optimization with Taq DNA Polymerase | NEB*). As a result, an additional minute was added to the extension time. These changes enabled the visualisation of bands representing the correct 2149 bp PCR amplified sequence (Figure 3.7A), indicating that the Clb2 promotor was successfully integrated upstream of Dpb11.

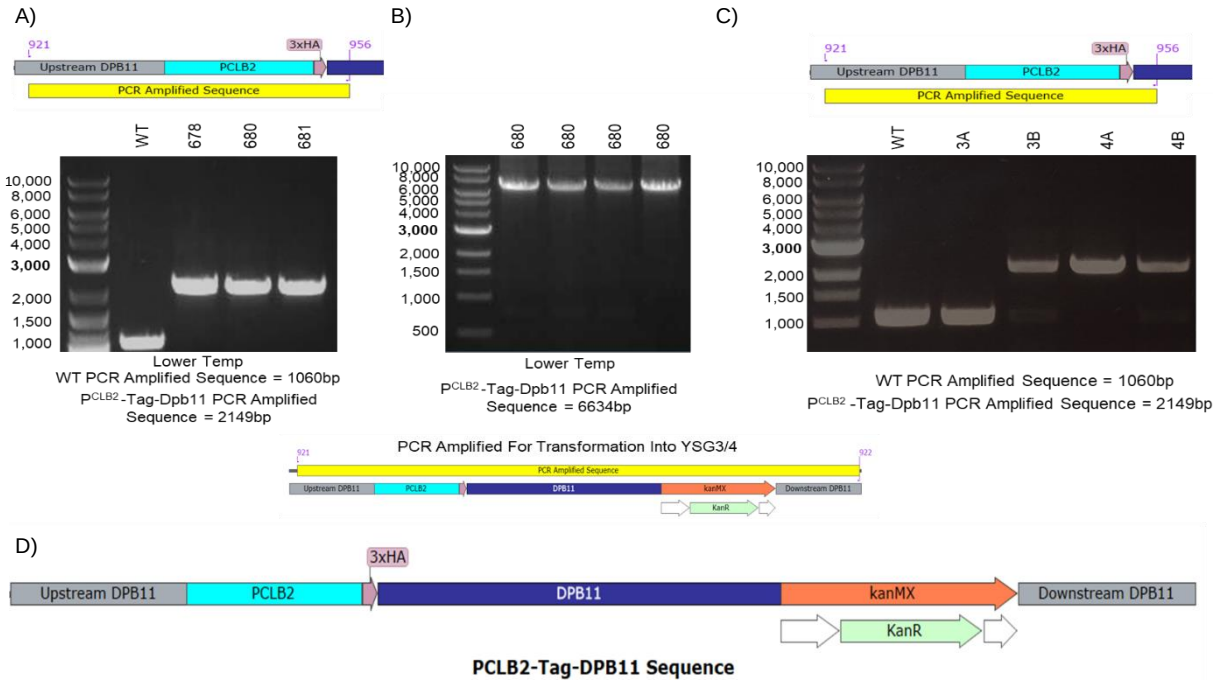

Figure 3.7 Gel electrophoresis of the pre-existing *tag-dpb11-md* mutants. Gel electrophoresis of the PCR amplified 2149 bp sequence containing the 6xHIS-3xHA N-terminal tag, upstream Dpb11 and Clb2 promotor. pre-existing *tag-dpb11-md* strains YSG678, YSG680, and YSG681 were examined. Primers 921 and 956. B) Complete cassette PCR of the pre-existing *tag-dpb11-md* strain YSG680. Primers 921 and 922. C) Repeat PCR from A) using transformed *tag-dpb11-md* strains 3A, 3B, 4A and 4B. Primers 921 and 956. D) The complete 6634 bp cassette sequence of *tag-dpb11-md*.

Given that the *tag-dpb11-md* mutation was only introduced into the YSG29 and YSG33 background strains, it was decided that integrating this mutation into the YSG3 and YSG4 backgrounds would validate whether the background strains had any impact on the meiotic phenotype. Initial PCR amplification of the complete cassette sequence using primers 921 and 922 displayed no banding. Subsequently, the annealing temperature was reduced by 2˚C, and the extension time was extended. A band representing a base pair length between 6 and 8 kb was observed during gel electrophoresis and determined to be the expected 6634 bp sequence (Figure 3.7B). This PCR was repeated four times to generate the high DNA concentration required for yeast transformation, as the four aliquots were combined during PCR cleanup. After nanodrop ensured that a high enough concentration was achieved, the sequence was transformed into YSG3 and YSG4. Using the same diagnostic PCR as (Figure 3.7A), the successful integration of the *tag-dpb11-md* cassette was observed within the 3B, 4A and 4B transformed strains, which were then labelled YSG793, YSG794, and YSG795, respectively.

3.1.2.2 Analysis and conclusions of *tag-dpb11-md* strains

Mating *tag-dpb11-md S. cerevisiae* mutants with their opposite mating types formed the diploids required for sporulation efficiency and spore viability. *tag-dpb11-md* strain YSG793 was mated with *tag-dpb11-md* strains YSG794 and YSG795, creating *tag-dpb11-md* diploid strains YSG876-YSG888, whilst *tag-dpb11-md* strain YSG678 was mated with *tag-dpb11-md* strains YSG680 and YSG681 to form diploids *tag-dpb11-md* strains YSG767-769 and YSG782-788. Following sporulation and dissection, spore viability and sporulation efficiency analysis observed some interesting findings when comparing the *tag-dpb11-md* YSG(29 x 33) diploids to the YSG(3 x 4) diploids created from the transformed haploids (Figure 3.8A/B).

The total spore viability of *tag-dpb11-md* (3 x 4) (96%, n = 128, SD = 1%) phenocopied WT (3 x 4) (p = 0.57) (97%, n = 95, SD = 2%), whereas *tag-dpb11-md* (29 x 33) (85%, n = 157,SD = 6%) showed a 12% (p = 0.0003) decrease in spore viability compared to WT (29 x 33) (96%, n = 96, SD = 2%). Notably the total sporulation efficiency of *tag-dpb11-md* (3 x 4) (75%, n = 1003, SD = 6%) did not phenocopy (p = 0.02) WT (3 x 4) (89%, n = 1791, SD = 6%) showing a 14% decrease, similar but to a less extent than the 85% (p = 1.85e-06) decrease observed between *tag-dpb11-md* (29 x 33) (12%, n = 1087, SD = 8%) and WT (29 x 33) (95%, n = 1034, SD = 1%). As shown in Figure 3.4B/C, changes to the background strain did not affect the spore viability observed within the *tag-dpb11* mutants. Since the only variation between the background strains was the addition of fluorescent proteins to separate locus and the meiotic phenotype remained consistent between YSG(3 x 4) and YSG(29 x 33), the different background was unlikely to result in the observed changes.

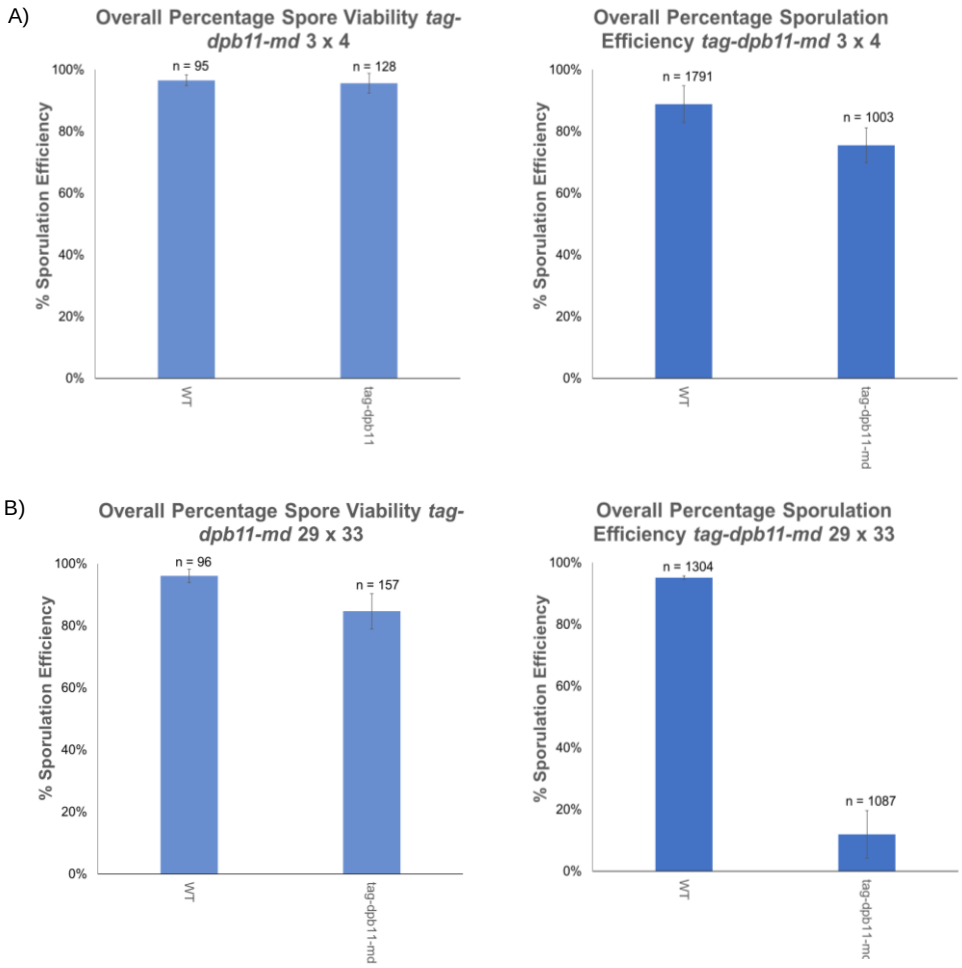

Figure 3.8: Spore viability and sporulation efficiency of *tag-dpb11-md* mutants A) Spore viability and sporulation efficiency of (3 x 4) WT control strains and the *tag-dpb11-md* (3 x 4) strains YSG876-YSG888. (p =0.54) (p =0.017) B) Spore viability and sporulation efficiency of the (29 x 33) WT control strains and the pre-existing *tag-dpb11-md* (29 x 33) strains YSG767-769 and YSG782-788. (p =0.00037) (p =1.85E-06) (Spore Viability: N = number of tetrads dissected. Sporulation Efficiency: N = number of sporulated/un-sporulated cells counted, Error Bars = Standard Deviation.)

To determine if the changes in meiotic phenotype observed in Figure 3.8A/B were a result of ineffective depletion of Dpb11 by the Clb2 promotor, a meiotic time course (2.2.8.3) was performed on WT controls YSG5 and YSG236 along with *tag-dpb11-md* (29 x 33) strains YSG767 and YSG76, and *tag-dpb11-md* (3 x 4) strains YSG883 and YSG878. The meiotic time course was performed, based on the meiotic depletion of Mec1 observed in *Mec1-md* (P^{CLB2}-Mec1) strains (Gray *et al.*, 2013). Protein preparation (2.2.7.1) of the samples indicated slight variation in protein expression between the *tag-dpb11-md* strains and WT within both backgrounds; however, the variation in band intensity may have resulted from different exposure times (Figure 3.9A). As the protein preparations were successful, the protein was transferred from the TCE gel onto a PVDF membrane via the process outlined in (2.2.7.3). A primary rabbit anti-HA antibody and a secondary fluorescent goat anti-rabbit antibody were used to visualise the levels of tagged Dpb11 expression via western blotting (2.2.7.4) (Figure 3.9B). Dpb11 has

a molecular weight of 87,258.6 DA, so banding between 75 kDa and 100 kDa was expected at T_0 before sequentially lowering in intensity within the first few hours (Gray *et al.*, 2013). Only non-specific banding was detected within the (3 x 4) and (29 x 33) strains (Figure 3.9B). The *tag-dpb11* strains were still under construction/analysis, so a 'WT' Dpb11 expression profile could not be examined and compared to the *tag-dpb11-md* strains. The expression of Dpb11 within vegetative *tag-dpb11* (and *dpb11-tag*) strains was subsequently examined separately.

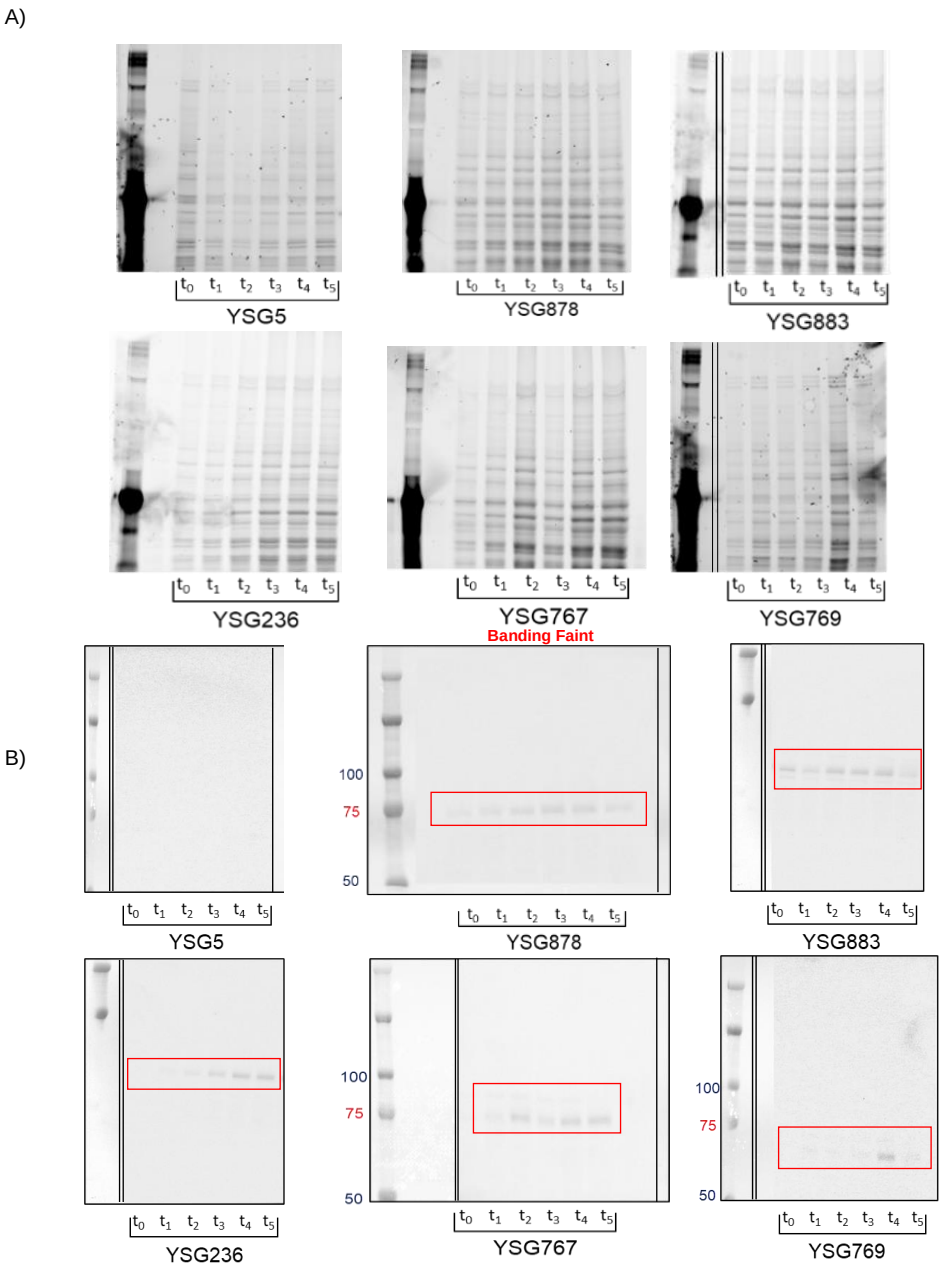

Figure 3.9 Protein extraction and western blot analysis of *tag-dpb11-md* (3 x 4) and (29 x 33) strains. A) Protein was extracted from samples taken at hourly intervals of a five-hour meiotic time. The strains examined were WT YSG5 and YSG236 and *tag-dpb11-md* YSG769, 767, 878 and 883. (7.5% TCE Gel 2.2.7.2). B) UV detector was used to visualise levels of Dpb11 protein expression from each of the samples (Antibodies: primary anti-HA, secondary goat anti-rabbit).

Protein extraction (2.2.7.1) was performed on inoculated WT and *tag-dpb11-md* strains. These steps were attempted twice, but both resulted in smearing present on the TCE gel, indicating an error during the protein preparation. Due to time constraints, a third attempt was not made. Since the levels of Dpb11 expression within the *tag-dpb11-md* strains could not be determined, no definitive conclusions could be

made on whether the insertion of the Clb2 promotor upstream from Dpb11 has resulted in the depletion of Dpb11 during meiosis. A band representing Dpb11 should be present at T_0 (Figure 3.8D); however, its absence suggests that future calibration is needed to display its expression profile accurately. The smearing of protein bands suggests an error in the protein procedure that went unnoticed, such as the collection of supernatant rather than the pellet.

If given extra time, another repeat of the protein extraction would be performed to examine WT levels of Dpb11 expression within vegetative *S. cerevisiae* strains. A meiotic time course including *tag-dpb11* and *tag-dpb11-md* strains would then allow the comparison of WT Dpb11 expression during meiosis to the P^{CLB2-}mediated meiotic depletion of Dpb11 within both backgrounds. Determining which of the two background strains (if any) are correctly depleting Dpb11 would ensure the conclusions made on Dpb11's importance during meiosis are correct. Alternatively, manually inducing/repressing Dpb11 expression during meiosis by placing the DPB11 gene under the GAL/ Cu^{2+} promotor could make a valuable comparison to the P^{CLB2} Dpb11 strains. Manually turning off the DPB11 gene at T_0 may lead to a more accurate representation of a Dpb11 knockout as the P^{CLB2} promotor has been shown to procedurally reduce protein expression within the first few hours following KAc inoculation (Gray *et al.*, 2013).

3.2 Construction and analysis of *dpb11-tag* and *dpb11-tag-md* strains

Despite vegetative N terminal tagged Dpb11 (*tag-dpb11)* strains showing a WT phenotype, initial observations indicated that an unknown variable resulted in a meiotic phenotype dissimilar to WT (Figure 3.5A). This outcome could be explained by the N-terminal 6xHis-3HA tag causing misfolding within Dpb11 and subsequently affecting its binding activity or molecular interference from the tag interacting with Dpb11's binding partners. Previous work has been carried out using C-terminally His-tagged Dpb11, so it was decided to create C terminal tagged Dpb11 (*dpb11-tag)* and meiotic depleted C terminal tagged Dpb11 (*dpb11-tag-md)* strains and characterise their meiotic phenotypes (Dhingra *et al.*, 2015).

Although later examination of the *tag-dpb11* strains determined that the N-terminal tag did not affect the meiotic phenotype (Figure 3.4B/C), we concluded it was best to continue with the analysis of *dpb11-tag* and *dpb11-tag-md* since (Navadgi-Patil and Burgers, 2009) showed that the C-terminal tail of Dpb11 was not required in DNA replication and the S phase checkpoint but indispensable for the G2/M checkpoint. If the *dpb11-tag* inhibits the binding activity of the Ddc2-Mec1 complex to its C-terminus, then a noticeable decrease in sporulation efficiency and spore viability could be observed (Mordes, Nam and Cortez, 2008).

3.2.1 Constructing C-terminal His tagged DPB11 *S. cerevisiae* strains

Tagging the C-terminal region of Dpb11 allows the quantification of protein expression via protein extraction, SDS PAGE and western blot analysis with the benefit of clarifying if an extension to the C-terminus affects the expression and activity of Dpb11 within vegetative and meiotic cells. Identical background strains, YSG3, YSG4, YSG29, and YSG33, were used to cross-examine the strains.

3.2.1.1 Construction and validation of *dpb11-tag*

To generate a high concentration of *dpb11-tag* cassette for use in *S. cerevisiae* transformation, the cassette was first designed into a vector (plasmid) using the New England Biolabs® NEBuilder® Assembly Tool. PCR amplification using NEBuilder® designed primers results in the fragments containing single-stranded DNA (tails) at each end that align to tails on adjacent fragments. During Gibson assembly, the fragments are incubated, allowing the fragments to bind together and form a complete plasmid. The plasmid backbone consisted of an origin of replication (Ori) alongside the ampicillin resistance gene (AmpR) and its promotor (P^{AmpR}). Plasmid-encoded initiation proteins recognise the Ori site initiating plasmid replication (del Solar *et al.*, 1998), while AmpR provides resistance to Ampicilin. LB-AMP plates select for *E. coli* that have successfully incorporated a plasmid containing the AmpR gene. While the Dpb11 and downstream Dpb11 regions provide homology between the cassette and the integration site, enabling integration into the *S. cerevisiae* genome.

Three fragments were designed to form the *dpb11-tag* plasmid, the first of which was 'END+KanMX+AmpR+ATG', a large fragment designed using the pre-existing *tag-dpb11* plasmid consisting of dpb11's end codon, the kanamycin resistance gene KanMX, downstream Dpb11, the origin of replication, the AmpR and its promotor and the dpb11 start codon. Two further fragments completed the *dpb11-tag* cassette, a DPB11 fragment consisting of the complete Dpb11 gene excluding its start and end codon and a 6His-3HA tag fragment.

A)

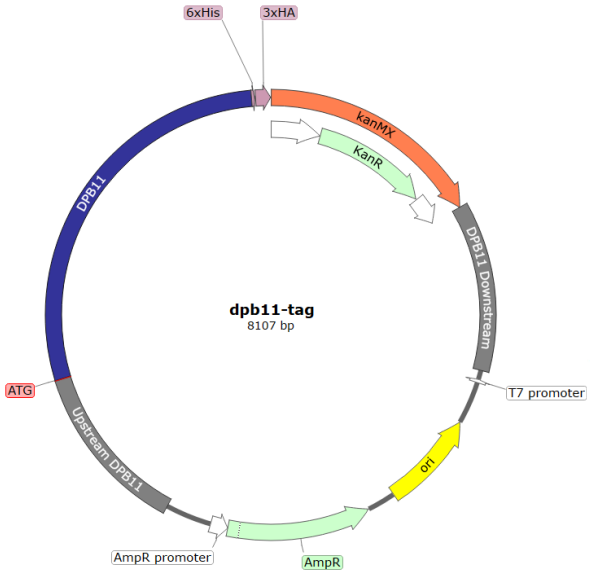

B)

Component Fragments

Name	Length	Produced by
END+KanMX+Ori+AmpR+ATG	5718	PCR
DPB11	2315	PCR
6His-3HA	134	PCR

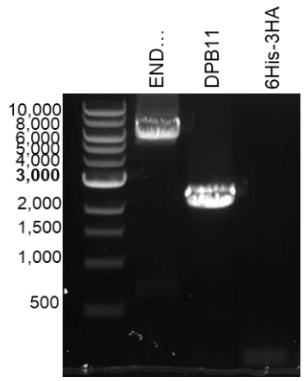

Figure 3.10: Design of *dpb11-tag plasmid* and construction of its fragments. A) Depiction of the *dpb11-tag* plasmid showing the 6xHis-3HA tag located at its C-terminus prior to the END codon. B) Table of fragment lengths required in the construction of *dpb11-tag* alongside the gel electrophoresis of each fragment following PCR amplification. PCR parameters: 'END+KanMX+AmpR+ATG' fragment, Primers 1170 and 1171. 'DPB11' fragment, Primers 1172 and 1173. '6His-3HA' fragment, Primers 1174 and 1175.

The 'END+KanMX+AmpR+ATG' fragment amplified from the *tag-dpb11* plasmid showed smearing but was believed to be the correct length as the bottom of the band was located below 6 kb (Figure 3.10B). In hindsight, similar to observations made in Figure 3.2, the fragment may be ~1 kb longer than expected, as this is where the bright banding ends. Due to the 6His-3HA fragment's 134 bp length, it exhibited a less pronounced band following its amplification (Figure 3.10B) from plasmid pSG11 (2.1.2.1), and until DNA sequencing of the complete plasmid, it was impossible to determine if the sequence was correct. The DPB11 fragment exhibited a high-intensity band at the correct location (Figure 3.10B) and was assumed to be correct. Following the nanodrop of each fragment, it was decided to continue with Gibson assembly.

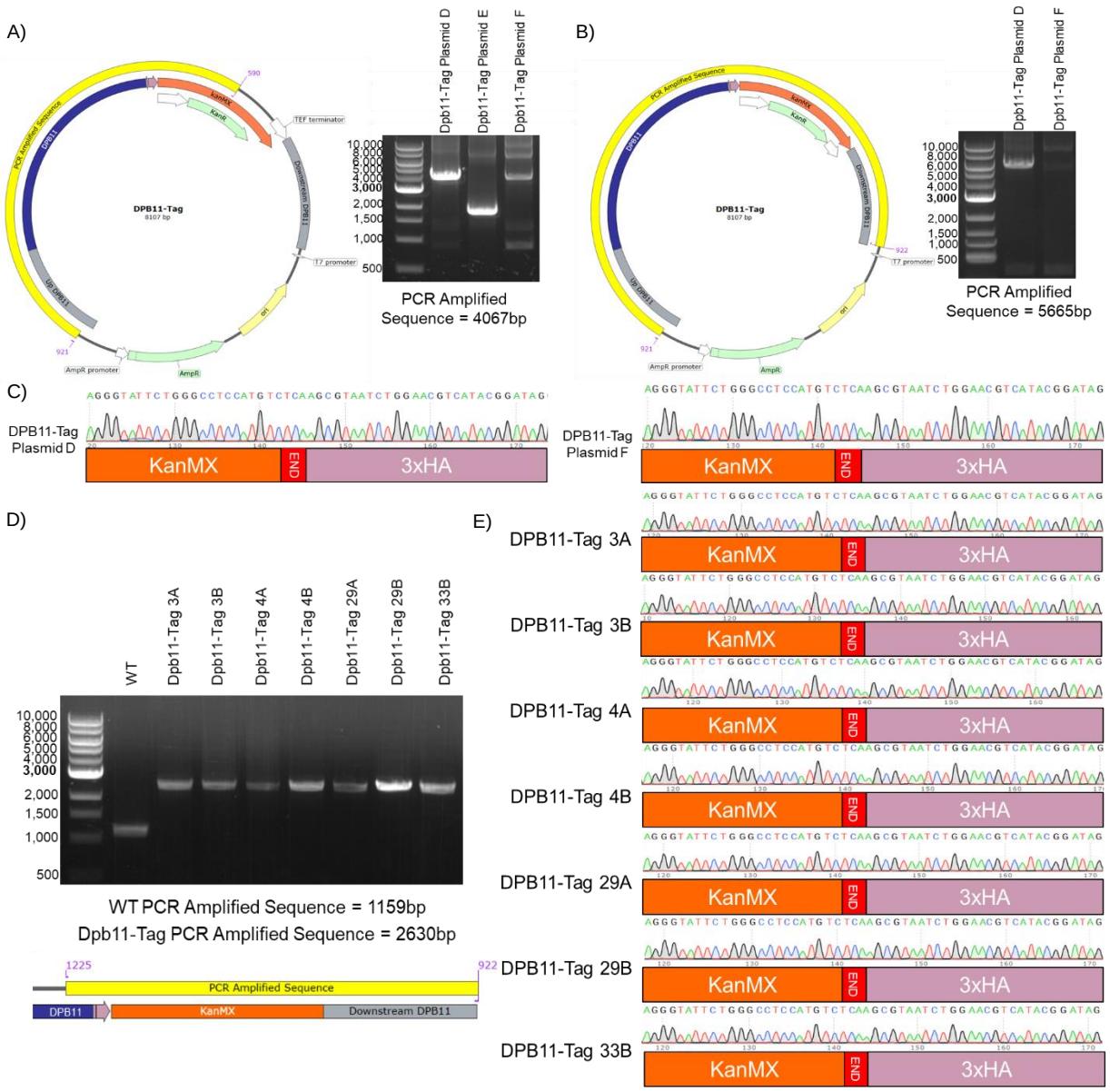

Figure 3.11 *dpb11-tag* plasmid validation and transformation. A) Diagnostic PCR amplification of *dpb11-tag* plasmids D, E, and F. Primers 921 and 590. B) Complete cassette PCR of *dpb11-tag* plasmids D, and F. Primers 921 and 922. C) DNA sequencing results of Plasmids D and F using reverse primer 1192. D) Diagnostic PCR of *dpb11-tag* transformed strains 3A, 3B, 4A, 4B, 29A, 29B, and 33B. Primers 1225 and 922. E) DNA sequencing of dpb11-tag transformed strains using reverse primer 1192.

Following Gibson assembly (2.2.5.1), three *E. coli* colonies (A, B, and C) were selected from the LB-Amp plate and inoculated in LB-Amp broth. After 13 hours of growth, a mini-prep was performed on each colony to isolate their plasmids. Each sample was nano-dropped to identify the presence of colonies before performing diagnostic PCRs. DNA sequencing indicated that the chosen plasmid (C)

had an addition point mutation within the 3HA region that would have resulted in the END codon being out of frame. Subsequently, three new colonies (D, E, and F) were inoculated from the LB-Amp selection plate. A diagnostic PCR of plasmids D, E and F (Figure 3.11A) indicated that at least two fragments had successfully integrated into plasmid D. DNA sequencing of plasmid D (Figure 3.11C) showed the 6His-3HA tag in-frame at the dpb11 C-terminus tailed by the END codon and KanMX. After a complete cassette PCR (Figure 3.11B) In preparation for transformation, a complete cassette PCR was performed on plasmid D (Figure 3.11B, similar band length to Figure 3.2C) and repeated to ensure a high enough concentration. Colonies 3A, 3B, 4A, 4B, 29A, 29B and 33B were inoculated from their G418 selection plates and underwent genomic DNA preparation. After ensuring the genomic DNA preparation was successful via nanodrop, a diagnostic PCR was performed using the forward primer Dpb11+ 2125 bp (1225) and the complete cassette reverse primer 922. Although this PCR ensured the successful integration of the *dpb11-tag* cassette at the correct location, the PCR amplified sequence for each transformation was still cleaned up and sent to sequencing with reverse primer 1192 to ensure no mutations were introduced during the transformation. Once the results detected no mutations within any *dpb11-tag* strain, they were labelled YSG963-969.

3.2.1.2 Analysis and conclusions of *dpb11-tag*

dpb11-tag YSG3 background colonies YSG963 and 964 were mated with the *dpb11-tag* YSG4 background colony YSG965 to create *dpb11-tag* diploids YSG1000-1005, whilst YSG29 *dpb11-tag* background colony YSG968 was mated with *dpb11-tag* YSG33 background colony YSG969 to create *dpb11-tag* diploids YSG1029-1031.The newly created diploids were inoculated and then sporulated for three days before spore viability and sporulation efficiency analysis.

The spore viability observed in both the *dpb11-tag* (94%, n = 94, SD = 4%) (3 x 4) background (p = 0.15) and the *dpb11-tag* (98%, n = 45, SD = 3%) (29 x 33) background (p = 0.29) strains was statistically similar to WT(97%, n = 95, SD = 2%)/(96%, n = 96, SD = 2%) (Figure 3.12A/B). Similarly the sporulation efficiency in both *dpb11-tag* (91%, n = 717, SD = 6%) (3 x 4) background (p = 0.63) and the *dpb11-tag* (95%, n = 649, SD = 1%) (29 x 33) background (p = 0.41) strains was statistically similar to WT (89%, n = 1791, SD = 6%)/(95%, n = 1034, SD = 1%) (Figure 3.12A/B). Therefore, it was concluded that tagging the C-terminus of Dpb11 had no notable impact on the meiotic phenotype of *S. cerevisiae* and potentially no impact on the expression and activity of Dpb11 (Figure 3.12A/B). This data aligns with the phenotype observed in the N-terminally tagged Dpb11 (*tag-dpb11)* diploid strains (Figure 3.4B/C, Figure 3.12C) YSG892, YSG893, YSG894, and YSG895, further proving that the non-WT meiotic phenotype initially observed was incorrect.

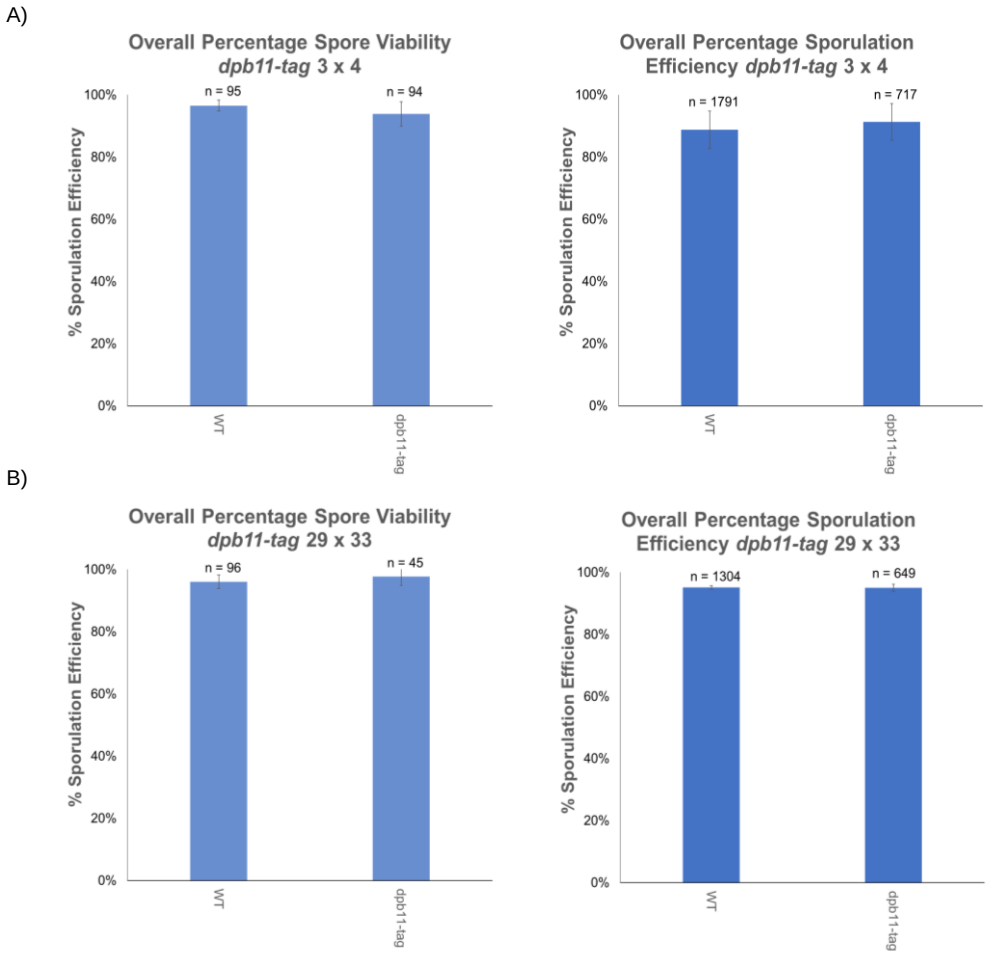

Figure 3.12: Spore viability and sporulation efficiency of *dpb11-tag* diploid strains. Spore viability and sporulation efficiency of (3 x 4) WT control strains and the *dpb11-tag* (3 x 4) diploids YSG1000-1005. (p =0.15) (p =0.63) B) Spore viability and sporulation efficiency of the (29 x 33) WT control strains and the *dpb11-tag* (29 x 33) diploids YSG1029-1031. (p =0.29) (p =0.41) (Spore Viability: N = number of tetrads dissected. Sporulation Efficiency: N = number of sporulated/un-sporulated cells counted, Error Bars = Standard Deviation.)

Further issues cropped up when amplifying the complete cassette sequence of *dpb11-tag* from plasmid D (Figure 3.11B), as the sequence was roughly 1 kb larger than expected. No extra sequence was identified in the Upstream+DPB11 gene region (Figure 3.11A), suggesting the region was located downstream of KanMX as disruption to KanMX would have resulted in the colonies not growing on the G418 selection plate. The large fragment was created from the pre-existing *tag-dpb11* fragment, which showed similar issues regarding a larger-than-expected complete sequence fragment (Figure 3.10B). Similar *to tag-dpb11*, no extra sequence could be detected within the downstream region following transformation (Figure 3.11D). To further clarify this, a repeat diagnostic PCR of the downstream region within the dpb11-tag transformants using primers 1225 and 922 could be completed with 2 minutes extra amplification time to account for the integration of a second downstream DPB11 fragment. Similar

to the pre-existing *tag-dpb11* plasmid A, a PCR from DPB11 into the plasmid backbone could help identify the extra region.

3.2.2 Constructing meiotic depleted C-terminal His tagged DPB11 *S. cerevisiae strains*

Alongside creating C-terminally tagged Dpb11 strains, it was decided to create C-terminally tagged meiotic depleted Dpb11 strains (*dpb11-tag-md*). Comparison of the meiotic phenotype between *tag-dpb11-md* and *dpb11-tag-md* would determine if C vs N terminally tagging Dpb11 had any effect on meiotic processes following Dpb11s depletion. Notably, it would also clarify the correct meiotic phenotype between the *tag-dpb11-md* background strains, as such transformation into background strains YSG3, 4, 29, and 33 was required.

3.2.2.1 Construction and validation of *dpb11-tag-md* A

Using NEBuilder® a *dpb11-tag-md plasmid* was designed from the premade *tag-dpb11-md* plasmid (2.1.2.3). Three fragments were required to transfer the tag from the N-terminus to the C-terminus in a similar method to 2.1.2.4. The central fragment consisted of the DPB11 END codon, KanMX marker, downstream DPB11, the bacterial Ori and AmpR/promotor, the DPB11 upstream, P^{CLB2}, and the DPB11 start codon. The two remaining fragments were the 3HA tag and the DPB11 complete gene. PCR amplification and nanodrop of the three fragments indicated that they were the correct size and concentration (Figure 3.13B), so it was decided to clean up the fragments and move on to Gibson assembly.

A)

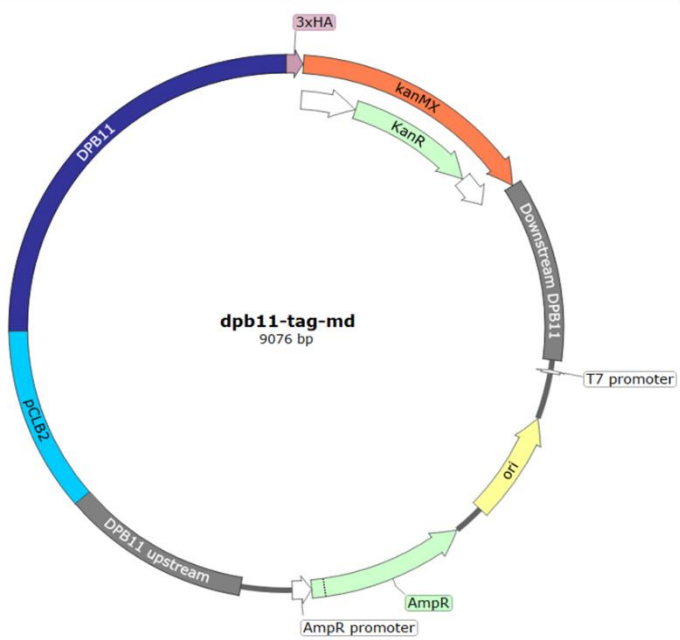

B)

Component Fragments

Name	Length	Produced by
3HA	110	PCR
KanMX+Ori+AmpR+pCLB2	6717	PCR
DPB11	2309	PCR

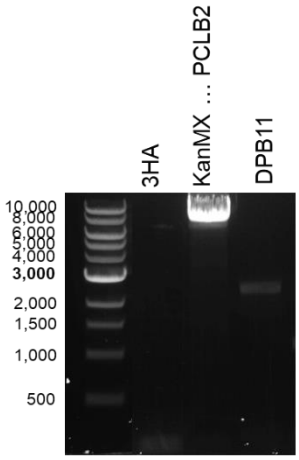

Figure 3.13 Design of *dpb11-tag-md A plasmid* and construction of its fragments. A) Depiction of the *dpb11-tag-md*. B) Table of fragment lengths required in the construction of *dpb11-tag-md* alongside the gel electrophoresis of each fragment following PCR amplification. PCR parameters: '3HA' fragment, Primers 1176 and 1177. 'KanMX+Ori+AmpR+pCLB2' fragment, Primers 1178 and 1179. 'DPB11' fragment, Primers 1180 and 1181.

Following incubation, the plasmids were transformed into *E. coli* (2.2.5.2). After inoculating selected colonies in LB-AMP, the cultures were mini-prepped and nano-dropped to ensure the presence of plasmids. Diagnostic PCRs were performed using primers 921 and 590 on Plasmids D-L, followed by complete cassette PCRs using primers 921 and 922 (Figure 3.14A/B). DNA sequencing of plasmids D-L revealed that six of the seven plasmids had unsuccessfully integrated the 3HA tag, and plasmid D had integrated an incorrectly amplified 3HA tag (Figure 3.14C). Since the 3HA-tag consists of three repeated HA sequences, primers 1176 and 1177 have a high homology with multiple regions within the tag, resulting in high levels of inconsistency between the PCR amplified sequences and due to the small size of the fragment, it had a small likelihood of integrating into the plasmid. Due to the successful integration of the 6xHis-3xHA tag at the C-terminus of Dpb11 within the *dpb11-tag* strains (Figure 3.11D), it was decided to design a new plasmid using *dpb11-tag* as a backbone.

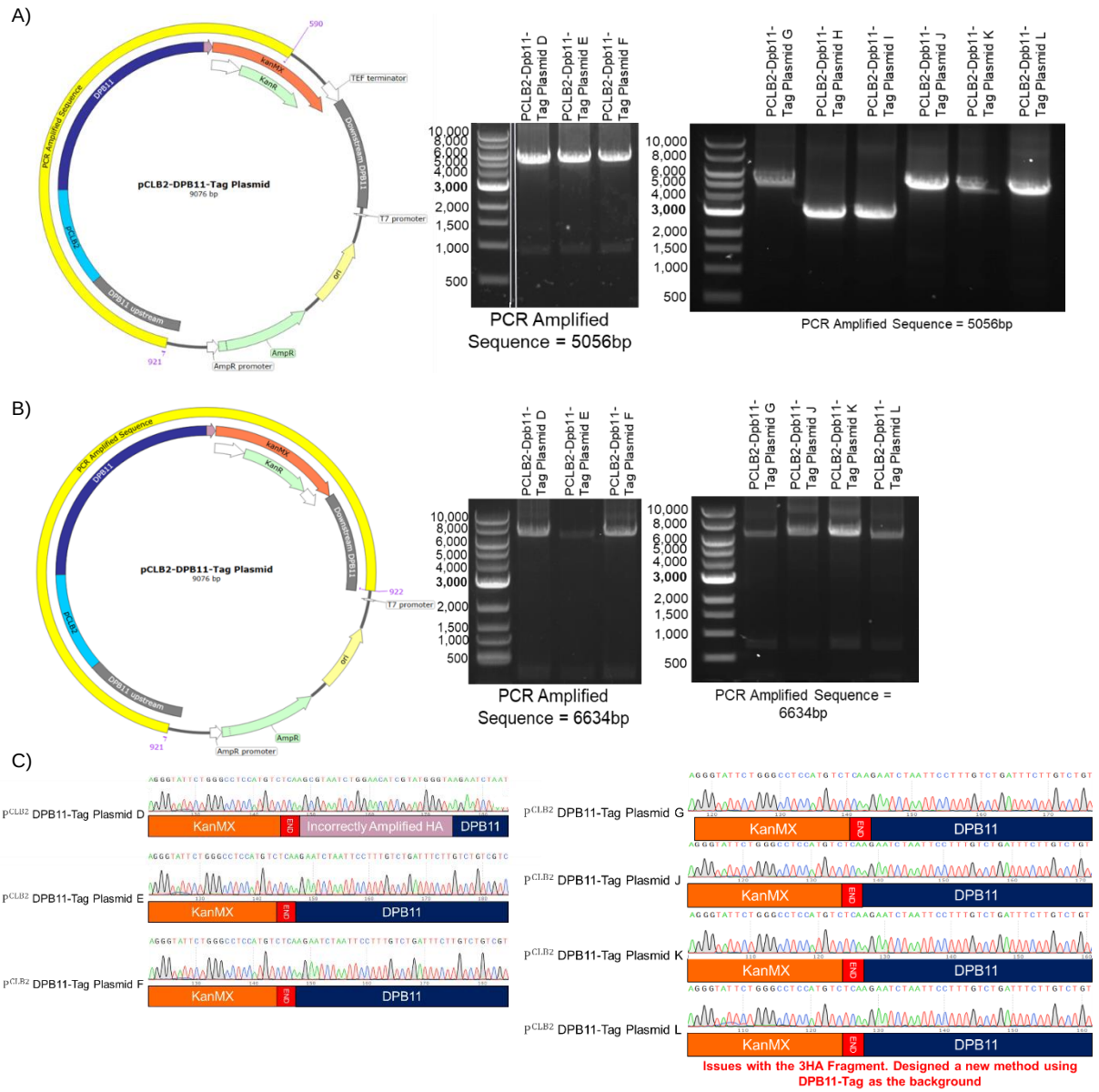

Figure 3.14 *dpb11-tag-md* A plasmid validation and transformation. A) Diagnostic PCR amplification of *dpb11-tag-md A* plasmids D-L. Primers 921 and 590. B) Complete cassette PCR of *dpb11-tag-md A* plasmids D-G and J-L. Primers 921 and 922. C) DNA sequencing results of plasmids D-G and J-L using reverse primer 1192.

3.2.2.2 Construction and validation of *dpb11-tag-md* B

Due to the inconsistencies observed in Figure 3.14 and the successful transformation of 6xHis-3xHA at the C terminus of DPB11, the next step was to design a *dpb11-tag-md* plasmid using the *dpb11-tag* plasmid as a backbone. Notably, this would result in a 6xHis-3HA tag located at the C-terminal region of the Dpb11 protein rather than the 3xHA tag in *tag-dpb11-md.* The meiotic phenotype of the *dpb11-tag* strains was unaffected by integrating a 6xHis-3HA tag at its C-terminus (Figure 3.11), so designing

a new plasmid using NEBuilder® was initiated. Two fragments were required to create the *dpb11-tag-md* plasmid: the 7889 kb backbone fragment made from *dpb11-tag* (2.1.2.4) and the Clb2 promoter fragment amplified from *tag-dpb11-md*. PCR amplification of the backbone fragment identified a ~1 kb larger than predicted sequence (Figure 3.15B). The extra sequence aligns with the observations in Figure 3.10, where the larger-than-expected fragment successfully integrated the correct cassette sequence into the *dpb11-tag* transformations.

The P^{CLB2} promotor fragment was successfully amplified and had the correct sized sequence (Figure 3.15B). As the plasmid was constructed using two fragments, the parameters for Gibson assembly needed to be adjusted accordingly. The fragments needed to be a total of 0.02–0.5 pmols rather than 0.2–1.0 pmoles, and the incubation time was reduced by 35 minutes. Bacterial transformation and selection were then conducted as previously outlined.

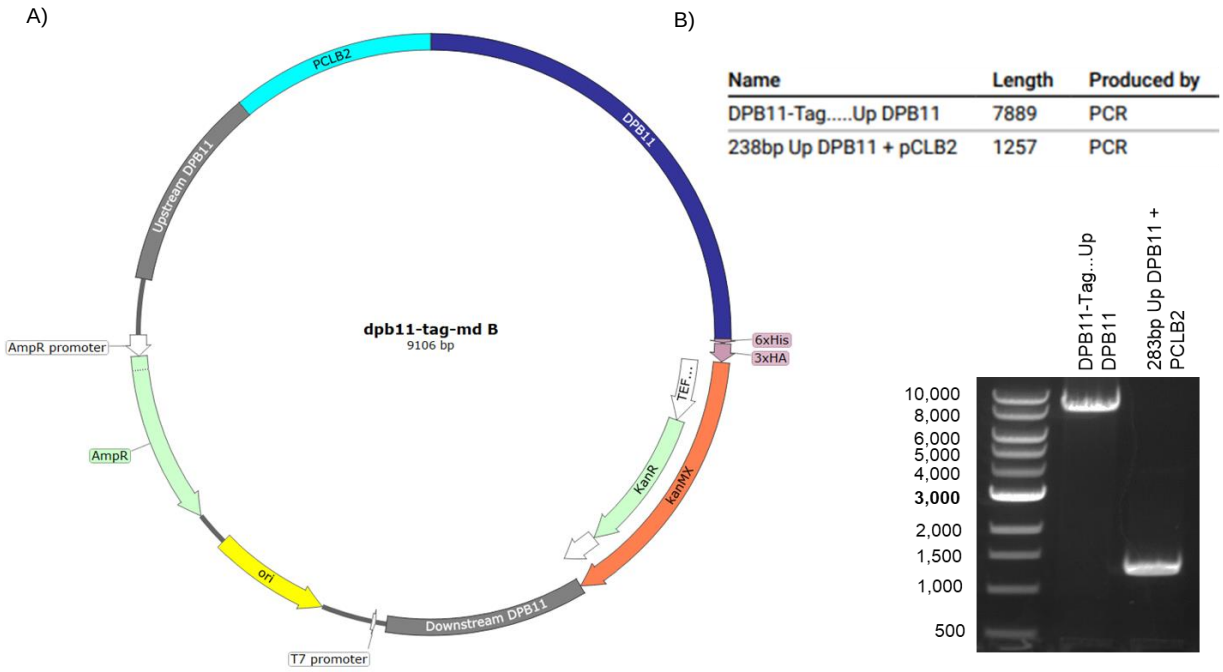

Figure 3.15: Design of *dpb11-tag-md B plasmid* and construction of its fragments. A) Depiction of the *dpb11-tag-md* plasmid. B) Table of fragment lengths required in the construction of *dpb11-tag-md B* alongside the gel electrophoresis of each fragment following PCR amplification. PCR parameters: 'DPB11-Tag….Up DPB11' fragment, Primers 1205 and 1206, '238 bp Up DPB11 + pCLB2' fragment, Primers 1203 and 1204.

Diagnostic PCRs of the mini-prepped plasmids A and B (Figure 3.16A/B) indicated that the complete cassette was the correct length and that the fragments had successfully integrated. The correct-sized complete cassette sequence indicated that the extra 1 kb region observed in Figure 3.15B was

integrated into the backbone rather than the cassette sequence. Since the tagged region of *dpb11-tag* was already sequenced, it was decided that sequencing the C-terminal 6xHis-3HA tag was unnecessary (Figure 3.11).

Using the method outlined in 2.2.5.3, the amplified cassette was transformed into YSG3, 4, 29. 33 successfully selecting colonies within backgrounds YSG3, 4, and 29. After Inoculation, DNA extraction and nano-drop analysis, diagnostic PCRs depicted the successful integration of the P^{CLB2} region upstream of DPB11 within transformed colonies 3B, 4E and 29B (Figure 3.16D). After mating *dpb11-tag-md* colony 29B with WT YSG33, the tetrads were dissected and replica-plated to cross the cassette region into the YSG33 background. The *dpb11-tag-md* strains 3B, 4E, 29B, replica-plated 29 and replica-plated 33 were labelled YSG970, 984, 971, 992 and 993, respectively.

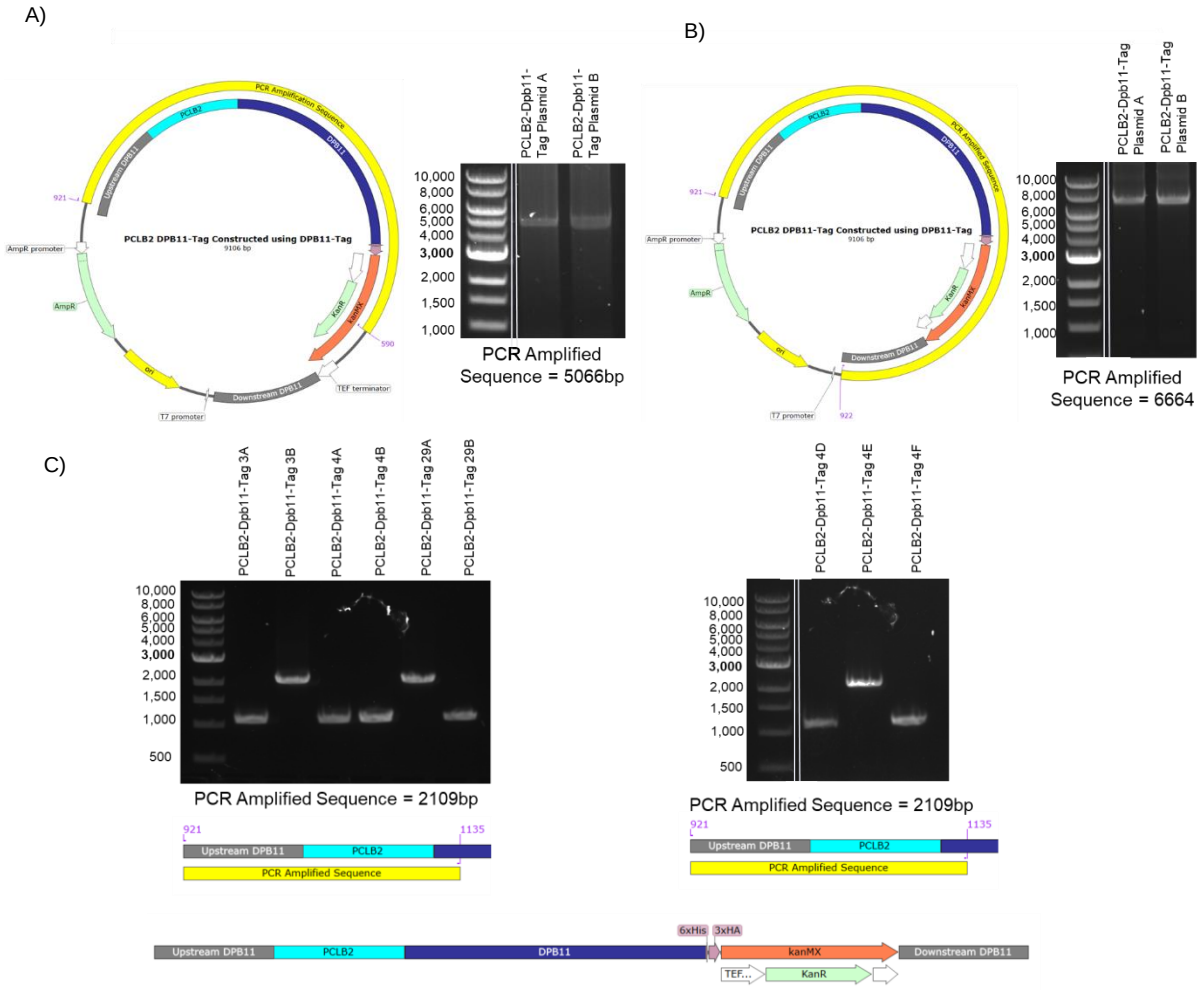

Figure 3.16: *dpb11-tag-md B* plasmid validation and transformation. A) Diagnostic PCR amplification of *dpb11-tag-md B* plasmids A and B. Primers 921 and 590. B) Complete cassette PCR of *dpb11-tag-md B* plasmids A and B. PCR parameters: Primers 921 and 922. C) Diagnostic PCR of *dpb11-tag-md B* transformed strains 3A, 3B, 4A, 4B, 4D, 4E, 4F, 29A and 29B. Primers 921 and 1135.

3.2.2.3 Analysis and conclusions of *dpb11-tag-md* B

Haploid *dpb11-tag-md* YSG3 background strain YSG970 was mated with *dpb11-tag-md* YSG4 background strain YSG984 to create *dpb11-tag-md* diploid colonies YSG1006-1008, whilst the *dpb11-tag-md* YSG29 background strain YSG992 was mated with the *dpb11-tag-md* YSG33 background strain YSG993 resulting in the formation of *dpb11-tag-md* diploid colonies YSG1034-1034. The spore viability of *dpb11-tag-md* (3 x 4) (96%, n = 48, SD = 2%) was statistically similar (p = 0.57, to the WT (3 x 4) controls (97%, n = 95, SD = 2%), whilst *dpb11-tag-md* (29 x 33) (99%, n = 79, SD = 2%) was 3% (p = 0.04) higher than the WT (96%, n = 96, SD = 2%) (Figure 3.17A/B). Similarly, the sporulation efficiency of *dpb11-tag-md* (3 x 4) (85%, n = 511, SD = 12%) and *dpb11-tag-md* (29 x 33) (94%, n = 508, SD = 2%) were statistically similar (p = 0.32, p = 0.23) to their WT counterparts (89%, n = 1791, SD = 6%)/ (95%, n = 1034, SD = 1%) (Figure 3.17A/B). Notably, the *dpb11-tag-md* (3 x 4) mutants showed a larger variety in the average (SD = 12) sporulation efficiency between each strain. To further explore this range, new diploid mutants could be created and then analysed to determine if the variation resulted from environmental factors rather than the mutation itself.

The meiotic-depleted stains phenocopying WT could indicate that Dpb11 does not play a significant role within the pachytene checkpoint. This indicates that Mec1 activity is completely independent of Dpb11, whose role could be replaced by a meiotic homolog similar to Rad9 and Rad53 being replaced by Hop1 and Mek1 (Chuang, Cheng and Wang, 2012) especially seeing as Dpb11 has no identified interactions with Rad9's meiotic homolog Hop1 (BioGrid Interactors Database). Similarly, Dpb11 may not be required for the hyperphosphorylation positive feedback loop exhibited by Mec1 during the DNA Damage checkpoint within the pachytene checkpoint (Mordes, Nam and Cortez, 2008). The main caveat with this theory is that the premade *tag-dpb11-md* (29 x 33) background strains exhibited a differing meiotic phenotype, indicating that Dpb11 does play a role during meiosis. Until Western blot analysis of Dpb11s expression profile under the Clb2 promotor is characterised, no concrete conclusions can be made. We hoped that creating *tag-dpb11-md mec1-md* doubles would shed more light on the situation (Chapter 13.3.2.2).

A)

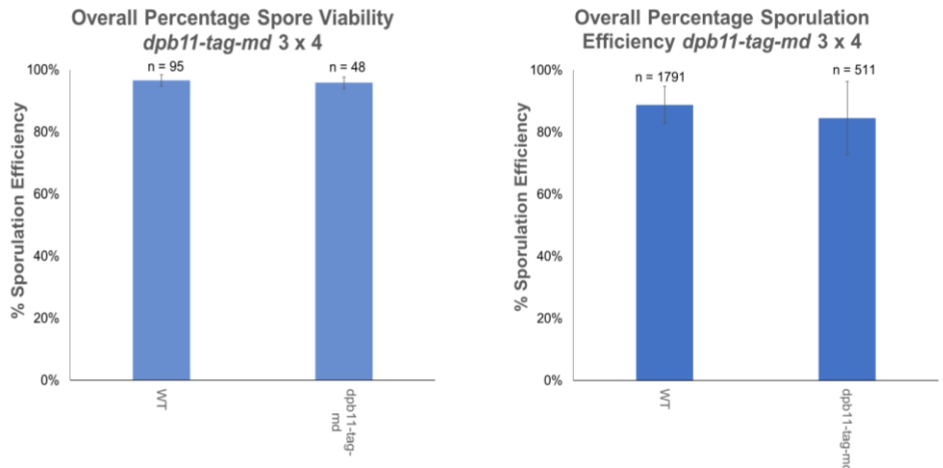

B)

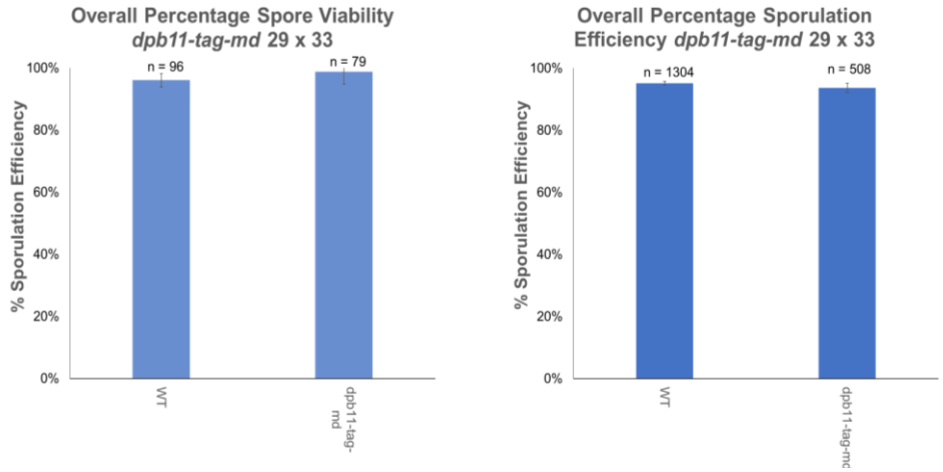

C)

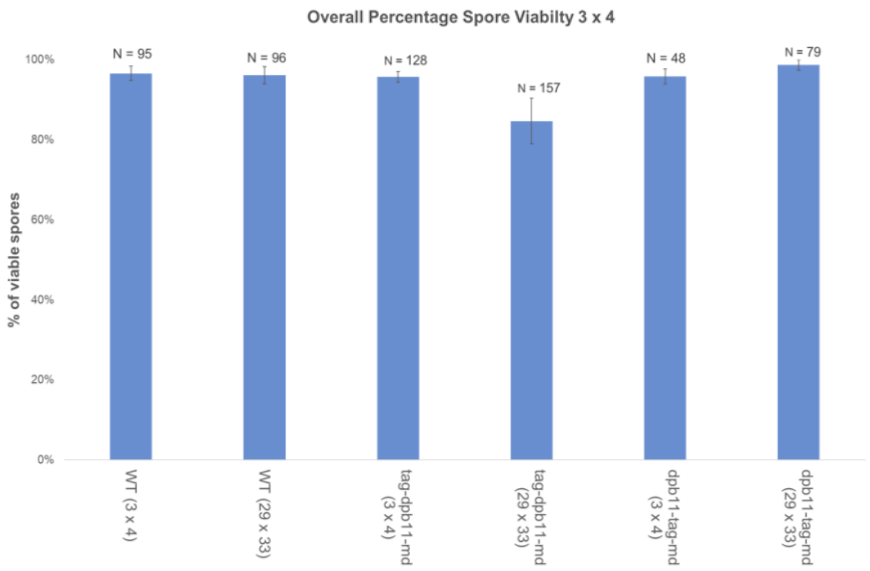

Figure 3.17: Spore viability and sporulation efficiency of *dpb11-tag-md* diploid strains. Spore viability and sporulation efficiency of (3 x 4) WT control strains and the *dpb11-tag-md* (3 x 4) diploids 1006-1008. (p =0.57) (p =0.32) B) Spore viability and sporulation efficiency of the (29 x 33) WT control strains and the *dpb11-tag-md* (29 x 33) diploids 1034-1034. (p =0.041) (p =0.23) C) Spore viability data from WT, *tag-dpb11-md* and *dpb11-tag-md* within the (3 x 4) and (29 x 33) backgrounds. (Spore Viability: N = number of tetrads dissected. Sporulation Efficiency: N = number of sporulated/un-sporulated cells counted, Error Bars = Standard Deviation.)

3.3 Construction and analysis of tagged *mec1* and *mec1-md* strains

Mec1 plays a vital role in the DNA damage checkpoint (Mordes, Nam and Cortez, 2008) and the pachytene checkpoint (Gray *et al.*, 2013). Research has shown that within the DNA damage checkpoint, Dpb11 is directly involved in the hyperphosphorylation activity of Mec1, but its requirement in Mec1 activity within the pachytene checkpoint has yet to be identified. Meiotic-depleted Mec1 (*mec1-md*) has been previously characterised by (Gray *et al.*, 2013), exhibiting 45-60% spore viability compared to the ~96/97% observed in WT. To determine if Dpb11 has roles during meiosis independent from Mec1, it was necessary to compare a *mec1-md, dpb11-md* double mutant to the single *mec1-md* strain. Therefore, a thorough analysis was required before creating any doubles to ensure the strains behaved as expected.

3.3.1 Constructing N and C-terminal His tagged MEC1 *S. cerevisiae* strains

Although research has been previously conducted on N-terminally tagged *mec1-md* (Gray *et al.*, 2013), it was decided that the creation of a *tag-mec1* strain was required to ensure the tag did not affect the strain's meiotic phenotype. Later, issues regarding the creation of *tag-mec1* led to the creation of the *mec1-tag*.

3.3.1.1 Construction and validation *tag-mec1* A

The first attempt at creating a *tag-mec1* plasmid required five PCR-amplified fragments. These included an upstream Mec1 fragment, a downstream Mec1 fragment, the Mec1 gene, a 6xHis Tag fragment and a KanMX fragment. pSG11 was used as the plasmid backbone created using a restriction digest of the pSG11 plasmid using enzymes NdeI and SacI. Gel electrophoresis of each fragment indicated successful PCR amplification, so they were subsequently cleaned up and assembled into a complete plasmid via Gibson assembly (Figure 3.18B). Following bacterial transformation and mini-prepping the selected colonies, it was determined via PCR and nanodrop that the colonies did not successfully integrate any plasmid (Figure 3.18C). Troubleshooting via further nanodrop and gel electrophoresis of each fragment indicated that the concentration of the Mec1 fragment was too low to create a plasmid successfully. The PCR was repeated three further times with varying amplification times and temperatures to increase the concentration of the Mec1 fragment; however, the fragment amplification was unsuccessful at each attempt. It was concluded that the large size of the fragment (7167 kb) being amplified from genomic DNA resulted in poor PCR products, similar to the complete cassette PCR amplification of transformed dpb11 strains. As such, a new approach was chosen that required the usage of smaller fragments.

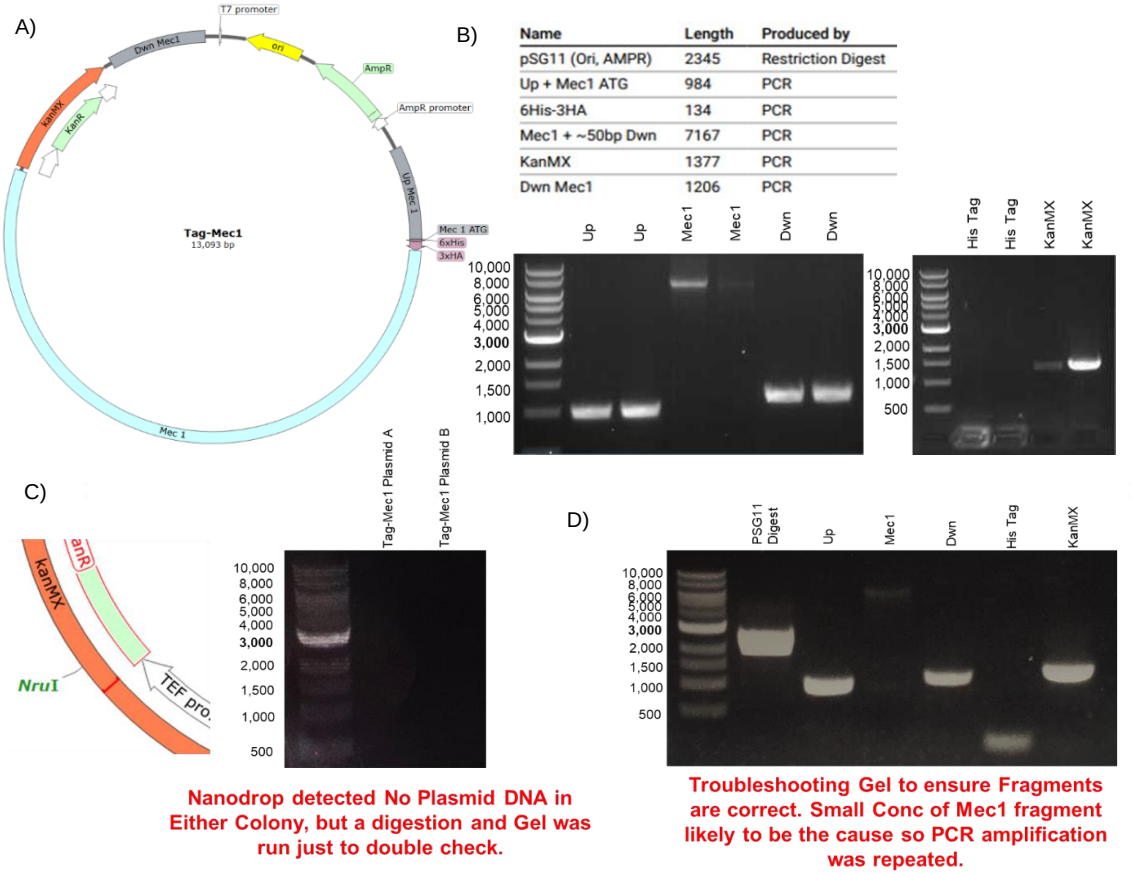

Figure 3.18: Design of *tag-mec1 A* plasmid and construction of its fragments. A) Diagram of the *tag-mec1* plasmid. B) Table of fragment lengths required in the construction of *tag-mec1* alongside the gel electrophoresis of each fragment following PCR amplification. Primers: 'Up + Mec1 ATG' fragment, Primers 1093 and 1094. 'KanMX' fragment, Primers 1099 and 1100. '6His-3HA' fragment, Primers 1095 and 1096. 'Mec1+ 50 bp' fragment, Primers 1097 and 1098. 'Dwn Mec1' fragment, Primers 1101 and 1102. C) Restriction Digest of *tag-mec1* A plasmids A and B using enzyme single cutter NruI, then visualised using gel electrophoresis. D) Diagnostic Gel electrophoresis of all the fragments that make up *tag-mec1* A.

3.3.1.2 Construction and validation of *tag-mec1* B

The second attempt at creating a *tag-mec1* plasmid involved splitting the Mec1 gene into two smaller (~3.5 kb) fragments with the remaining fragments unchanged. PCR amplification of the 1st half of Mec1 was successful (Figure 3.19B); however, following three attempts of the 2nd half of Mec1 at different PCR parameters, the amplification remained unsuccessful. From this, we concluded that either a structure within the 2nd half of Mec1 interfered with its PCR amplification or the primer at the C-terminus of Mec1 was ineffective at binding to the DNA. It was decided that a new strategy using only the first half of Mec1 would be created.

A)

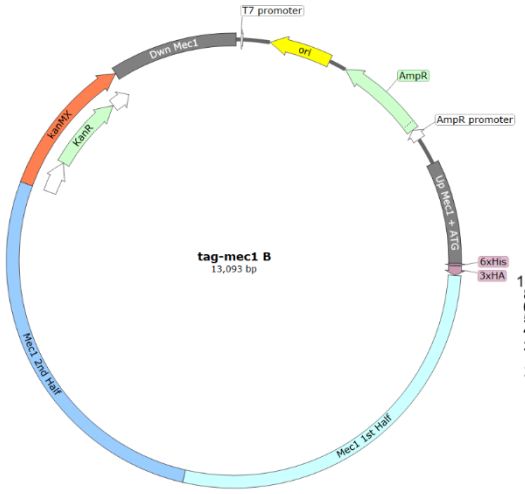

B)

Name	Length	Produced by
pSG11 (Ori, AMPR)	2345	Restriction Digest
Up + Mec1 ATG	984	PCR
6His-3HA	134	PCR
Mec1 1st Half	3626	PCR
Mec1 2nd Half	3561	PCR
KanMX	1377	PCR
Dwn Mec1	1206	PCR

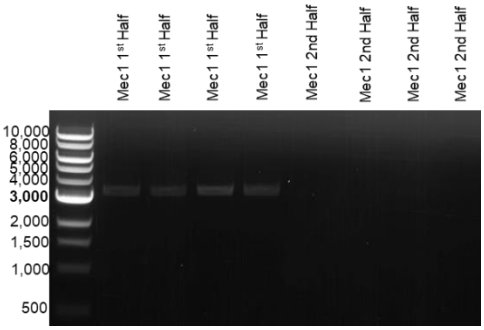

Figure 3.19: Design of *tag-mec1 B plasmid* and construction of its fragments. A) Depiction of the *tag-mec1* plasmid. B) Table of fragment lengths required in the construction of *tag-mec1 B* alongside the gel electrophoresis of each Mec1's 1st and 2nd half fragments following PCR amplification. PCR parameters: 'Mec1 1st Half' fragment, Primers 1097 and 1142. 'Mec1 2nd Half' fragment, Primers 1098 and 1143.

3.3.1.3 Construction and validation of *tag-mec1* C

The third attempt at creating *tag-mec1* was halted midway through development following the realisation that integrating KanMX upstream from the Mec1 gene would interfere with Mec1s promotor region promoting Mec1 expression. Following this realisation, it was decided to start fresh with a new plasmid with a C-terminally tagged Mec1 gene as integrating the KanMX selection marker before the upstream Mec1 region would be outside the homology region and potentially interfere with Mec1 promotor and after the 1st half of Mec1 would result in the integration of KanMX within the Mec1 gene. Placing KanMX before the upstream region may also interfere with sequence homology. As such, it was decided that a new strategy 3xHA tagging the C-terminal region of Mec1 was required under the assumption that the previous primer resulted in the impaired amplification of Mec1.

A)

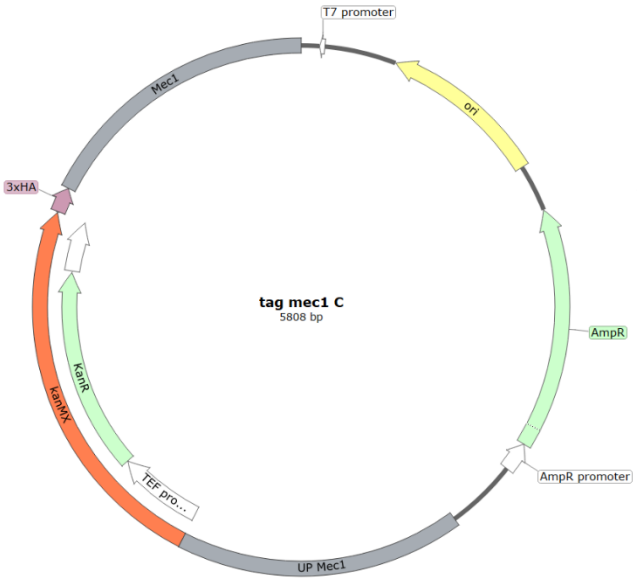

B)

Name	Length	Produced by
pSG11 Ori + AmpR	2345	Restriction Digest
Up Mec1	1026	PCR
KanMX	1377	PCR
ATG+3HA	113	PCR
Mec1 (1kb)	1047	PCR

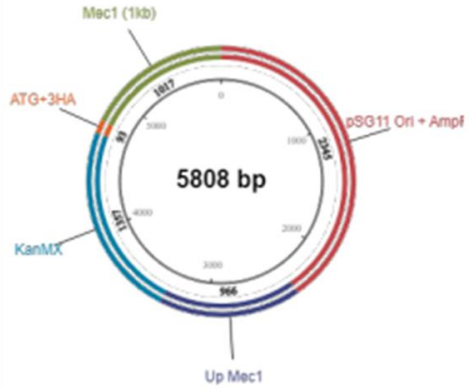

Figure 3.20: Design of *tag-mec1-C* plasmid and construction of its fragments. A) Depiction of the *tag-Mec1*. B) Table of tag-mec1 C fragments alongside a diagram of the fragment's alignment.

3.3.1.4 Construction and validation of *mec1-tag*

When creating the C-terminal tagged Mec1, it was essential that the Mec1 fragment was small enough to amplify from genomic DNA successfully and kept enough homology to integrate into the genome. The plasmid was designed using four fragments: the final ~1 kb of Mec1, the 6xHis-3HA-end codon-KanMX region from *dpb11-tag-md*, downstream mec1 and the plasmid backbone. PCR amplification of the 'Final 1 kb of Mec1' fragment and secondary (lower temp) PCR of the upstream and downstream revealed correctly sized bands. The fragments were then nano-dropped, cleaned up, and their pmoles were calculated. Alongside the digested pSG11 (Figure 3.18), the fragments were incubated via Gibson assembly. Following bacterial transformation, the successful colonies were inoculated in LB-AMP and then mini-prepped to purify their plasmids. Diagnostic PCRs of the plasmids identified indicated a correct band at 2167 bp and a secondary band at 4 kb (Figure 3.22A/B). The band's presence in every reaction mixture indicated that it represented the undigested plasmid. PCR amplification of the complete cassette produced a correctly sized band of 3804 bp, which was cleaned up in preparation for yeast transformation.

A)

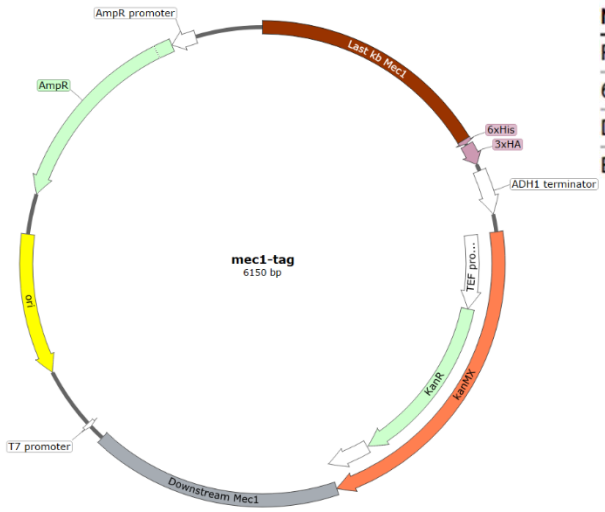

B)

Name	Length	Produced by
Final 1kb of Mec1	1030	PCR
6His3HA + End + KanMX	1782	PCR
Downstream Mec1	1073	PCR
Backbone	2345	Restriction Digest

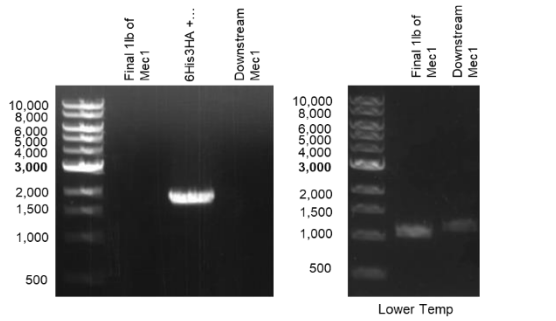

Figure 3.21: Design of *mec1-tag plasmid* and construction of its fragments. A) Diagram of the *mec1-tag* plasmid. B) Table of fragment lengths required in the construction of *mec1-tag* alongside the gel electrophoresis of its fragments following PCR amplification. PCR parameters: 'Final 1kb of Mec1' fragment, Primers 1226 and 1227. 6His3HA + End + KanMX' fragment, Primers 1228 and 1229. 'Downstream Mec1' fragment, Primers 1230 and 1231.

The aim was to transform the cassette into the background YSG3, 4, 29 and 33. However, the KanMX sequence was not present in any of the transformed strains, and therefore, it was concluded that none of the transformations were successful. Interestingly, the transformed strains showed extra bands alongside the WT banding, although it remains unclear what these represent. At this stage, no further time was available to continue researching *tag-mec1/mec1-tag* strains.

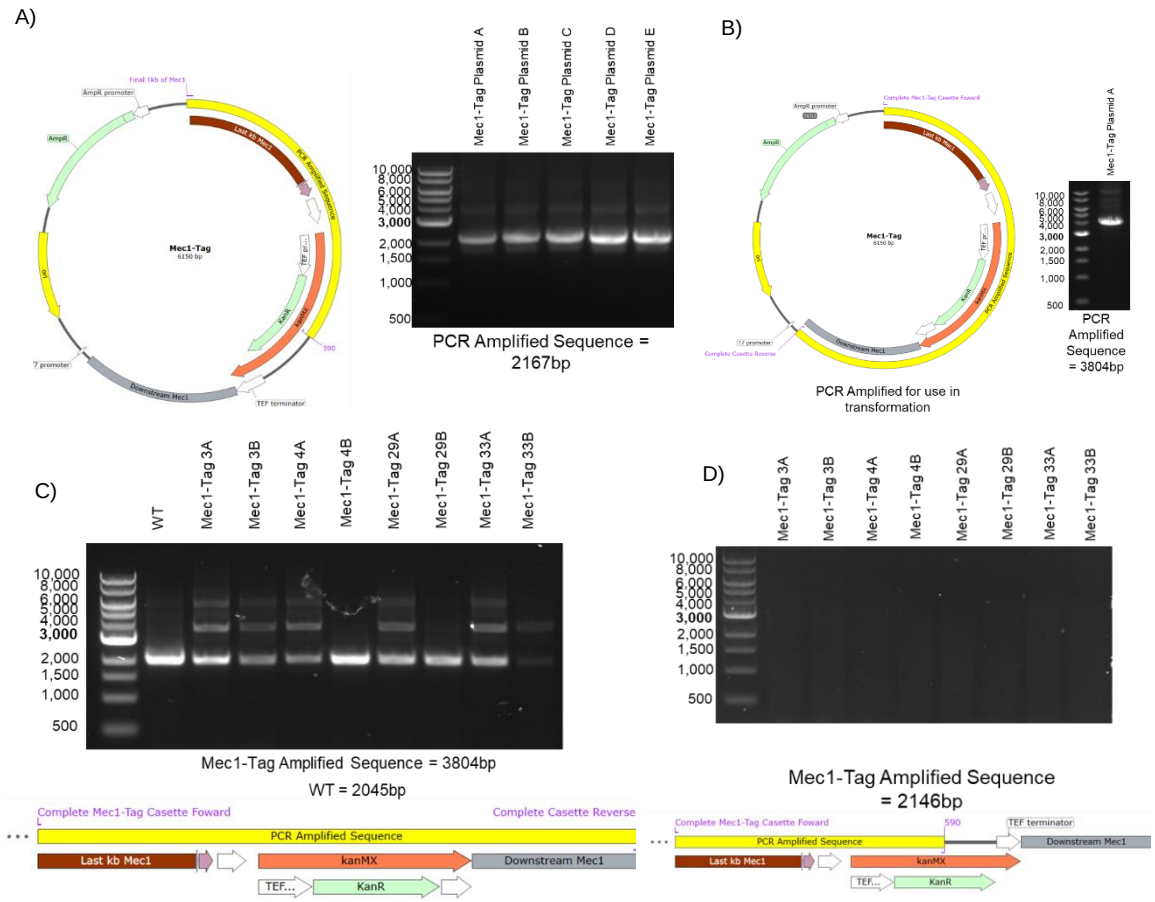

Figure 3.22: *mec1-tag* plasmid validation and transformation. A) Diagnostic PCR amplification of *mec1-tag* plasmids A-F. PCR parameters: Primers 1226 and 590, 72˚C annealing temp and 2.5 min amplification time. B) Complete cassette PCR of *mec1-tag* plasmid A. Primers MEC1-Tag 'CompleteSeq_Fwd' and 'MEC1-Tag CompleteSeq_Rev'. C) Diagnostic PCR of *mec1-tag* transformed strains 3A, 3B, 4A, 4B, 29A, 29B, 33A and 33B.: Primers 'CompleteSeq_Fwd' and 'MEC1-Tag CompleteSeq_Rev'. D) Diagnostic PCR amplification of *mec1-tag* transformed strains 3A, 3B, 4A, 4B, 29A, 29B, 33A and 33B. Primers 'MEC1-Tag CompleteSeq_Fwd' and 590.

To clarify if the integration of the His-tag at the N-terminus of Mec1 affects the meiotic phenotype of the mutant strains, the *mec1-tag* transformation needs to be completed, followed by comparing the sporulation efficiency and spore viability to the WT control strains.

3.3.2 Constructing meiotic depleted N-terminal His tagged MEC1 *S. cerevisiae* strains

The goals for this section were to create *mec1-md* within the YSG3, YSG29 and YSG33 background strains and characterise the meiotic phenotypes of each to see if they align with data within (Gray *et al.*, 2013). This C-terminally tagged *mec1-md* YSG4 background strain YSG15 was already created, so it could be used as a base for creating strains within this research.

3.3.2.1 Validation and construction of *mec1-md*

To transfer the *mec1-md* cassette sequence to the YSG3 background, the *mec1-md* YSG4 background strain YSG15 and WT strain YSG3 were mated together on a YPD+ALU plate. The patch was then inoculated in KAc to initiate sporulation before being dissected. After replicating the dissected plates onto G418, YSG1 and YSG2 plates. The first dissected plate had every dissected spore grow on the YSG2 plate, and none grow on the YSG1 plate, suggesting a mistake during the procedure. The second attempt had similar issues, so it was decided to create *mec1-md* in the YSG3 background via transformation.

The mec1-md complete cassette was amplified in preparation for yeast transformation using primers 84 and 85. After gel electrophoresis indicated the correct size cassette was amplified, it was nanodrop dropped and then cleaned up. The selected colonies were inoculated after yeast transformation and underwent Genomic DNA Preparation. Diagnostic PCRs revealed the successful integration of the mec1-md cassette into the YSG3B, 29A, 33A and 33B strains that were subsequently labelled *mec1-md* strains YSG789, YSG790, YSG791, and YSG792, respectively.

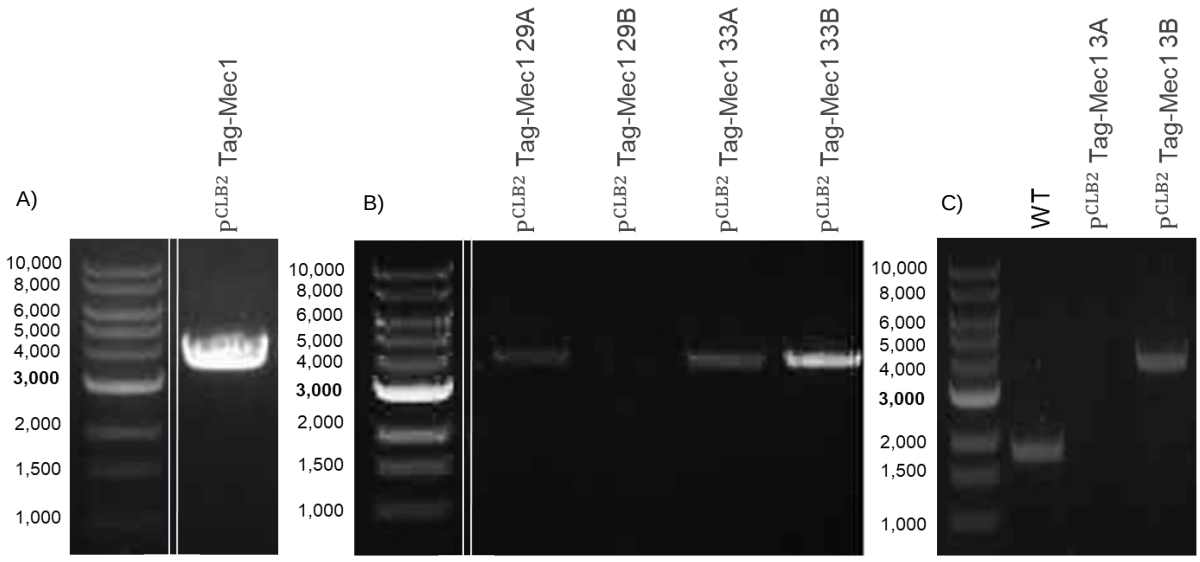

Figure 3.23 *tag-mec1-md* validation and transformation. A) Complete cassette PCR of *tag-mec1-md* YSG15 genomic DNA. PCR parameters: Primers 84 and 85. B) Complete cassette PCR of transformed *tag-mec1-md* strains 3A, 3B, 29A, 29B. PCR parameters: Primers 84 and 85.

3.3.2.2 Analysis and conclusions of *mec1-md*

To characterise the meiotic phenotype of meiotic depleted mec1 diploids YSG796, YSG797, and YSG798 were generated from mating the *mec1-md* YSG3 background strain YSG970 with the *mec1-md* YSG4 background strain YSG15. Similarly, the *mec1-md* diploids YSG830 and YSG854-856 were created from the *mec1-md* YSG29 background strain YSG790 and the *mec1-md* YSG33 strain YSG791. Inoculation of the diploid colonies and sporulation in KAc allowed for sporulation efficiency and spore viability analysis.

Although both the *mec1-md* (3 x 4) (84%, n = 48, SD = 4%) and *mec1-md* (29 x 33) (51%, n = 61, SD = 8%) diploids showed statistically significant reductions in spore viability (13%, p = 0.01 and 45%, p = 1.00e-06) compared to their WT counterparts, they were also statistically different from each other (33%, p = 0.001) (Figure 3.24A/B). Interestingly, no significant difference (p = 0.85) in sporulation efficiency was observed between the *mec1-md* (3 x 4) (40%, n = 527, SD = 4%) and *mec1-md* (29 x 33) (43%, n = 517, SD = 11%) strains. Both *mec1-md* backgrounds showed a significant difference (49%, p = 3.77e-6 and 50%, p = 0.004) in sporulation efficiency compared to WT (Figure 3.24A/B).

Results obtained from previous work (Gray *et al.*, 2013) using the same *mec1-md* cassette more closely align with the data obtained from the (29 x 33) background *mec1-md* strains, which showed a ~50% spore viability. Since both backgrounds showed sporulation efficiencies of ~50%, it was theorised that the spore viability data from the YSG(3 x 4) background could be erroneous and potentially a result of dissecting structures that resembled tetrads, following the construction of *mec1-md, tag-dpb11* double (3 x 4) spore viability analysis observed no statistical difference when compared to *mec1-md* (3 x 4) (Figure 3.27A). This could indicate that one of the two haploids used to create the (3 x 4) *mec1-md* diploids may not be depleting Mec1.

To further examine the *mec1-md* mutants, a repeat complete cassette PCR of each haploid could be completed to evaluate the presence of the P^{CLB2} within each strain. If the promotor is present in the haploids, the next step is to ensure that Mec1 is successfully depleted during meiosis. A meiotic time course of the *mec1-md* diploids could be completed by taking samples at hourly intervals for 5 hours. A western blot of protein extracted from these samples run on a TCE gel and then transferred to a PVDF membrane would visualise mec1 expression using primary rabbit anti-HA antibodies and secondary goat anti-rabbit fluorescent antibodies. The expression levels could then be compared to data from (Gray *et al.*, 2013) to see which phenotype more closely represents meiotic-depleted Mec1.

A)

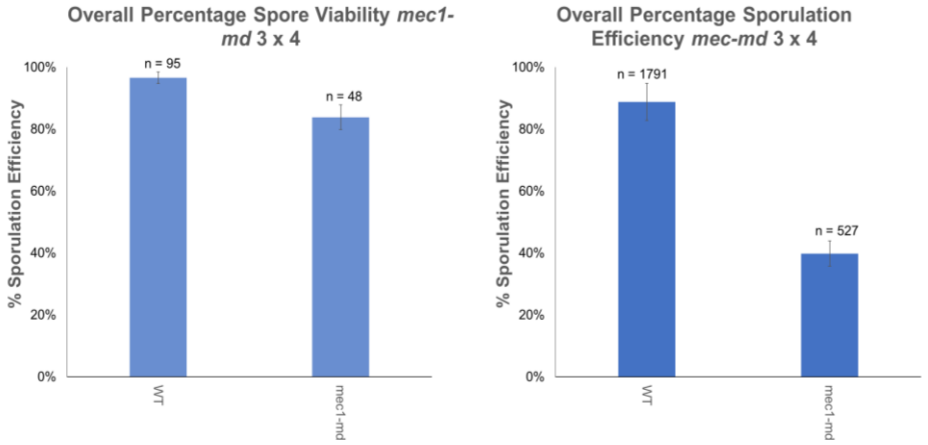

B)

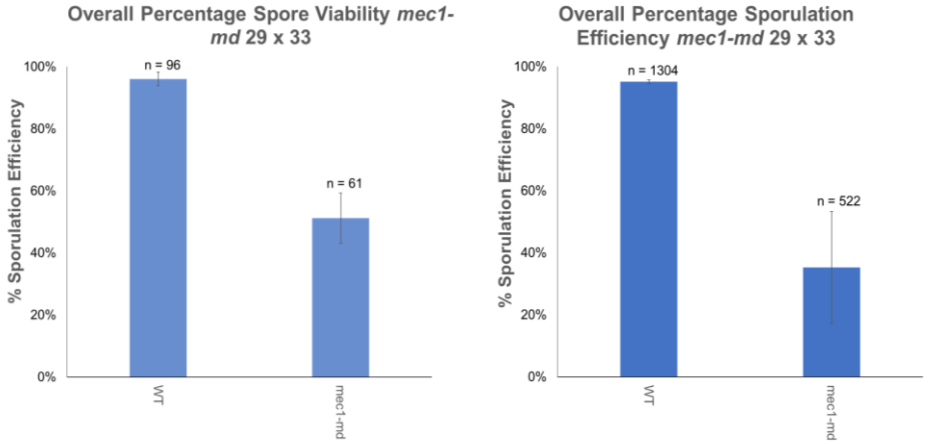

Figure 3.24 Spore viability and sporulation efficiency of *tag-mec1-md* diploid strains. Spore viability and sporulation efficiency of (3 x 4) WT control strains and the *tag-mec1-md* (3 x 4) diploids YSG796-798. (p =0.0002) (p =3.77E-06) B) Spore viability and sporulation efficiency of the (29 x 33) WT control strains and the *tag-mec1-md* (29 x 33) diploids YSG830, and YSG854-856. (p =1.002E-06) (p =0.0047) (Spore Viability: N = number of tetrads dissected. Sporulation Efficiency: N = number of sporulated/un-sporulated cells counted, Error Bars = Standard Deviation.)

3.4 Construction of double mutants

Creating a haploid strain with two different mutations when the single mutant strains have already been created uses a similar method to crossing a cassette from one background into the opposite. The two mutants that needed to be in a single strain were mated together, inoculated the following day, and washed and transferred to KAc to initiate sporulation. After three days of sporulation, the tetrads were dissected and left to grow on a YPD+ALU dissection plate. The strains were then replica-plated and left to grow for two days. Tetrads that showed two colonies growing on the G418 plate and two not growing were selected as this arrangement guarantees both colonies have both mutations.

tag-dpb11 strain YSG858 was mated with *mec1-md* strain YSG15 to create *tag-dpb11 mec1-md* double mutants as outlined to create haploid strains (a) YSG928 and (α) YSG929. These strains were mated together, and single diploid colonies were inoculated, sporulated, and dissected. The diploid *tag-dpb11 mec1-md* doubles were labelled YSG1009-1011. Using the methods previously outlined, (3 x 4) background haploid doubles *dpb11-tag mec1-md* (a YSG985, α YSG986), *tag-dpb11-md mec1-md* (a YSG987, α YSG988), and *dpb11-tag-md mec1-md* (a YSG989, α YSG990, YSG991) were created (Further details in Table 2-1.). Similarly (29 x 33) background haploid doubles *tag-dpb11 mec1-md* (a YSG994, α YSG995), *dpb11-tag + mec1-md* (a YSG996, α YSG997), *tag-dpb11-md mec1-md* (a YSG871, α YSG872, YSG873), and *dpb11-tag-md mec1-md* (a YSG998, α YSG999) were created (Further details in Table 2-1.).

The haploid mutants were mated together, streaked for singles, inoculated, and then sporulated in KAc. The resulting (3 x 4) background diploids were as follows: *dpb11-tag mec1-md* (YSG1012-1016), *tag-dpb11-md mec1-md* (YSG1017-1019), and *dpb11-tag-md mec1-md* (YSG1020-1022) (Further details in Table 2-1.). The (29 x 33) background diploid mutants generated *tag-dpb11-md mec1-md* (YSG939-943) were also created. Various issues arose during the creation of the double mutants. The *dpb11-tag-md mec1-md* (29 x 33) diploids showed a WT phenotype (Figure 3.25) resulting from an error during replica-plating, *tag-dpb11 mec1-md* (29 x 33) diploids showed no signs of sporulation, and contamination during the final month of research resulted in the complete loss of multiple weeks of research. If given extra time the re-creation of *dpb11-tag-md mec1-md* (29 x 33), *tag-dpb11 mec1-md* (29 x 33), and *dpb11-tag mec1-md* (3 x 4)/(29 x 33) would be a priority. Spore viability and sporulation efficiency analysis of these strains would help create a more complete data set as it would allow the comparison of C vs. N terminally tagging dpb11 within a meiotic-depleted Mec1 strain.

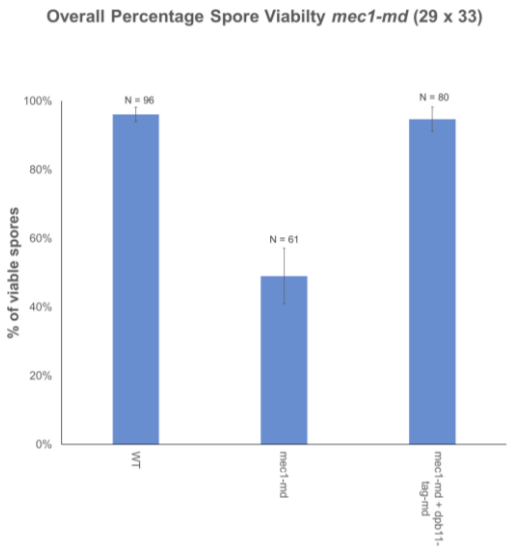

Figure 3.25 Spore viability and sporulation efficiency comparison of *mec1-md*, to *mec1-md* + *dpb11-tag-md*. Spore viability and sporulation efficiency of (29 x 33) WT control strains, *mec1-md strains* YSG830, and YSG854-856, and *tag-mec1-md dpb11-tag-md* (29 x 33) diploids A, B, C, and D. This data indicated an issue with the *tag-mec1-md dpb11-tag-md* diploids (Spore Viability: N = number of tetrads dissected. Sporulation Efficiency: N = number of sporulated/un-sporulated cells counted, Error Bars = Standard Deviation.)

3.5 Conclusions

When examining whether Dpb11 has roles both dependent and independent on Mec1 during meiosis, it is essential to ensure that within meiotic-depleted Dpb11 strains, the expression profile of Dpb11 indicates a drop during meiosis. The *tag-dpb11-md* and *dpb11-tag-md* strains remain inconclusive on whether Dpb11 expression is curbed as the spore viability of the *tag-dpb11-md* (3 x 4) (n = 128, p = 0.54), *dpb11-tag-md* (3 x 4) (n = 48, p = 0.57), and (29 x 33) (n = 79, 3% increase p = 0.04) strains phenocopied WT (Figure 3.26A/Figure 3.27A). This could indicate that Dpb11 is not being correctly depleted within these strains as the *tag-dpb11-md* (29 x 33) (85%, n = 157) strains exhibited an 11% (p=0.0004) decrease in spore viability compared to WT (Figure 3.27A). Interestingly, the sporulation efficiency of the *tag-dpb11-md* (3 x 4) (75%, n = 1003) did not phenocopy WT (p = 0.017) (Figure 3.26B), whilst *dpb11-tag-md* (3 x 4) (n = 511) and (29 x 33) (n = 508) did (p = 0.32, p = 0.15) (Figure 3.26B/Figure 3.27B). This could indicate the partial depletion of Dpb11 within *tag-dpb11-md* (3 x 4) as (29 x 33) diploids created from the pre-existing *tag-dpb11-md* strains YSG678, YSG680, and YSG681 showed an 83% decrease compared to WT versus the 14% decrease observed in *tag-dpb11-md* (3 x 4) diploids.

To further clarify, if Dpb11 expression is depleted within *tag-dpb11-md or dpb11-tag-md,* these mutations were integrated into *mec1-md* strains. Within the YSG(3 x 4) background, spore viability

analysis of *mec1-md tag-dpb11-md* and *mec1-md dpb11-tag-md* doubles resulted in a ~28% ($n = 49$, $p = 0.004$) and ~17% ($n = 76$, $p = 0.04$) reduction compared to the *mec1-md* single mutant (Figure 3.26A). A change in the meiotic phenotype indicated that the expression of Dpb11 has changed; however, whether this resulted from complete Dpb11 depletion or partial depletion cannot be confirmed. The change to the meiotic phenotype following Dpb11 depletion within strains already lacking Mec1 (*mec1-md*) could indicate that Dpb11 has roles independent from Mec1 during meiosis. Previous studies have investigated Dpb11's involvement in joint molecule resolution, where it forms the central domain unit between the Slx4/Rtt107 scaffold complex and Mus81-Mms4 during meiosis (Gritenaite *et al.*, 2014; Cussiol *et al.*, 2015), disruption of which may lead to mis-segregation of chromosomes and result in lower spore viability.

Since *dpb11-md* displayed a WT meiotic phenotype within the YSG(3 x 4) background, this could indicate that Mec1 can alleviate/ replace these roles during meiosis. This is corroborated by research suggesting that Mek1 indirectly regulates Holliday junction resolution through its activation by Mec1/Tel1-dependent phosphorylation of the Rad9 homolog Hop1 (Chuang, Cheng and Wang, 2012; Hollingsworth and Gaglione, 2019). Dpb11 has no predicted or observed interactions with Hop1 (Biogrid Database) but plays a vital role in Rad9's phosphorylation by Mec1 during mitosis (Vialard *et al.*, 1998).

Data obtained from the western blot (Figure 3.8D) of *tag-dpb11-md* should have indicated the expression levels of Dpb11, but the expression of Dpb11 within vegetative *tag-dpb11* and *dpb11-tag* must first be characterised to calibrate the western blot of the meiotic depleted strains correctly. Similarly, further PCR analysis of the *tag-dpb11, dpb11-tag* and *dpb11-tag-md* strains+ plasmids must be carried out to determine what the extra region downstream from DPB11 is within the plasmid and if it has been integrated into the strains. The WT spore viability observed in *tag-dpb11-md* (3 x 4) did not result from this extra region, as the cassette used was created directly from the YSG680 genomic DNA.

A)

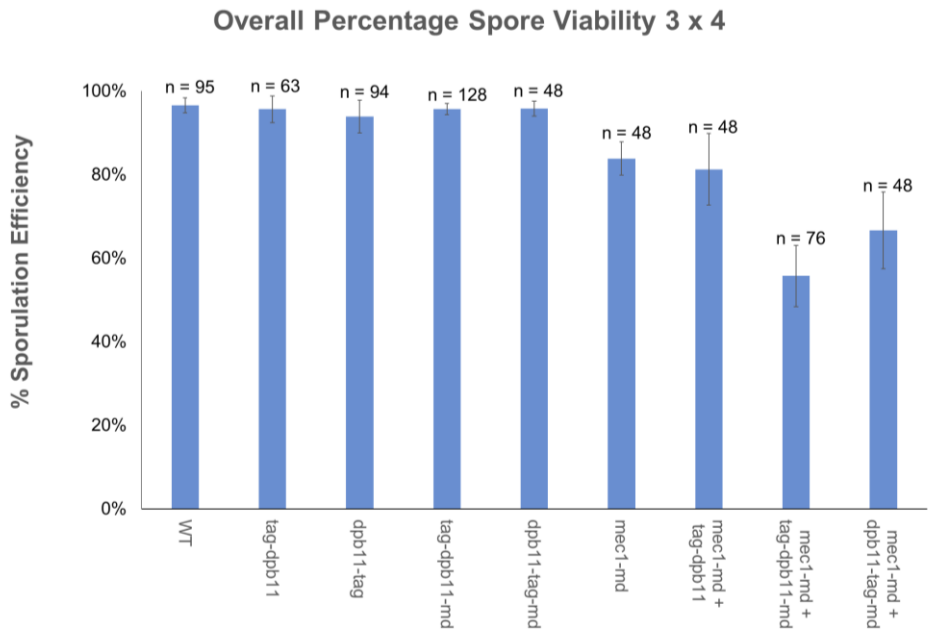

B)

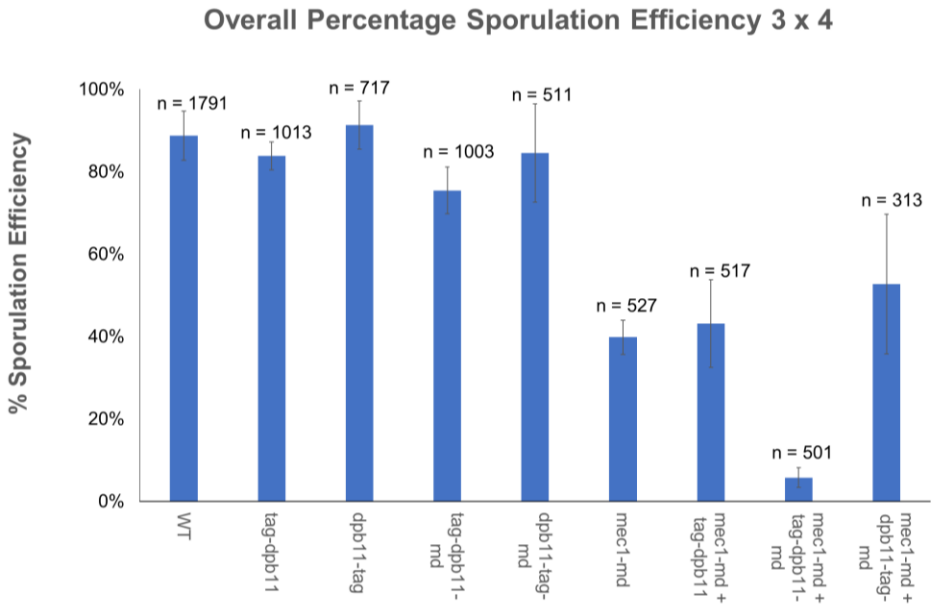

Figure 3.26 Spore viability and sporulation efficiency all (3 x 4) strains. A) Spore viability and of l YSG3 x YSG4 diploid strains discussed in this research B) Sporulation efficiency of all YSG3 x YSG4 diploid strains discussed in this research (Spore Viability: N=number of tetrads dissected, Sporulation Efficiency: N=number of sporulated/un-sporulated cells counted, Error Bars = Standard Deviation.)

A WT spore viability was observed within *tag-dpb11* (3 x 4) (n = 63, p = 0.55) and (29 x 33) (n = 80, 1% increase p = 0.04) along with *dpb11-tag* (3 x 4) (n = 94, p = 0.15) and (29 x 33) (n = 45, p = 0.29) shows that integration of the His-tag at the N or C terminal region does not affect Dpb11 activity. This was further supported by sporulation efficiency analysis of both mutations phenocopying WT within both backgrounds (More details in 3.1.1.3,3.2.1.2, Figure 3.26B, and Figure 3.27B).

Both background strains showed decreased spore viability when comparing the *mec1-md* mutants to the *tag-dpb11-md/dpb11-tag-md* single mutants (Figure 3.26A/Figure 3.27A). Within the YSG(3 x 4) background, *mec1-md* (n = 48) showed a 12% (p = 0.001) decrease in spore viability, compared to *tag-dpb11-md* (n = 128) and a 12% (p = 0.009) decrease compared to *dpb11-tag-md* (n = 48).Similarly, when analysing the sporulation efficiency, a 35% (p = 0.0002) decrease was observed between *tag-dpb11-md* (n=1003) and *mec1-md* (n = 527) and a 45% (p = 0.004) decrease was observed between *dpb11-tag-md* (n=511) and *mec1-md* (n = 527). This data indicates that during meiosis, Mec1 has roles independent of Dpb11. The C-terminus of the 9-1-1 checkpoint clamp is capable of activating Mec1 without the need for Dpb11 to bridge the two together (Navadgi-Patil and Burgers, 2009). Similarly, Dpb11 has shown to be completely redundant in Mec1 activation during G1 (Navadgi-Patil and Burgers, 2009), which could indicate a similar scenario is occurring within the pachytene checkpoint. Dpb11-independent roles of Mec1 could result in the WT Spore viability observed in the (3 x 4) *tag-dpb11-md* as Mec1 activates pathways normally reliant on Mec1 independent activity of Dpb11 (observed in the *mec1-md tag-dpb11-md* double)

The ~12% increase in spore viability between the YSG(29 x 33) *mec1-md tag-dpb11-md double* and *mec1-md* was not statistically significant (p = 0.09) enough to make any conclusions (Figure 3.27B), especially since its sporulation efficiency (n=727) decreased by 33% (p =0.004) compared to *mec1-md* (n =522). In conclusion, a comparison of spore viability and sporulation efficiency between *tag-dpb11-md* and *dpb11-tag-md* indicates that integration of the P^{CLB2} has impacted Dpb11 expression; however, to what extent remains unclear. A change in expression is supported by a further decrease in spore viability and sporulation efficiency following the integration of *tag-dpb11-md* or *dpb11-tag-md* into *mec1-md,* which also indicated that Dpb11 has Mec1-independent roles during meiosis. A WT phenotype observed within the *tag-dpb11* and *dpb11-tag* strains proved that the His-tag does not impair potential Dpb11 activity during meiosis. However, It remains unclear if Dpb11 has any roles dependent on Mec1 as a WT phenotype was observed in the *tag-dpb11-md* (3 x 4) and *dpb11-tag-md* (3 x 4 and 29 x 33) strains, whereas the *tag-dpb11-md* (29 x 33) strain exhibited a decrease in spore viability and sporulation efficiency compared to WT. *mec1-md* had lower spore viability and sporulation efficiency when compared to the dpb11-md strains, suggesting that Mec1 activity is not dependent on Dpb11.

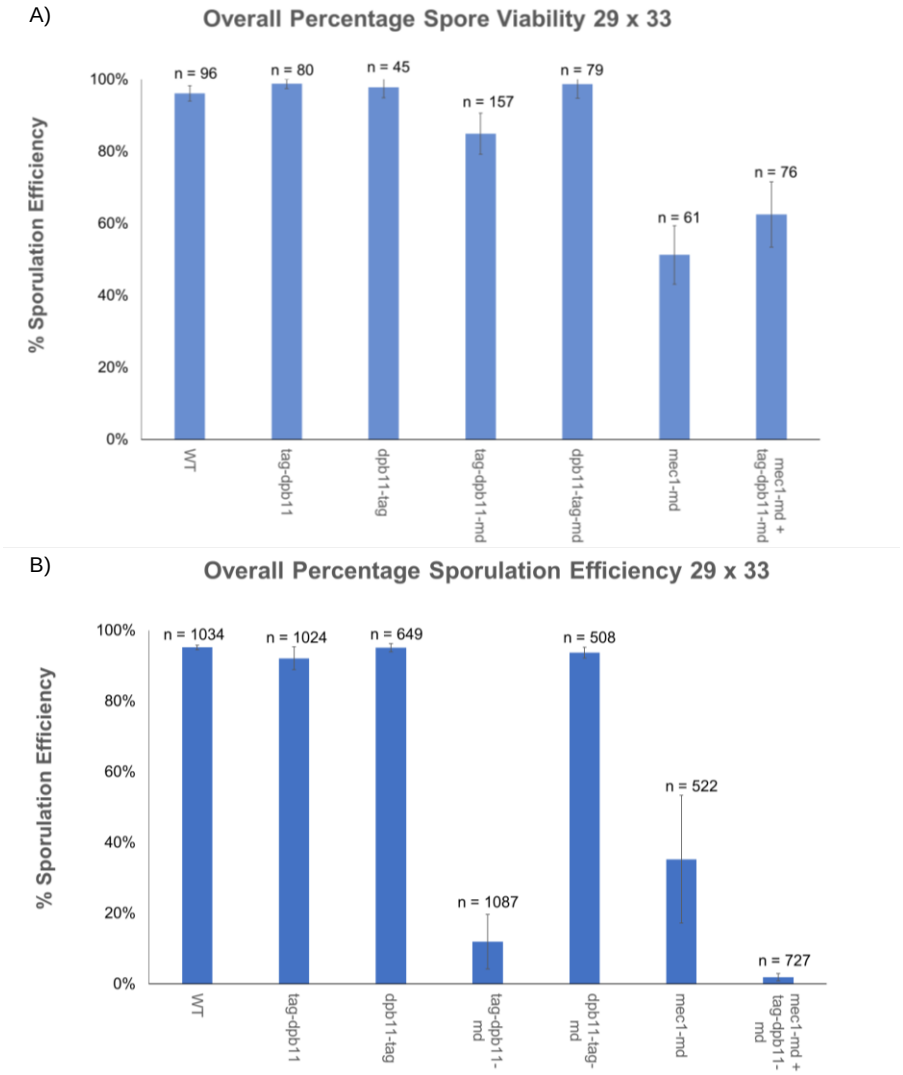

Figure 3.27 Spore viability and sporulation efficiency all (29 x 33) strains. A) Spore viability and of YSG29 x YSG33 diploid strains discussed in this research strains) B) Sporulation efficiency of YSG29 x YSG33 diploid strains discussed in this research (Spore Viability: N=number of tetrads dissected, Sporulation Efficiency: N=number of sporulated/un-sporulated cells counted, Error Bars = Standard Deviation.)

Chapter 4: Future Perspectives

Using this research as a backbone, further experiments could clarify and expand upon the work already completed. The first of which is a western blot analysis of vegetative *tag-dpb11/dpb11-tag* to then use as a baseline for a western blot analysis of the 1–5-hour *tag-dpb11*-md meiotic time course samples obtained in this study. If Dpb11 is shown to be depleted during meiosis within the *tag-dpb11-md* mutants, then further experiments could be conducted using these strains. Fluorescent Microscopy could be performed using the YSG(29 x 33) strains to visualise the crossovers occurring between each strain (Thacker *et al.*, 2011) and give indications on the impact depletion of Dpb11/Mec1 has on crossover frequency. Similarly, the mutations could be integrated into SK1 and S288C background for nanopore sequencing. Nanopore sequencing detects individual nucleotides by measuring the alterations in electric current as they pass through nanoscale pores and is capable of reading very long sequences (Gong *et al.*, 2017). The identified sequence can then be compared to the background SK1 and S288C sequences to identify any potential crossovers of genetic information.

Identifying the extra region within the *tag-dpb11* plasmid is of utmost importance to ensure that no extra region has been transformed into the strains that could affect the expression of Dpb11. This initial pre-existing plasmid was used as a backbone within *dpb11-tag* and *dpb11-tag-md.* A PCR of the DPB11 gene into the plasmid backbone should amplify the extra region. This fragment can then be DNA sequenced to accurately determine the incorrectly integrated fragment. New primers can be generated using NEBuilder® for use in amplification and sequencing.

A post-translational modification (PTM) was observed on Dpb11 during meiosis (unpublished data), so enzyme assays could help identify the type of phosphorylation occurring by treating dpb11 with enzymes designed to target PTMs and checking for the disappearance of the larger band via western blot. The protein could be truncated to determine where the PTM was located until the band is no longer present. Mec1 is a notable PIKK kinase that could be responsible for this PTM, so evaluation of the PTM following the depletion of Mec1 could indicate its involvement. Mutation of the PTM region could signify its importance within Mec1 activity.

A way of evaluating the checkpoint activity within the mutant strains could be to introduce the strains to varying levels of DNA-damaging agents and visualise the growth of colonies at each level. If the checkpoint remains intact, the growth rate should remain consistent with a WT control. If performed on tag-dpb11-md and dpb11-tag-md, the importance of Dpb11 within the checkpoint during meiosis could be evaluated.

Ime2 is a meiosis-specific kinase expressed only during meiosis (Guttmann-Raviv, Martin and Kassir, 2002). Subsequently, its promoter, contrary to P^{CLB2}, promotes protein expression only during meiosis. Placing DPB11-1, a C-terminally truncated Dpb11, under the Ime2 promoter will enable us to determine the importance of Dpb11-Ddc2 binding in Mec1/Dpb11 activity. This is due to the C terminal regions' vital role in Dpb11 Ddc2 Binding (Mordes, Nam and Cortez, 2008). Placing P^{IME2}-Dpb11-1 into the P^{CLB2}-Dpb11 cassette will enable WT characteristics before meiosis and ensure the cells remain inviable.

Sporulating *S. cerevisiae* cells using potassium acetate resulted in high levels of variation in sporulation between strains containing the same mutation. This variation most likely resulted from inadequate washing, but even a perfect wash will likely result in small amounts of YPD remaining in the sporulation media. Therefore, an alternative method of initiating sporulation could be created by placing IME2 under a manually inducible promotor such as GAL. Manual activation would enable the synchronous activation of meiosis and reduce the number of cells undergoing premature meiosis within the YPD+ALU media.

Hop1 (Rad9s meiotic homolog) has yet to be identified as a binding partner of Dpb11. As Dpb11 plays a vital role in Rad9s phosphorylation by Mec1 (Figure 1.6), a similar mechanism may occur between Dpb11 and Hop1 during meiosis. First, a tagged form of Hop1 must be generated for a protein binding assay with Dpb11. If Dpb11 and Hop1 show binding activity, further examination can be performed. Dpb11 binds to Rad9 during mitosis using its BRCT 1/2 domain, so a mutation in the BRCT 1/2 domain may inhibit Dpb11-Hop1 binding.

TopBP1 is the human homolog of Dpb11 and activates the Mec1 human homolog ATR (Kumagai *et al.*, 2006) via an interaction with the human checkpoint clamp RAD9-HUS1-RAD1 (9-1-1) (Delacroix *et al.*, 2007). Like Dpb11, its structure also consists of multiple BRCT domains (Day *et al.*, 2018). Notably, TopBP1 is involved in the checkpoint mechanism during meiosis (Perera *et al.*, 2004). TopBP1 undergoes a structural change within the checkpoint to reveal its ATR activation domain (ADD) (Mordes *et al.*, 2008). Dpb11 has a Mec1 activation domain, but it is structurally different from TopBP1's ADD, so it may be helpful to determine if Dpb11's structure undergoes a similar change during the activation of Mec1 during meiosis. Identifying the observed Mec1-independent activity of Dpb11 could help deepen our understanding of the roles TopBP1 plays outside of the meiotic checkpoint within humans (Garcia, Furuya and Carr, 2005). Examination of mice concluded that a mutation in the BRCT 5 subunit of TopBP1 resulted in infertility (Ascencao *et al.*, 2023); therefore, increasing our understanding of Dpb11 and its potential mechanisms during meiosis could lead to the development of treatments for infertility induced by a mutation within the checkpoint mechanism.

Chapter 5: References

Alani, E. *et al.* (1992) 'Characterization of DNA-binding and strand-exchange stimulation properties of y-RPA, a yeast single-strand-DNA-binding protein', *Journal of molecular biology*, 227(1), pp. 54–71.

Alcasabas, A.A. *et al.* (2001) 'Mrc1 transduces signals of DNA replication stress to activate Rad53', *Nature Cell Biology*, 3(11), pp. 958–965. Available at: https://doi.org/10.1038/ncb1101-958.

Allers, T. and Lichten, M. (2001) 'Differential Timing and Control of Noncrossover and Crossover Recombination during Meiosis', *Cell*, 106(1), pp. 47–57. Available at: https://doi.org/10.1016/S0092-8674(01)00416-0.

Araki, H. *et al.* (1995) 'Dpb11, which interacts with DNA polymerase II(epsilon) in Saccharomyces cerevisiae, has a dual role in S-phase progression and at a cell cycle checkpoint', *Proceedings of the National Academy of Sciences of the United States of America*, 92(25), pp. 11791–11795. Available at: https://doi.org/10.1073/pnas.92.25.11791.

Ascencao, C.F.R. *et al.* (2023) *A TOPBP1 Allele Causing Male Infertility Uncouples XY Silencing Dynamics From Sex Body Formation*. preprint. elife. Available at: https://doi.org/10.7554/eLife.90887.1.

Baker, B.S. *et al.* (1976) 'The genetic control of meiosis', *Annual Review of Genetics*, 10, pp. 53–134. Available at: https://doi.org/10.1146/annurev.ge.10.120176.000413.

Bonilla, C.Y., Melo, J.A. and Toczyski, D.P. (2008) 'Colocalization of sensors is sufficient to activate the DNA damage checkpoint in the absence of damage', *Molecular cell*, 30(3), pp. 267–276.

Bork, P. *et al.* (1997) 'A superfamily of conserved domains in DNA damage-responsive cell cycle checkpoint proteins', *FASEB journal: official publication of the Federation of American Societies for Experimental Biology*, 11(1), pp. 68–76.

Börner, G.V., Kleckner, N. and Hunter, N. (2004) 'Crossover/Noncrossover Differentiation, Synaptonemal Complex Formation, and Regulatory Surveillance at the Leptotene/Zygotene Transition of Meiosis', *Cell*, 117(1), pp. 29–45. Available at: https://doi.org/10.1016/S0092-8674(04)00292-2.

Broach, J.R., Pringle, J.R. and Jones, E.W. (1991) *Molecular and cellular biology of the yeast Saccharomyces*. Cole Spring Harbor Laboratory Press.

Burgess, S.M., Powers, T. and Mell, J.C. (2017) 'Budding Yeast *S accharomyces Cerevisiae* as a Model Genetic Organism', in John Wiley & Sons, Ltd (ed.) *eLS*. 1st edn. Wiley, pp. 1–12. Available at: https://doi.org/10.1002/9780470015902.a0000821.pub2.

Callender, T.L. *et al.* (2016) 'Mek1 Down Regulates Rad51 Activity during Yeast Meiosis by Phosphorylation of Hed1', *PLOS Genetics*. Edited by M. Lichten, 12(8), p. e1006226. Available at: https://doi.org/10.1371/journal.pgen.1006226.

Carballo, J.A. *et al.* (2008) 'Phosphorylation of the Axial Element Protein Hop1 by Mec1/Tel1 Ensures Meiotic Interhomolog Recombination', *Cell*, 132(5), pp. 758–770. Available at: https://doi.org/10.1016/j.cell.2008.01.035.

Cartagena-Lirola, H. *et al.* (2008) 'Role of the Saccharomyces cerevisiae Rad53 checkpoint kinase in signaling double-strand breaks during the meiotic cell cycle', *Molecular and Cellular Biology*, 28(14), pp. 4480–4493. Available at: https://doi.org/10.1128/MCB.00375-08.

Chen, E.S.-W. *et al.* (2014) 'Use of Quantitative Mass Spectrometric Analysis to Elucidate the Mechanisms of Phospho-priming and Auto-activation of the Checkpoint Kinase Rad53 in Vivo', *Molecular & Cellular Proteomics*, 13(2), pp. 551–565. Available at: https://doi.org/10.1074/mcp.M113.034058.

Chen, X. *et al.* (2015) 'Phosphorylation of the Synaptonemal Complex Protein Zip1 Regulates the Crossover/Noncrossover Decision during Yeast Meiosis', *PLOS Biology*. Edited by D. Durocher, 13(12), p. e1002329. Available at: https://doi.org/10.1371/journal.pbio.1002329.

Chu, S. *et al.* (1998) 'The Transcriptional Program of Sporulation in Budding Yeast', *Science*, 282(5389), pp. 699–705. Available at: https://doi.org/10.1126/science.282.5389.699.

Chuang, C.-N., Cheng, Y.-H. and Wang, T.-F. (2012) 'Mek1 stabilizes Hop1-Thr318 phosphorylation to promote interhomolog recombination and checkpoint responses during yeast meiosis', *Nucleic Acids Research*, 40(22), pp. 11416–11427. Available at: https://doi.org/10.1093/nar/gks920.

Claeys Bouuaert, C. *et al.* (2021) 'Structural and functional characterization of the Spo11 core complex', *Nature Structural & Molecular Biology*, 28(1), pp. 92–102. Available at: https://doi.org/10.1038/s41594-020-00534-w.

Colomina, N. (1999) 'G1 cyclins block the Ime1 pathway to make mitosis and meiosis incompatible in budding yeast', *The EMBO Journal*, 18(2), pp. 320–329. Available at: https://doi.org/10.1093/emboj/18.2.320.

Coughlan, A.Y. *et al.* (2020) 'The yeast mating-type switching endonuclease HO is a domesticated member of an unorthodox homing genetic element family', *eLife*, 9, p. e55336. Available at: https://doi.org/10.7554/eLife.55336.

Cussiol, J.R. *et al.* (2015) 'Dampening DNA damage checkpoint signalling via coordinated BRCT domain interactions', *The EMBO Journal*, 34(12), pp. 1704–1717. Available at: https://doi.org/10.15252/embj.201490834.

Dahmann, C. and Futcher, B. (1995) 'Specialization of B-type cyclins for mitosis or meiosis in S. cerevisiae', *Genetics*, 140(3), pp. 957–963. Available at: https://doi.org/10.1093/genetics/140.3.957.

Day, M. *et al.* (2018) 'BRCT domains of the DNA damage checkpoint proteins TOPBP1/Rad4 display distinct specificities for phosphopeptide ligands', *eLife*, 7, p. e39979. Available at: https://doi.org/10.7554/eLife.39979.

Delacroix, S. *et al.* (2007) 'The Rad9–Hus1–Rad1 (9–1–1) clamp activates checkpoint signaling via TopBP1', *Genes & Development*, 21(12), pp. 1472–1477. Available at: https://doi.org/10.1101/gad.1547007.

Deshpande, I. *et al.* (2017) 'Structural Basis of Mec1-Ddc2-RPA Assembly and Activation on Single-Stranded DNA at Sites of Damage', *Molecular Cell*, 68(2), pp. 431-445.e5. Available at: https://doi.org/10.1016/j.molcel.2017.09.019.

Dhingra, N. *et al.* (2015) 'Dpb11 Protein Helps Control Assembly of the Cdc45·Mcm2-7·GINS Replication Fork Helicase', *Journal of Biological Chemistry*, 290(12), pp. 7586–7601. Available at: https://doi.org/10.1074/jbc.M115.640383.

Dirick, L. *et al.* (1998) 'Regulation of Meiotic S Phase by Ime2 and a Clb5,6-Associated Kinase in *Saccharomyces cerevisiae*', *Science*, 281(5384), pp. 1854–1857. Available at: https://doi.org/10.1126/science.281.5384.1854.

Dresser, M.E. and Giroux, C.N. (1988) 'Meiotic chromosome behavior in spread preparations of yeast.', *The Journal of cell biology*, 106(3), pp. 567–573. Available at: https://doi.org/10.1083/jcb.106.3.567.

Dubrana, K. *et al.* (2007) 'The processing of double-strand breaks and binding of single-strand-binding proteins RPA and Rad51 modulate the formation of ATR-kinase foci in yeast', *Journal of cell science*, 120(23), pp. 4209–4220.

Enserink, J.M. and Kolodner, R.D. (2010) 'An overview of Cdk1-controlled targets and processes', *Cell Division*, 5(1), p. 11. Available at: https://doi.org/10.1186/1747-1028-5-11.

Esponda, P. and Giménez-Martín, G. (1972) 'The attachment of the synaptonemal complex to the nuclear envelope: An ultrastructural and cytochemical analysis', *Chromosoma*, 38(4), pp. 405–417. Available at: https://doi.org/10.1007/BF00320159.

Esposito, M.S. *et al.* (1969) 'Acetate utilization and macromolecular synthesis during sporulation of yeast', *Journal of Bacteriology*, 100(1), pp. 180–186. Available at: https://doi.org/10.1128/jb.100.1.180-186.1969.

Evrin, C. *et al.* (2009) 'A double-hexameric MCM2-7 complex is loaded onto origin DNA during licensing of eukaryotic DNA replication', *Proceedings of the National Academy of Sciences*, 106(48), pp. 20240–20245. Available at: https://doi.org/10.1073/pnas.0911500106.

Featherstone, C. and Jackson, S.P. (1999) 'DNA double-strand break repair', *Current Biology*, 9(20), pp. R759–R761. Available at: https://doi.org/10.1016/S0960-9822(00)80005-6.

Field, J. *et al.* (1988) 'Purification of a RAS-responsive adenylyl cyclase complex from Saccharomyces cerevisiae by use of an epitope addition method', *Molecular and Cellular Biology*, 8(5), pp. 2159–2165. Available at: https://doi.org/10.1128/mcb.8.5.2159-2165.1988.

Garcia, V. *et al.* (2011) 'Bidirectional resection of DNA double-strand breaks by Mre11 and Exo1', *Nature*, 479(7372), pp. 241–244. Available at: https://doi.org/10.1038/nature10515.

Garcia, V., Furuya, K. and Carr, A.M. (2005) 'Identification and functional analysis of TopBP1 and its homologs', *DNA repair*, 4(11), pp. 1227–1239. Available at: https://doi.org/10.1016/j.dnarep.2005.04.001.

Gardner, R., Putnam, C.W. and Weinert, T. (1999) 'RAD53, DUN1 and PDS1 define two parallel G2/M checkpoint pathways in budding yeast', *The EMBO journal*, 18(11), pp. 3173–3185. Available at: https://doi.org/10.1093/emboj/18.11.3173.

Gilbert, C.S., Green, C.M. and Lowndes, N.F. (2001) 'Budding Yeast Rad9 Is an ATP-Dependent Rad53 Activating Machine', *Molecular Cell*, 8(1), pp. 129–136. Available at: https://doi.org/10.1016/S1097-2765(01)00267-2.

Gong, L. *et al.* (2017) *Nanopore Sequencing Reveals High-Resolution Structural Variation in the Cancer Genome*. preprint. Genomics. Available at: https://doi.org/10.1101/209718.

Goossens, K.V.Y. *et al.* (2015) 'Molecular mechanism of flocculation self-recognition in yeast and its role in mating and survival', *mBio*, 6(2), pp. e00427-15. Available at: https://doi.org/10.1128/mBio.00427-15.

Gottlieb, S.F. *et al.* (2023) 'Genetics, Nondisjunction', in *StatPearls*. Treasure Island (FL): StatPearls Publishing. Available at: http://www.ncbi.nlm.nih.gov/books/NBK482240/ (Accessed: 27 September 2023).

Gottlieb, S.F., Gulani, A. and Tegay, D.H. (2023) 'Genetics, Meiosis', in *StatPearls*. Treasure Island (FL): StatPearls Publishing. Available at: http://www.ncbi.nlm.nih.gov/books/NBK482462/ (Accessed: 25 September 2023).

Gray, S. *et al.* (2013) 'Positive regulation of meiotic DNA double-strand break formation by activation of the DNA damage checkpoint kinase Mec1(ATR)', *Open Biology*, 3(7), p. 130019. Available at: https://doi.org/10.1098/rsob.130019.

Gritenaite, D. *et al.* (2014) 'A cell cycle-regulated Slx4-Dpb11 complex promotes the resolution of DNA repair intermediates linked to stalled replication', *Genes & Development*, 28(14), pp. 1604–1619. Available at: https://doi.org/10.1101/gad.240515.114.

Guidelines for PCR Optimization with Taq DNA Polymerase | NEB (no date). Available at: https://www.neb.com/en-gb/tools-and-resources/usage-guidelines/guidelines-for-pcr-optimization-with-taq-dna-polymerase (Accessed: 19 September 2023).

Guttmann-Raviv, N., Martin, S. and Kassir, Y. (2002) 'Ime2, a meiosis-specific kinase in yeast, is required for destabilization of its transcriptional activator, Ime1', *Molecular and Cellular Biology*, 22(7), pp. 2047–2056. Available at: https://doi.org/10.1128/MCB.22.7.2047-2056.2002.

He, R. and Zhang, Z. (2022) 'Rad53 arrests leading and lagging strand DNA synthesis via distinct mechanisms in response to DNA replication stress', *BioEssays*, 44(9), p. 2200061. Available at: https://doi.org/10.1002/bies.202200061.

Ho, B. *et al.* (2022) *Mec1-Independent Activation of the Rad53 Checkpoint Kinase Revealed by Quantitative Analysis of Protein Localization Dynamics*. preprint. Genetics. Available at: https://doi.org/10.1101/2022.08.04.502543.

Hochuli, E. *et al.* (1988) 'Genetic Approach to Facilitate Purification of Recombinant Proteins with a Novel Metal Chelate Adsorbent', *Nature Biotechnology*, 6(11), pp. 1321–1325. Available at: https://doi.org/10.1038/nbt1188-1321.

Hochwagen, A. and Amon, A. (2006) 'Checking Your Breaks: Surveillance Mechanisms of Meiotic Recombination', *Current Biology*, 16(6), pp. R217–R228. Available at: https://doi.org/10.1016/j.cub.2006.03.009.

Hollingsworth, N.M. and Gaglione, R. (2019) 'The meiotic-specific Mek1 kinase in budding yeast regulates interhomolog recombination and coordinates meiotic progression with double-strand break repair', *Current Genetics*, 65(3), pp. 631–641. Available at: https://doi.org/10.1007/s00294-019-00937-3.

Hosoya, N. and Miyagawa, K. (2021) 'Synaptonemal complex proteins modulate the level of genome integrity in cancers', *Cancer Science*, 112(3), pp. 989–996. Available at: https://doi.org/10.1111/cas.14791.

Ilves, I. *et al.* (2010) 'Activation of the MCM2-7 Helicase by Association with Cdc45 and GINS Proteins', *Molecular Cell*, 37(2), pp. 247–258. Available at: https://doi.org/10.1016/j.molcel.2009.12.030.

Jimenez, A. and Davies, J. (1980) 'Expression of a transposable antibiotic resistance element in Saccharomyces', *Nature*, 287(5785), pp. 869–871. Available at: https://doi.org/10.1038/287869a0.

Kawai, S. *et al.* (2004) 'Molecular insights on DNA delivery into Saccharomyces cerevisiae', *Biochemical and Biophysical Research Communications*, 317(1), pp. 100–107. Available at: https://doi.org/10.1016/j.bbrc.2004.03.011.

Kawai, S., Hashimoto, W. and Murata, K. (2010) 'Transformation of Saccharomyces cerevisiae and other fungi: methods and possible underlying mechanism', *Bioengineered Bugs*, 1(6), pp. 395–403. Available at: https://doi.org/10.4161/bbug.1.6.13257.

Kaye, J.A. *et al.* (2004) 'DNA Breaks Promote Genomic Instability by Impeding Proper Chromosome Segregation', *Current Biology*, 14(23), pp. 2096–2106. Available at: https://doi.org/10.1016/j.cub.2004.10.051.

Keeney, S. (2001) 'Mechanism and control of meiotic recombination initiation', in *Current Topics in Developmental Biology*. Elsevier, pp. 1–53. Available at: https://doi.org/10.1016/S0070-2153(01)52008-6.

Keeney, S. and Kleckner, N. (1995) 'Covalent protein-DNA complexes at the 5' strand termini of meiosis-specific double-strand breaks in yeast.', *Proceedings of the National Academy of Sciences*, 92(24), pp. 11274–11278. Available at: https://doi.org/10.1073/pnas.92.24.11274.

Kumagai, A. *et al.* (2006) 'TopBP1 Activates the ATR-ATRIP Complex', *Cell*, 124(5), pp. 943–955. Available at: https://doi.org/10.1016/j.cell.2005.12.041.

Labib, K. (2010) ‘How do Cdc7 and cyclin-dependent kinases trigger the initiation of chromosome replication in eukaryotic cells?’, *Genes & Development*, 24(12), pp. 1208–1219. Available at: https://doi.org/10.1101/gad.1933010.

Liu, J., Wu, T.C. and Lichten, M. (1995) ‘The location and structure of double-strand DNA breaks induced during yeast meiosis: evidence for a covalently linked DNA-protein intermediate.’, *The EMBO Journal*, 14(18), pp. 4599–4608. Available at: https://doi.org/10.1002/j.1460-2075.1995.tb00139.x.

Lydall, D. *et al.* (1996) ‘A meiotic recombination checkpoint controlled by mitotic checkpoint genes’, *Nature*, 383(6603), pp. 840–843. Available at: https://doi.org/10.1038/383840a0.

MacKenzie, A.M. and Lacefield, S. (2020) ‘CDK Regulation of Meiosis: Lessons from S. cerevisiae and S. pombe’, *Genes*, 11(7), p. 723. Available at: https://doi.org/10.3390/genes11070723.

Maine, E.M. (2013) ‘Gametogenesis’, in *Brenner’s Encyclopedia of Genetics*. Elsevier, pp. 154–156. Available at: https://doi.org/10.1016/B978-0-12-374984-0.00575-1.

Majka, J. and Burgers, P.M.J. (2003) ‘Yeast Rad17/Mec3/Ddc1: a sliding clamp for the DNA damage checkpoint’, *Proceedings of the National Academy of Sciences of the United States of America*, 100(5), pp. 2249–2254. Available at: https://doi.org/10.1073/pnas.0437148100.

Majka, J., Niedziela-Majka, A. and Burgers, P.M.J. (2006) ‘The checkpoint clamp activates Mec1 kinase during initiation of the DNA damage checkpoint’, *Molecular Cell*, 24(6), pp. 891–901. Available at: https://doi.org/10.1016/j.molcel.2006.11.027.

Masumoto, H., Sugino, A. and Araki, H. (2000) ‘Dpb11 Controls the Association between DNA Polymerases α and ε and the Autonomously Replicating Sequence Region of Budding Yeast’, *Molecular and Cellular Biology*, 20(8), pp. 2809–2817. Available at: https://doi.org/10.1128/MCB.20.8.2809-2817.2000.

McIntosh, J.R. (2021) ‘Anaphase A’, *Seminars in Cell & Developmental Biology*, 117, pp. 118–126. Available at: https://doi.org/10.1016/j.semcdb.2021.03.009.

McMahill, M.S., Sham, C.W. and Bishop, D.K. (2007) ‘Synthesis-Dependent Strand Annealing in Meiosis’, *PLoS Biology*. Edited by M. Lichten, 5(11), p. e299. Available at: https://doi.org/10.1371/journal.pbio.0050299.

Mitchell, A.P. (1994) ‘Control of meiotic gene expression in Saccharomyces cerevisiae’, *Microbiological Reviews*, 58(1), pp. 56–70. Available at: https://doi.org/10.1128/mr.58.1.56-70.1994.

Mordes, D.A. *et al.* (2008) ‘TopBP1 activates ATR through ATRIP and a PIKK regulatory domain’, *Genes & Development*, 22(11), pp. 1478–1489. Available at: https://doi.org/10.1101/gad.1666208.

Mordes, D.A., Nam, E.A. and Cortez, D. (2008) ‘Dpb11 activates the Mec1–Ddc2 complex’, *Proceedings of the National Academy of Sciences*, 105(48), pp. 18730–18734. Available at: https://doi.org/10.1073/pnas.0806621105.

Muramatsu, S. *et al.* (2010) ‘CDK-dependent complex formation between replication proteins Dpb11, Sld2, Pol ε, and GINS in budding yeast’, *Genes & Development*, 24(6), pp. 602–612. Available at: https://doi.org/10.1101/gad.1883410.

Navadgi-Patil, V.M. and Burgers, P.M. (2009) ‘The unstructured C-terminal tail of the 9-1-1 clamp subunit Ddc1 activates Mec1/ATR via two distinct mechanisms’, *Molecular Cell*, 36(5), pp. 743–753. Available at: https://doi.org/10.1016/j.molcel.2009.10.014.

Neale, M.J. and Keeney, S. (2006) ‘Clarifying the mechanics of DNA strand exchange in meiotic recombination’, *Nature*, 442(7099), pp. 153–158. Available at: https://doi.org/10.1038/nature04885.

Neale, M.J., Pan, J. and Keeney, S. (2005) 'Endonucleolytic processing of covalent protein-linked DNA double-strand breaks', *Nature*, 436(7053), pp. 1053–1057. Available at: https://doi.org/10.1038/nature03872.

Niu, H. *et al.* (2005) 'Partner Choice during Meiosis Is Regulated by Hop1-promoted Dimerization of Mek1', *Molecular Biology of the Cell*, 16(12), pp. 5804–5818. Available at: https://doi.org/10.1091/mbc.e05-05-0465.

Ohouo, P.Y. *et al.* (2013) 'DNA-repair scaffolds dampen checkpoint signalling by counteracting the adaptor Rad9', *Nature*, 493(7430), pp. 120–124. Available at: https://doi.org/10.1038/nature11658.

Osborn, A.J. and Elledge, S.J. (2003) 'Mrc1 is a replication fork component whose phosphorylation in response to DNA replication stress activates Rad53', *Genes & Development*, 17(14), pp. 1755–1767. Available at: https://doi.org/10.1101/gad.1098303.

Parvinen, M. and Söderström, K.-O. (1976) 'Chromosome rotation and formation of synapsis', *Nature*, 260(5551), pp. 534–535. Available at: https://doi.org/10.1038/260534a0.

Perera, D. *et al.* (2004) 'TopBP1 and ATR colocalization at meiotic chromosomes: role of TopBP1/Cut5 in the meiotic recombination checkpoint', *Molecular Biology of the Cell*, 15(4), pp. 1568–1579. Available at: https://doi.org/10.1091/mbc.e03-06-0444.

Petronczki, M., Siomos, M.F. and Nasmyth, K. (2003) 'Un Ménage à Quatre', *Cell*, 112(4), pp. 423–440. Available at: https://doi.org/10.1016/S0092-8674(03)00083-7.

Pfander, B. and Diffley, J.F.X. (2011) 'Dpb11 coordinates Mec1 kinase activation with cell cycle-regulated Rad9 recruitment', *The EMBO journal*, 30(24), pp. 4897–4907. Available at: https://doi.org/10.1038/emboj.2011.345.

Princz, L.N., Gritenaite, D. and Pfander, B. (2015) 'The Slx4-Dpb11 scaffold complex: coordinating the response to replication fork stalling in S-phase and the subsequent mitosis', *Cell Cycle (Georgetown, Tex.)*, 14(4), pp. 488–494. Available at: https://doi.org/10.4161/15384101.2014.989126.

Prugar, E. *et al.* (2017) 'Coordination of Double Strand Break Repair and Meiotic Progression in Yeast by a Mek1-Ndt80 Negative Feedback Loop', *Genetics*, 206(1), pp. 497–512. Available at: https://doi.org/10.1534/genetics.117.199703.

Puddu, F. *et al.* (2008) 'Phosphorylation of the budding yeast 9-1-1 complex is required for Dpb11 function in the full activation of the UV-induced DNA damage checkpoint', *Molecular and cellular biology*, 28(15), pp. 4782–4793.

Remus, D. *et al.* (2009) 'Concerted Loading of Mcm2–7 Double Hexamers around DNA during DNA Replication Origin Licensing', *Cell*, 139(4), pp. 719–730. Available at: https://doi.org/10.1016/j.cell.2009.10.015.

Rizzo, M.A. and Piston, D.W. (2005) 'High-contrast imaging of fluorescent protein FRET by fluorescence polarization microscopy', *Biophysical Journal*, 88(2), pp. L14-16. Available at: https://doi.org/10.1529/biophysj.104.055442.

Roeder, G. (2000) 'The pachytene checkpoint', *Trends in Genetics*, 16(9), pp. 395–403. Available at: https://doi.org/10.1016/S0168-9525(00)02080-1.

Rouse, J. and Jackson, S.P. (2002) 'Lcd1p recruits Mec1p to DNA lesions in vitro and in vivo', *Molecular cell*, 9(4), pp. 857–869.

Rubin-Bejerano, I. *et al.* (1996) 'Induction of Meiosis in *Saccharomyces cerevisiae* Depends on Conversion of the Transcriptional Repressor Ume6 to a Positive Regulator by Its Regulated Association with the Transcriptional Activator Ime1', *Molecular and Cellular Biology*, 16(5), pp. 2518–2526. Available at: https://doi.org/10.1128/MCB.16.5.2518.

Russell, P.J. (2010) *Biology: exploring the diversity of life*. 1st Canadian ed. Toronto: Nelson Education.

Salari, Roshanak and Salari, Rosita (2017) 'Investigation of the Best Saccharomyces cerevisiae Growth Condition', *Electronic Physician*, 9(1), pp. 3592–3597. Available at: https://doi.org/10.19082/3592.

Scherthan, H. *et al.* (2007) 'Chromosome mobility during meiotic prophase in Saccharomyces cerevisiae', *Proceedings of the National Academy of Sciences of the United States of America*, 104(43), pp. 16934–16939. Available at: https://doi.org/10.1073/pnas.0704860104.

Shaner, N.C. *et al.* (2004) 'Improved monomeric red, orange and yellow fluorescent proteins derived from Discosoma sp. red fluorescent protein', *Nature Biotechnology*, 22(12), pp. 1567–1572. Available at: https://doi.org/10.1038/nbt1037.

Sheu, Y.-J. *et al.* (2022) 'Prevalent and dynamic binding of the cell cycle checkpoint kinase Rad53 to gene promoters', *eLife*, 11, p. e84320. Available at: https://doi.org/10.7554/eLife.84320.

Shrivastav, M., De Haro, L.P. and Nickoloff, J.A. (2008) 'Regulation of DNA double-strand break repair pathway choice', *Cell Research*, 18(1), pp. 134–147. Available at: https://doi.org/10.1038/cr.2007.111.

Smith, H.E. *et al.* (1990) 'Role of *IME1* Expression in Regulation of Meiosis in *Saccharomyces cerevisiae*', *Molecular and Cellular Biology*, 10(12), pp. 6103–6113. Available at: https://doi.org/10.1128/mcb.10.12.6103-6113.1990.

Smith, H.E. *et al.* (1993) 'Genetic evidence for transcriptional activation by the yeast IME1 gene product.', *Genetics*, 133(4), pp. 775–784. Available at: https://doi.org/10.1093/genetics/133.4.775.

Smith, H.E. and Mitchell, A.P. (1989) 'A Transcriptional Cascade Governs Entry into Meiosis in *Saccharomyces cerevisiae*', *Molecular and Cellular Biology*, 9(5), pp. 2142–2152. Available at: https://doi.org/10.1128/mcb.9.5.2142-2152.1989.

del Solar, G. *et al.* (1998) 'Replication and control of circular bacterial plasmids', *Microbiology and molecular biology reviews: MMBR*, 62(2), pp. 434–464. Available at: https://doi.org/10.1128/MMBR.62.2.434-464.1998.

Stuart, D. and Wittenberg, C. (1998) '*CLB5* and *CLB6* are required for premeiotic DNA replication and activation of the meiotic S/M checkpoint', *Genes & Development*, 12(17), pp. 2698–2710. Available at: https://doi.org/10.1101/gad.12.17.2698.

Sun, Z. *et al.* (1996) 'Spk1/Rad53 is regulated by Mec1-dependent protein phosphorylation in DNA replication and damage checkpoint pathways', *Genes & development*, 10(4), pp. 395–406.

Székvölgyi, L. and Nicolas, A. (2010) 'From meiosis to postmeiotic events: homologous recombination is obligatory but flexible', *The FEBS journal*, 277(3), pp. 571–589.

Takayama, Y. *et al.* (2003) 'GINS, a novel multiprotein complex required for chromosomal DNA replication in budding yeast', *Genes & Development*, 17(9), pp. 1153–1165. Available at: https://doi.org/10.1101/gad.1065903.

Tanaka, S. *et al.* (2007) 'CDK-dependent phosphorylation of Sld2 and Sld3 initiates DNA replication in budding yeast', *Nature*, 445(7125), pp. 328–332. Available at: https://doi.org/10.1038/nature05465.

Tanaka, S. *et al.* (2013) 'Efficient initiation of DNA replication in eukaryotes requires Dpb11/TopBP1-GINS interaction', *Molecular and Cellular Biology*, 33(13), pp. 2614–2622. Available at: https://doi.org/10.1128/MCB.00431-13.

Thacker, D. *et al.* (2011) 'Exploiting spore-autonomous fluorescent protein expression to quantify meiotic chromosome behaviors in Saccharomyces cerevisiae', *Genetics*, 189(2), pp. 423–439. Available at: https://doi.org/10.1534/genetics.111.131326.

Trelles-Sticken, E., Loidl, J. and Scherthan, H. (1999) 'Bouquet formation in budding yeast: Initiation of recombination is not required for meiotic telomere clustering', *Journal of Cell Science*, 112(5), pp. 651–658. Available at: https://doi.org/10.1242/jcs.112.5.651.

Vialard, J.E. *et al.* (1998) 'The budding yeast Rad9 checkpoint protein is subjected to Mec1/Tel1-dependent hyperphosphorylation and interacts with Rad53 after DNA damage', *The EMBO journal*, 17(19), pp. 5679–5688.

Winter, E. (2012) 'The Sum1/Ndt80 Transcriptional Switch and Commitment to Meiosis in Saccharomyces cerevisiae', *Microbiology and Molecular Biology Reviews*, 76(1), pp. 1–15. Available at: https://doi.org/10.1128/MMBR.05010-11.

Yu, X. *et al.* (2003) 'The BRCT Domain Is a Phospho-Protein Binding Domain', *Science*, 302(5645), pp. 639–642. Available at: https://doi.org/10.1126/science.1088753.

Zakharyevich, K. *et al.* (2010) 'Temporally and Biochemically Distinct Activities of Exo1 during Meiosis: Double-Strand Break Resection and Resolution of Double Holliday Junctions', *Molecular Cell*, 40(6), pp. 1001–1015. Available at: https://doi.org/10.1016/j.molcel.2010.11.032.

Zickler, D. and Kleckner, N. (2015) 'Recombination, Pairing, and Synapsis of Homologs during Meiosis', *Cold Spring Harbor Perspectives in Biology*, 7(6), p. a016626. Available at: https://doi.org/10.1101/cshperspect.a016626.

Zou, L. and Elledge, S.J. (2003) 'Sensing DNA damage through ATRIP recognition of RPA-ssDNA complexes', *Science*, 300(5625), pp. 1542–1548.